



ΕΛΛΗΝΙΚΗ  
ΕΠΙΣΤΗΜΟΝΙΚΗ  
ΕΤΑΙΡΕΙΑ  
ΕΔΑΦΟΜΗΧΑΝΙΚΗΣ  
& ΓΕΩΤΕΧΝΙΚΗΣ  
ΜΗΧΑΝΙΚΗΣ

Αρ. 14 – ΜΑΙΟΣ 2008

# Τα Νέα

14

## της Ε Ε Ε Ε Γ Μ

### ΤΑΚΤΙΚΗ ΓΕΝΙΚΗ ΣΥΝΕΛΕΥΣΗ ΤΗΣ ΕΕΕΕΓΜ Τρίτη 13<sup>η</sup> Μαΐου 2008

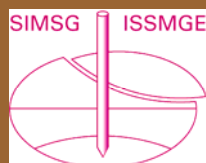
Την Τρίτη 13 Μαΐου 2008 διεξήχθη στην Αίθουσα Εκδηλώσεων της Σχολής Πολιτικών Μηχανικών του ΕΜΠ η τακτική Γενική Συνέλευση της ΕΕΕΕΓΜ, η οποία ήταν και εκλογοαπολογιστική. Η συνέλευση αυτή ήταν η πρώτη που συνεκλήθη μετά την τελευταία τροποποίηση του Άρθρου 7 του Καταστατικού, με την οποία καθιερώθηκε η δυνατότητα συμμετοχής στις ψηφοφορίες αρχαιρεσιών και δι' αλληλογραφίας.

Στη συνέλευση συμμετείχαν 60 μέλη της ΕΕΕΕΓΜ, ενώ 31 μέλη εψήφισαν δι' αλληλογραφίας.

Ο Πρόεδρος της Εκτελεστικής Επιτροπής Μιχάλης Παχάκης παρουσίασε την Έκθεση Πεπραγμένων της από την προηγούμενη εκλογική Γενική Συνέλευση της 24.05.2005 και ενημέρωσε ιδιαίτερα το σώμα για την διεκδίκηση, την ανάληψη και την προετοιμασία του επομένου XV European Conference on Soil Mechanics and Geotechnical Engineering στην Αθήνα τον Σεπτέμβριο 2011.

Ο Ταμίας της Εκτελεστικής Επιτροπής Μανώλης Βουζαράς παρουσίασε τον οικονομικό απολογισμό του οικονομικού έτους 2007 και ο Ορέστης Παπαγεωργίου, εκπροσωπώντας της Εξελεγκτική Επιτροπή, παρουσίασε την έκθεση της Εξελεγκτικής Επιτροπής.

Τα πεπραγμένα της Εκτελεστικής Επιτροπής και ο οικονομικός απολογισμός έγιναν ομοφώνως δεκτά από το σώμα.

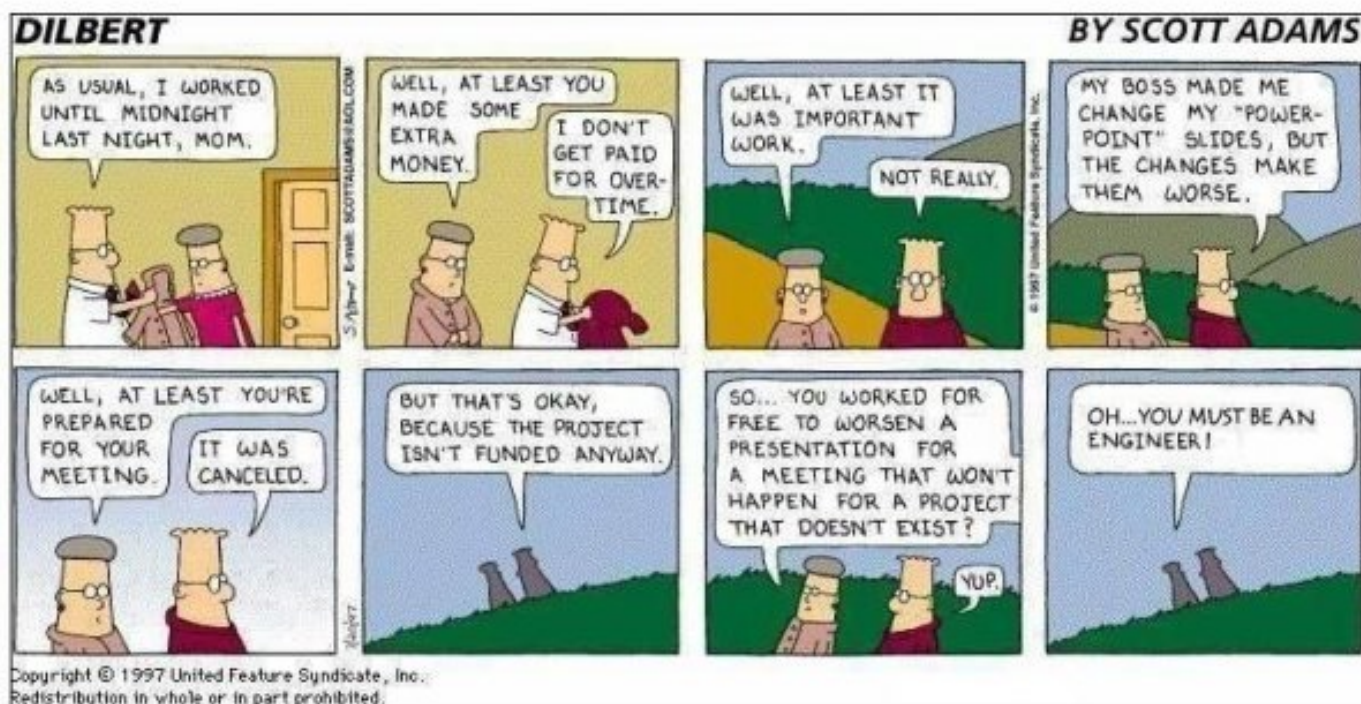


(συνέχεια στην σελίδα 3)

## Π Ε Ρ Ι Ε Χ Ο Μ Ε Ν Α

Τακτική Γενική Συνέλευση της ΕΕΕΕΓΜ	1
Άρθρα	8
- C. Tsatsanifos "Contribution of geotechnical engineering in the rehabilitation of buildings and infrastructures"	8
- E. Hoek, C. Carranza-Torres, M. Diederichs and B. Corkum "Integration of geotechnical and structural design in tunnelling"	24

Φαίνεται ότι δεν συμβαίνουν μόνο στην Ελλάδα ...



(συνέχεια από την σελίδα 1)

## **ΕΚΘΕΣΗ ΠΕΠΡΑΓΜΕΝΩΝ (24.05.2005 + 13.05.2008)**

### **1. ΕΙΣΑΓΩΓΗ**

Η παρούσα Γενική Συνέλευση είναι απολογιστική και εκλογική.

Τα τρία χρόνια που πέρασαν με τη θητεία της απερχόμενης Εκτελεστικής Επιτροπής ήταν αρκετά πλούσια σε γεγονότα και δραστηριότητες που εμπίπτουν στους σκοπούς της Επισημονικής μας Εταιρείας σύμφωνα με το Καταστατικό της.

### **2. Η ΕΚΤΕΛΕΣΤΙΚΗ ΕΠΙΤΡΟΠΗ**

Η προηγούμενη Εκλογική Γενική Συνέλευση της ΕΕΕΕΓΜ (τότε ΕΕΕΕΘ) που ήταν και καταστατική έλαβε χώρα στις 24.05.2005.

Από αυτήν εξελέγη η Εκτελεστική Επιτροπή που συγκροτήθηκε σε σώμα στις 23.06.2005 με την ακόλουθη σύνθεση:

Πρόεδρος	:	Μιχάλης Παχάκης
Α' Αντιπρόεδρος	:	Χρήστος Τσατσάνιφος
Β' Αντιπρόεδρος	:	Σπύρος Καβουνίδης
Γεν. Γραμματέας	:	Ανδρέας Αναγνωστόπουλος
Ταμίας	:	Μανόλης Βουζαράς
Έφορος	:	Γιώργος Ντούλης
Μέλη	:	Παναγιώτης Βέππας Μιχάλης Καββαδάς Δημήτρης Κούμουλος

Ως αναπληρωματικά μέλη εξελέγησαν οι κάτωθι:

1. Γιώργος Μπουκοβάλας
2. Κώστας Κορωνιώτης
3. Γιώργος Ντουλιάς
4. Σπύρος Παπασπύρου

Στην ίδια Γενική Συνέλευση εξελέγησαν για την Εξελεγκτική Επιτροπή οι κάτωθι:

1. Ορέστης Παπαγεωργίου
2. Αλέξανδρος Ζουριδής
3. Αριστοτέλης Καμαριώτης

Η Εκτελεστική Επιτροπή κατά την τριετή περίοδο της θητείας της συνεδρίασε 24 φορές.

Παράλληλα δεδομένου ότι τα μέλη της ήταν και μέλη της Οργανωτικής Επιτροπής του 5<sup>ου</sup> Πανελληνίου Συνεδρίου Γεωτεχνικής και Γεωπεριβαλλοντικής Μηχανικής, που συνδιοργανώθηκε με το ΤΕΕ, έλαβε μέρος σε πολυάριθμες συνεδριάσεις της ευρείας Οργανωτικής Επιτροπής στο ΤΕΕ, της οποίας προήδρευε ο Γεν. Γραμματέας της ΕΕΕΕΓΜ ομ. καθ. ΕΜΠ Α. Αναγνωστόπουλος.

### **3. ΓΕΝΙΚΕΣ ΣΥΝΕΛΕΥΣΕΙΣ**

Στο διάστημα της τριετίας η Ε.Ε. συγκάλεσε δύο ετήσιες τακτικές Γενικές Συνελεύσεις, σύμφωνα με το Καταστατικό:

- Στις 16.06.2006 (απολογιστική και καταστατική ως προς το άρθρο 7)
- Στις 11.12.2007 (απολογιστική)

### **4. ΤΡΟΠΟΠΟΙΗΣΗ ΤΟΥ ΚΑΤΑΣΤΑΤΙΚΟΥ**

Σύμφωνα με τις αποφάσεις των Γενικών Συνελεύσεων της 24.05.2005 και της 16.06.2006, η Ε.Ε. πρόβη στις απαραίτητες ενέργειες για την τροποποίηση του Καταστατικού της Εταιρείας. Στις 16.02.2007 εκδόθηκε η απόφαση του Πρωτοδικείου Αθηνών με την οποία εγκρίθηκε η τροποποίηση και στις 30.03.2007 έγινε η καταχώρηση στο Βιβλίο Σωματείων

του Πρωτοδικείου. Από την ημερομηνία αυτή ισχύει το τροποποιημένο καταστατικό.

Υπενθυμίζεται ότι οι τροποποιήσεις αφορούν κυρίως την επωνυμία της εταιρείας που έγινε ΕΛΛΗΝΙΚΗ ΕΠΙΣΤΗΜΟΝΙΚΗ ΕΤΑΙΡΕΙΑ ΕΔΑΦΟΜΗΧΑΝΙΚΗΣ & ΓΕΩΤΕΧΝΙΚΗΣ ΜΗΧΑΝΙΚΗΣ ώστε να συμφωνεί με την επωνυμία της αντίστοιχης Διεθνούς Εταιρείας (ISSMGE) της οποίας είναι μέλος και στον τρόπο διεξαγωγής των αρχαιρεσιών για την ανάδειξη των μελών της Εκτελεστικής και της Εξελεγκτικής Επιτροπής με τον οποίο δίνεται η δυνατότητα υποβολής υποψηφιοτήτων και αποστολής ψηφοδελτίων ταχυδρομικώς.

Το τροποποιημένο καταστατικό και η διαδικασία ψηφοφορίας, όπως αυτή εγκρίθηκε από τη Γ.Σ. της 16.06.2006, δημοσιεύτηκαν στο τεύχος αρ. 8 των «Νέων της ΕΕΕΕΓΜ» που εκδόθηκε και διανεμήθηκε με την ευκαιρία του εορτασμού των 40 χρόνων της εταιρείας.

### **5. ΝΕΑ ΜΕΛΗ**

Από την τελευταία Γενική Συνέλευση μέχρι σήμερα ενεγράφησαν στην ΕΕΕΕΓΜ τα κάτωθι μέλη (κατά σειράν εγγραφής):

1. Μαυρομάτη Ζωή – Χριστίνα, Πολιτικός Μηχανικός
2. Σακελλαρίου Σοφία, Πολιτικός Μηχανικός
3. Ιωσηφίδου Κωνσταντίνα, Πολιτικός Μηχανικός
4. Κωνσταντής Θωμάς, Πολιτικός Μηχανικός
5. Αναστασόπουλος Κωνσταντίνος, Πολιτικός Μηχανικός
6. Πατέλης Ηλίας, Πολιτικός Μηχανικός – Γεωλόγος
7. Χλιμίντζας Γεώργιος, Δρ. Πολιτικός Μηχανικός
8. Μαραγκός Νικόλαος, Πολιτικός Μηχανικός
9. Παπασταμάτης Ζήσης, Πολιτικός Μηχανικός
10. Παπαχατζάκη Ζαχαρούλα – Ρέα, Πολιτικός Μηχανικός MSc
11. Βούρβαχης Ιωάννης, Πολιτικός Μηχανικός
12. Παπαδρόσος Νικόλαος, Πολιτικός Μηχανικός
13. Σκυλάκης Εμμανουήλ, Πολιτικός Μηχανικός MSc
14. Αναστασόπουλος Ιωάννης, Δρ. Πολιτικός Μηχανικός
15. Δούλαλα – Rigby Χάιδω, Πολιτικός Μηχανικός
16. Μαρονικολάκη Ειρήνη, Πολιτικός Μηχανικός
17. Παπαδάκος Γεώργιος, Πολιτικός Μηχανικός
18. Ξενάκη Βασιλική, Δρ. Πολιτικός Μηχανικός
19. Ιωαννίδης Κωνσταντίνος, Πολιτικός Μηχανικός
20. Μαρίνος Βασίλειος, Τεχνικός Γεωλόγος MSc, DIC
21. Ιακωβίδου Μαρία, Πολιτικός Μηχανικός MSc, DIC
22. Παπαχαλαράμπος Γεώργιος, Πολιτικός Μηχανικός MSc, DIC
23. Σιταρένιος Παναγιώτης, Πολιτικός Μηχανικός
24. Μουλίνος Γεράσιμος, Δρ. Πολιτικός Μηχανικός
25. Κεραμίδας Ευτύχιος, Πολιτικός Μηχανικός MSc, DIC
26. Κοζμπούλης Απόστολος, Πολιτικός Μηχανικός MEng
27. Ανδριανόπουλος Κων/νος, Δρ. Πολιτικός Μηχανικός
28. Άρμπερ Πήτερ, Πολιτικός Μηχανικός
29. Ανδρέου Παναγιώτης, Πολιτικός Μηχανικός
30. Γιαννακού Αμαλία, Πολιτικός Μηχανικός
31. Ζευγόλης Ιωάννης, Πολιτικός Μηχανικός
32. Καβουκλής Παναγιώτης, Πολιτικός Μηχανικός
33. Κακδέρη Καλλιόπη, Πολιτικός Μηχανικός
34. Μανάκου Μαρία, Γεωλόγος
35. Μάνου Δήμητρα, Πολιτικός Μηχανικός
36. Μπασδέκης Αναστάσιος, Γεωλόγος
37. Προυντζόπουλος Γεώργιος, Πολιτικός Μηχανικός
38. Σαρόγλου Χαράλαμπος, Γεωλόγος
39. Φορτσάκης Πέτρος, Πολιτικός Μηχανικός

Επίσης ενεκρίθη η εγγραφή των κάτωθι:

1. Νάκου Φωφώ, Πολιτικός Μηχανικός, Γεωλόγος
2. Ιωαννίδης Ιωάννης, Πολιτικός Μηχανικός
3. Γρυπάρης Φαίδων, Πολιτικός Μηχανικός
4. Βρεττός Χρήστος, Δρ. Πολιτικός Μηχανικός
5. Μαρονικολάκη Αικατερίνη, Πολιτικός Μηχανικός
6. Ρίζου Χριστίνη, Πολιτικός Μηχανικός
7. Αλεξανδρής Χρήστος, Πολιτικός Μηχανικός

8. Αργυρούδης Σωτήριος, Πολιτικός Μηχανικός
9. Κίρτας Εμμανουήλ, Πολιτικός Μηχανικός
10. Κτενίδου Όλγα – Τζόαν, Πολιτικός Μηχανικός
11. Χατζηαντωνίου Κλεονίκη, Πολιτικός Μηχανικός
12. Κανελαίδης Κωνσταντίνος, Πολιτικός Μηχανικός
13. Λιώτης Ευστάθιος, Δρ. Μηχανικός Μεταλλείων – Μεταλλουργός
14. Ζαχαράκη Καλλιόπη, Πολιτικός Μηχανικός, Μ.Δ.Ε.
15. Ελεζόγλου Κωνσταντίνος, Θρασύβουλος: Μηχ. Μεταλλείων – Μεταλλουργός, MSc, DIC
16. Κουρετζής Γεώργιος, Δρ. Πολιτικός Μηχανικός

## 6. ΕΚΔΗΛΩΣΗ ΓΙΑ ΤΑ 40 ΧΡΟΝΙΑ ΤΗΣ ΕΕΕΕΓΜ

Στις 15 Μαΐου 2007 έλαβε χώρα στην αίθουσα του ΕΒΕΑ πανηγυρική εκδήλωση για τα 40 χρόνια από την ίδρυση της ΕΕΕΕΘ/ΕΕΕΕΓΜ, κατά την οποία επιδόθηκαν αναμνηστικές πλακέτες στα Ιδρυτικά Μέλη, στους διατελέσαντες Πρόεδρους της Εκτελεστικής Επιτροπής και στον επί 26 συνεχή έτη Γεν. Γραμματέα της.

Στην εκδήλωση δόθηκε διάλεξη από τον συνάδελφο και πρώην Πρόεδρο Ηλία Σωτηρόπουλο με θέμα: «Εδαφομηχανική – Παρελθόν, Παρόν και Μέλλον» και ακολούθησε δεξίωση.

Επίσης κυκλοφόρησε πανηγυρικό τεύχος των «Νέων της ΕΕΕΕΓΜ» (αρ. 8).

## 7. ΑΘΗΝΑΪΚΕΣ ΔΙΑΛΕΞΕΙΣ

- α. Στις 23.01.2006 δόθηκε η 4<sup>η</sup> Αθηναϊκή Διάλεξη Γεωτεχνικής Μηχανικής με προσκεκλημένο ομιλητή τον καθηγητή της Ecole National des Ponts et Chaussées Alain Pecker με θέμα: "Enhanced seismic design of shallow foundations: example of the Rion – Antirion bridge".
- β. Στις 17 Μαρτίου 2008 δόθηκε η 5<sup>η</sup> Αθηναϊκή Διάλεξη Γεωτεχνικής Μηχανικής με προσκεκλημένο ομιλητή τον ομότιμο καθηγητή του ΕΜΠ Ανδρέα Αναγνωστόπουλο με θέμα: «Καθιζήσεις επιφανειακών θεμελιώσεων».

Και οι δύο διαλέξεις είχαν εξαιρετική επιτυχία λόγω του ενδιαφέροντος περιεχομένου τους και του τρόπου παρουσίασής τους και υπήρξε μαζική προσέλευση ακροατών. Στην πρώτη εξ αυτών παρευρέθη και ο Αντιπρόεδρος για την Ευρώπη της ISSMGE καθηγητής Roger Frank.

Οι Αθηναϊκές διαλέξεις, που δίνονται ανά διετία, είναι πλέον καθιερωμένος θεσμός της Εταιρείας μας και αποτελούν επισημονικό γεγονός.

## 8. ΑΛΛΕΣ ΔΙΑΛΕΞΕΙΣ

- Διάλεξη του καθηγητή ENPC **Roger Frank**, Αντιπροέδρου για την Ευρώπη της ISSMGE. Θέμα: «Μικροπασσαλοι: Έρευνα και Εφαρμογή» (30.05.2005).
- Διάλεξη του καθηγητή ΕΜΠ **Παύλου Μαρίνου**. Θέμα: «Οι Νέες Σήραγγες Βάσης των Άλπειων: Οι Σήραγγες του Νέου Αιώνα» (07.11.2005).
- Διάλεξη του καθηγητή **Robert Mair**, του Πανεπιστημίου του Cambridge (επανάληψη της "Rankine Lecture", 2006) με θέμα: "Tunneling and Geotechnics – New Horizons" (14.09.2006).
- Διάλεξη της συναδέλφου **Άντας Αθανασοπούλου**, Πολ. Μηχ. MSc, υποψήφιας διδάκτορος Πανεπ. Berkeley με θέμα: «Διερεύνηση της Συμπεριφοράς των Συστημάτων Αντιπλημμυρικής Προστασίας της Νέας Ορλεάνης κατά τον Τυφώνα "Κατρίνα" της 29<sup>ης</sup> Αυγούστου 2005» (σε συνεργασία με την ΕΕΕΕΘ του ΤΕΕ) (19.12.2006).
- Διάλεξη του καθηγητή **Mounir Khalel Berrah** της Ecole National Polytechnique της Αλγερίας με θέμα: «The Complete Stochastic Deamplification Approach:

An Efficient Tool to Describe the Spatial Variability of Earthquake Motion" (σε συνεργασία με το ΕΜΠ) (18.06.2007).

- Διάλεξη του καθηγητή **Antonio Gens**, του Πανεπιστημίου της Catalonia (επανάληψη της "Rankine Lecture", 2007) με θέμα: "Soil – Environment Interactions in Geotechnical Engineering" (17.04.2008).

Διαλέξεις Νέων Διδασκτόρων Γεωτεχνικών Μηχανικών με θέματα της διδακτορικής τους διατριβής (σε συνεργασία με την ΕΕΕΕΘ του ΤΕΕ).

- **Ανδρέα Αντωνίου**, με θέμα: «Εφαρμογή Γεωγραφικών Συστημάτων Πληροφοριών στη Γεωτεχνική Μηχανική» (13.03.2006).
- **Γεωργίου Χλιμίντζα**, με θέμα: «Εκτίμηση Μόνιμων Μετακινήσεων λόγω Σεισμού σε Εδαφικά Πρανή με Χρήση Απλοποιημένης Ανάλυσης Ολισθήσεων» (13.03.2006).
- **Πρόδρομου Ψαρρόπουλου**, Δρ. Πολ. Μηχ. ΕΜΠ, με θέμα: «Εδαφοδυναμική Προσομοίωση στη Σεισμική Ανάλυση Βάθρων και ακροβάθρων Γεφυρών» (11.12.2006).
- **Έλενας Κούμουλου**, με θέμα: «Προσομοίωση στον Φυγοκεντριστή της Κίνησης Βαρέων μη Υδατοδιαλυτών Υγρών Ρυπαντών» (11.12.2006).

## 9. ΗΜΕΡΙΔΕΣ – WORKSHOPS – ΔΙΕΘΝΗ ΣΥΝΕΔΡΙΑ ΣΤΗΝ ΕΛΛΑΔΑ

Κατά την περίοδο που εξετάζεται, έλαβαν χώρα στην Ελλάδα με ευρεία και ενεργό συμμετοχή των μελών της ΕΕΕΕΓΜ οι ακόλουθες ημερίδες, workshops και διεθνή συνέδρια.

- 13 ÷ 16.06.2005 "International Workshop on Degradation, Instabilities and Bifurcation in Geomechanics", στην Αθήνα (χορηγία 1500€ της ΕΕΕΕΓΜ).
- 11 ÷ 12.10.2005 1<sup>ο</sup> Ελληνοϊαπωνικό Workshop με θέμα «Αντισεισμικός Σχεδιασμός, Παρατήρηση Συμπεριφοράς και Αναβάθμιση Θεμελιώσεων», στην Αθήνα.
- 05.12.2005 Ημερίδα με θέμα: «Ρύπανση Εδάφους: Πρόληψη και Αποκατάσταση» στην Αθήνα, (συνδιοργάνωση Γεωτ. Τομέα ΕΜΠ και ΕΕΕΕΓΜ).
- 11.01.2007 Ημερίδα «Γεωτεχνικές Εφαρμογές Γεωσυνθετικών Υλικών», στην Αθήνα, (συνδιοργάνωση ΕΕΕΕΘ/ΤΕΕ και ΕΣΓΥ).
- 01.02.2007 Ημερίδα "Νέες Εξελιγμένες Μέθοδοι Μηχανικής Διάνοιξης Σηράγγων", στην Αθήνα, (συνδιοργάνωση ΕΕΕΕΘ/ΤΕΕ, ΕΕΣΥΕ και Πολυτεχνικού Συλλόγου).
- 20 ÷ 22.06.2007 Διεθνές Συνέδριο με θέμα "Advanced Characterization of Pavement and Soil Engineering Materials", στην Αθήνα, (συνδιοργάνωση ΕΜΠ, Delft και Πανεπ. Illinois, υπό την αιγίδα των ISAP, ISCP και HESPER).
- 25 ÷ 28.06.2007 4<sup>ο</sup> Διεθνές Συνέδριο Γεωτεχνικής Σεισμικής Μηχανικής (4<sup>th</sup> Int. Conf. on Earthquake Geotechnical Engineering), στη Θεσσαλονίκη, (συνδιοργάνωση από την επιτροπή TC4 της ISSMGE, το Εργαστήριο Γεωτεχνικής του Αριστοτελείου Πανεπιστημίου και την ΕΕΕΕΓΜ).

Λεπτομερείς αναφορές στις εκδηλώσεις αυτές έχουν περιληφθεί στα τεύχη των «Νέων της ΕΕΕΕΓΜ».

## 10. 16<sup>ο</sup> ΔΙΕΘΝΕΣ ΣΥΝΕΔΡΙΟ ΕΔΑΦΟΜΗΧΑΝΙΚΗΣ ΚΑΙ ΓΕΩΤΕΧΝΙΚΗΣ ΜΗΧΑΝΙΚΗΣ

Το συνέδριο πραγματοποιήθηκε στην Osaka της Ιαπωνίας (12 ÷ 16 Σεπτεμβρίου 2005).

Η ΕΕΕΕΓΜ συμμετείχε με 6 ανακοινώσεις μελών της. Επίσης τα μέλη Ι. Βαρδουλάκης, Δ. Κούμπος, Γ. Γκαζέτας και Χ. Τσατσανίφους συμμετείχαν στα προεδρεία.

## 11. 5<sup>ο</sup> ΠΑΝΕΛΛΗΝΙΟ ΣΥΝΕΔΡΙΟ ΓΕΩΤΕΧΝΙΚΗΣ ΚΑΙ ΠΕΡΙΒΑΛΛΟΝΤΙΚΗΣ ΜΗΧΑΝΙΚΗΣ

Το 5<sup>ο</sup> Πανελλήνιο Συνέδριο που συνδιοργανώθηκε με το ΤΕΕ πραγματοποιήθηκε με επιτυχία στην Ξάνθη στο διάστημα 31.05 έως 02.06.2006.

Έλαβαν μέρος 560 σύνεδροι και υποβλήθηκαν 227 εργασίες. Επίσης έγιναν 12 ειδικές ομιλίες και μια εναρκτήρια διάλεξη από προσκεκλημένο ομιλητή (Χ. Βρεπτός). Το συνέδριο χαιρέτησε μεταξύ άλλων ο Αντιπρόεδρος για την Ευρώπη της ISSMGE κ. R. Frank. Με πρωτοβουλία της ΕΕΕΕΓΜ προσκλήθηκαν στο συνέδριο εκπρόσωποι των Εθνικών Γεωτεχνικών Ενώσεων των χωρών της Ανατολικής Ευρώπης για να συμμετάσχουν σε ειδική συνεδρία με θέμα την διδασκαλία και πρακτική της Γεωτεχνικής Μηχανικής στις χώρες αυτές.

## 12. 14<sup>ο</sup> ΠΑΝΕΥΡΩΠΑΪΚΟ ΣΥΝΕΔΡΙΟ ΣΤΗ ΜΑΔΡΙΤΗ

Το Συνέδριο πραγματοποιήθηκε στη Μαδρίτη στο διάστημα 24 ÷ 27 Σεπτεμβρίου, με συμμετοχή 830 συνέδρων, μεταξύ των οποίων 16 μέλη της ΕΕΕΕΓΜ και τρεις Έλληνες σύνεδροι εγκατεστημένοι στο εξωτερικό. Ο Γενικός Γραμματέας Α. Αναγνωστόπουλος ήταν μέλος της Διεθνούς Επιστημονικής Επιτροπής του Συνεδρίου και ο Αντιπρόεδρος Χ. Τσατσανίφους ήταν Γενικός εισηγητής στην Κύρια Συνεδρία 4.

Τα μέλη μας Γ. Μπουκοβάλας και Κ. Πιπλάκης συμμετείχαν στο workshop της επιτροπής ERTC12 στα πλαίσια του Συνεδρίου.

Ο συνάδελφος Γ. Αναγνώστου, Καθηγητής στο Πανεπιστήμιο της Ζυρίχης ήταν panelist στη Συνεδρία Συζήτησης 3.1.

Τα μέλη μας Γ. Γκαζέτας και Γ. Αθανασόπουλος ήταν panelist στις Συνεδρίες Συζήτησης 1.1 και 4.3 αντίστοιχα, αλλά δεν μπόρεσαν να παρευρεθούν στο Συνέδριο, λόγω άλλων υποχρεώσεων.

Εκ μέρους της ΕΕΕΕΓΜ υπεβλήθησαν στο Συνέδριο και δημοσιεύτηκαν στα Πρακτικά, έξι (6) άρθρα μελών της.

Λεπτομέρειες για το Συνέδριο υπάρχουν στο τεύχος 10 των «Νέων της ΕΕΕΕΓΜ».

## 13. ΔΙΕΚΔΙΚΗΣΗ ΚΑΙ ΑΝΑΛΗΨΗ ΤΗΣ ΔΙΟΡΓΑΝΩΣΗΣ ΤΟΥ 15<sup>ου</sup> ΠΑΝΕΥΡΩΠΑΪΚΟΥ ΣΥΝΕΔΡΙΟΥ

Η Εκτελεστική Επιτροπή, ακολουθώντας τις ισχύουσες διαδικασίες της ISSMGE, υπέβαλε στις 17.04.2007 έγγραφο αίτημα προς τον Γεν. Γραμματέα και τον Αντιπρόεδρο για την Ευρώπη, για την ανάληψη της διοργάνωσης του 15<sup>ου</sup> Πανευρωπαϊκού Συνεδρίου Εδαφομηχανικής και Γεωτεχνικής Μηχανικής στην Αθήνα το Σεπτέμβριο του 2011, με θέμα "Geotechnics of Hard Soils – Weak Rocks".

Ακολούθως προέβη στις απαραίτητες ενέργειες για την προετοιμασία του σχετικού φακέλου διεκδίκησης, προκειμένου να διεκδικήσει την ψήφο των υπολοίπων Ευρωπαϊκών Γεωτεχνικών Ενώσεων μελών της International Society for Soil Mechanics & Geotechnical Engineering (ISSMGE), κατά τη Γενική τους Συνέλευση στα πλαίσια του 14<sup>ου</sup> ECSMGE στη Μαδρίτη.

Η σύνταξη του φακέλου απαιτεί τη συνεργασία με εξειδικευμένο Γραφείο διοργάνωσης διεθνών συνεδρίων. Για το σκοπό αυτό η Ε. Ε. αφού έλαβε και αξιολόγησε προσφορές από τέσσερα τέτοια Γραφεία επέλεξε το Γραφείο «TRIAENA TOURS & CONGRESS» S.A.

Με τη βοήθεια του Γραφείου αυτού συντάχθηκε ο φάκελος διεκδίκησης και ταχυδρομήθηκε στις Ευρωπαϊκές Γεωτεχνικές Ενώσεις και στους αξιωματούχους της ISSMGE αρκετές μέρες πριν από την Γενική Συνέλευση της 25<sup>ης</sup> Σεπτεμβρίου 2007 στη Μαδρίτη.

Στη Γενική Συνέλευση παρέστησαν ο Πρόεδρος, ο Α' Αντιπρόεδρος και ο Γεν. Γραμματέας της ΕΕΕΕΓΜ και την παρουσίαση της διεκδίκησης έκανε ο δεύτερος εξ αυτών συνάδελφος Χ. Τσατσανίφους.

Αντίπαλος της ΕΕΕΕΓΜ και της Αθήνας, ήταν η British Geotechnical Association (BGA) και το Εδιμβούργο.

Κατά την ψηφοφορία η ΕΕΕΕΓΜ κέρδισε τη διοργάνωση με ψήφους 22 έναντι 9 επί 31 ψηφισάντων.

Ήδη η Ε.Ε. προχώρησε στις διαδικασίες σύστασης Οργανωτικής Επιτροπής που θα ενεργοποιηθεί αμέσως μετά την εκλογή και συγκρότηση της νέας Ε.Ε.

Λεπτομέρειες θα ανακοινωθούν μέσω των «Νέων της ΕΕΕΕΓΜ».

Με απόφαση της Γ.Σ. της 11.12.2007 έπειτα από εισήγηση της Ε.Ε. ο Πρόεδρος εξουσιοδοτήθηκε να υπογράψει σύμβαση συνεργασίας με το προαναφερθέν Γραφείο. Η σύμβαση υπογράφηκε στις 14.04.2008.

## 14. ΥΠΟΣΤΗΡΙΞΗ ΣΥΜΜΕΤΟΧΗΣ ΝΕΩΝ ΓΕΩΤΕΧΝΙΚΩΝ ΜΗΧΑΝΙΚΩΝ ΣΕ ΔΙΕΘΝΕΙΣ ΕΚΔΗΛΩΣΕΙΣ

Με δαπάνες της ΕΕΕΕΓΜ έλαβαν μέρος σε Διεθνή και Ευρωπαϊκά Συνέδρια Νέων Γεωτεχνικών Μηχανικών (YGEC) οι κάτωθι συνάδελφοι:

- Ι. Αναστασόπουλος: 3<sup>ο</sup> Διεθνές YGEC, Osaka, Ιαπωνίας (15 Σεπτεμβρίου, 2005)
- Π. Ανδρέου: 17<sup>ο</sup> Ευρωπαϊκό YGEC, Ζάγκρεμπ Κροατίας (20÷22 Ιουλίου, 2006)
- Α. Αραπάκου, Α. Δρουδάκης: 17<sup>ο</sup> Ευρωπαϊκό YGEC, Ανκόνα, Ιταλίας, (17÷20 Ιουνίου, 2007)

Επίσης εγκρίθηκε η συμμετοχή στο 19<sup>ο</sup> Ευρωπαϊκό YGEC, που θα γίνει στο Győr της Ουγγαρίας, από 4 έως 6 Σεπτεμβρίου 2008, των συναδέλφων:

- Α. Παπαδοπούλου, και
- Γ. Αναγνωστόπουλου

## 15. ΔΙΕΘΝΕΙΣ ΣΧΕΣΕΙΣ

### 15.1 Γενική Συνέλευση της ISSMGE – Εκλογή Προέδρου (Osaka Ιαπωνίας, Σεπτ. 2005)

Η Γ.Σ. της ISSMGE έλαβε χώρα στις 11.09.2005 στα πλαίσια του 16<sup>ου</sup> Διεθνούς Συνεδρίου Εδαφομηχανικής και Θεμελιώσεων στη Osaka της Ιαπωνίας. Στη Γ.Σ. κατά την οποία έγινε και εκλογή Προέδρου συμμετείχαν 53 Εθνικές Ενώσεις και άλλες 12 Ενώσεις εκπροσωπήθηκαν με εξουσιοδότηση από τις παρούσες. Η ΕΕΕΕΓΜ εκπροσωπήθηκε από τους αντιπροέδρους Χ. Τσατσανίφο και Σ. Καβουνίδη.

Στη Γ.Σ. εκτός από την εκλογή Προέδρου (P. Séco e Pinto) και την παρουσίαση των δραστηριοτήτων των Τεχνικών Επιτροπών, ελήφθη απόφαση για τη δημιουργία Ομοσπονδίας Διεθνών Γεω-Τεχνικών Ενώσεων (Federation of International Geo-Engineering Societies – FIGS) με συμμετοχή των ISSMGE, ISRM και IAEG.

## 15.2 Γενική Συνέλευση ISSMGE (Brisbane Αυστραλίας, Οκτ. 2007)

Η Συνέλευση έγινε στο Brisbane της Αυστραλίας στα πλαίσια του 10<sup>th</sup> Australia – New Zealand Conference on Geomechanics, 21 ÷ 24 Οκτωβρίου 2007.

Η ΕΕΕΕΓΜ δεν εκπροσωπήθηκε, αλλά εξουσιοδότησε τον Αντιπρόεδρο για την Ευρώπη (R. Frank) να δώσει εκ μέρους της θετική ψήφο για τη σύσταση της Ομοσπονδίας Διεθνών Γεω-Τεχνικών Ενώσεων (Federation of International Geotechnical Engineering Societies – FIGS) όπου οι τρεις διεθνείς ενώσεις (ISSMGE, ISRM και IAEG) διατηρούν την αυτονομία τους, αλλά συνεργάζονται σε κοινές δράσεις, συνιστώντας Κοινές Τεχνικές Επιτροπές (Joint Technical Committees) για διάφορα θέματα.

## 15.3 Συμμετοχή σε Τεχνικές Επιτροπές της Διεθνούς Ένωσης

Σημαντική υπήρξε η συμμετοχή μελών μας στις Τεχνικές Επιτροπές (Technical Committees) της ISSMGE:

TC 3	Geotechnics of Pavements Α. Λοΐζος (core member)
TC 4	Earthquake Geotechnical Engineering & Associated Problems Κ. Πιπιλάκης (core member) Γ. Γκαζέτας Γ. Μπουκοβάλας
TC 5	Environmental Geotechnics Μ. Πανταζίδου Δ. Κούμουλους
TC 17	Ground Improvement Α. Πλατής
TC 18	Deep Foundations Α. Κωμοδρόμος
TC 28	Underground construction in Soft Ground Conditions Π. Βέττας Σ. Σχινά
TC 33	Geotechnics of Soil Erosion Μ. Σακελλαρίου
TC 34	Prediction Methods in Large Strain Geomechanics Ι. Βαρδουλάκης (core member)
ERTC 12	Implementation of Eurocode 8 Κ. Πιπιλάκης Γ. Γκαζέτας Γ. Μπουκοβάλας Μ. Παχάκης (για τη συμβατότητα με τον EC-7)

Οι Κοινές Τεχνικές Επιτροπές (JTCs) της FIGS, στις οποίες έχουν επίσης δηλώσει συμμετοχή μέλη μας δεν έχουν ενεργοποιηθεί.

Με απόφαση του Προέδρου της ISSMGE επανενεργοποιήθηκε πρόσφατα η TC 19 (Preservation of Monuments and Historic Sites), στην οποία συμμετέχουν τα μέλη μας:

Χ. Τσατσανίφους (Chairman)  
Π. Ψαρρόπουλος (Secretary)  
Κ. Πιπιλάκης (core member)  
Ε. Χιώτης

Η ΕΕΕΕΓΜ είναι η υπεύθυνη εθνική ένωση της ISSMGE για τη δραστηριότητα της επιτροπής αυτής.

## 15.4 Επαφές με Αξιωματούχους της ISSMGE

Υπήρξαν συναντήσεις και φιλοξενία (γεύμα) του Προέδρου της ISSMGE (P. Sêco e Pinto) και του Αντιπροέδρου για την Ευρώπη (R. Frank) τόσο στην Αθήνα όσο και στη Μαδρίτη στα πλαίσια της διεκδίκησης της διοργάνωσης του 15<sup>ου</sup> ES-MGE.

## 16. ΕΥΡΩΚΩΔΙΚΑΣ 7

Ολοκληρώθηκε η μετάφραση του Ευρωκώδικα 7 (Γεωτεχνικός Σχεδιασμός – Μέρος 1: Γενικοί Κανόνες) και η σύνταξη του Εθνικού Προσαρτήματος για την Ελλάδα από ομάδα εργασίας αποτελούμενη από τους Α. Αναγνωστόπουλο, Μ. Καββαδά, Κ. Κωνσταντινίδου, Η. Μιχάλη, Β. Παπαδόπουλο και Μ. Παχάκη. Τα σχετικά κείμενα υποβλήθηκαν ήδη στον ΟΑΣΠ (που ενεργεί για λογαριασμό του ΥΠΕΧΩΔΕ) για τα περαιτέρω.

Επίσης προχωρεί η μετάφραση και του 2<sup>ου</sup> Μέρους (ENV 1997-2) που αφορά το σχεδιασμό με βάση τις επιτόπου και εργαστηριακές δοκιμές.

## 17. ΤΡΑΠΕΖΑ ΕΔΑΦΟΤΕΧΝΙΚΩΝ ΔΕΔΟΜΕΝΩΝ

Τα μέλη της Ε.Ε. της ΕΕΕΕΓΜ μαζί με μέλη της Επιστημονικής Επιτροπής Ειδικότητας Πολιτικών Μηχανικών και της Ειδικής Επιστημονικής Επιτροπής Εδαφομηχανικής και Θεμελιώσεων του ΤΕΕ, υπό μορφή άτυπης επιτροπής, έλαβαν μέρος σε συνεδριάσεις στο Τεχνικό Επιμελητήριο, με σκοπό τη διατύπωση και προώθηση προς την Πολιτεία πρότασης για την ίδρυση Ελληνικής Τράπεζας Εδαφοτεχνικών Δεδομένων. Η πρωτοβουλία προήλθε από τον ομότιμο καθηγητή ΕΜΠ κ. Θ. Τάσιο, ο οποίος συμμετείχε στις συνεδριάσεις. Συγκροτήθηκε ολιγομελής ομάδα εργασίας για τη μελέτη του θέματος και διατύπωση συγκεκριμένων προτάσεων προς την άτυπη επιτροπή.

## 18. ΕΚΔΟΣΕΙΣ

- Άρχισε και συνεχίζεται, με επιμέλεια του Αντιπροέδρου Χ. Τσατσανίφους, η έκδοση του ενημερωτικού δελτίου «ΤΑ ΝΕΑ ΤΗΣ ΕΕΕΕΓΜ». Μέσα στην εξεταζόμενη περίοδο εκδόθηκαν δέκα τρία (13) τεύχη (αρ. 1 έως 13) εκ των οποίων τα τρία (3, 8 και 9) σε πολυτελή έκδοση. Το τεύχος 9 εκδόθηκε στην αγγλική και διανεμήθηκε στις ευρωπαϊκές γεωτεχνικές ενώσεις με το φάκελο διεκδίκησης του 15<sup>ου</sup> Πανευρωπαϊκού Συνεδρίου.
- Συγκεντρώθηκαν τα γραπτά κείμενα των προσκεκλημένων και ειδικών ομιλιών, καθώς και των χαιρετισμών του 5<sup>ου</sup> Πανελληνίου Συνεδρίου Γεωτεχνικής (Ξάνθη, 2006) με φροντίδα του Προέδρου και του συναδέλφου Γ. Ντουινιά και έπειτα από κάποια στοιχειώδη εκδοτική επεξεργασία εκδόθηκε μέσω του ΤΕΕ ο 4<sup>ος</sup> Τόμος των Πρακτικών (διατίθεται δωρεάν στους συμμετέσχοντες από το Γραφείο Διεθνών Σχέσεων και Συνεδρίων του ΤΕΕ).

## 19. ΙΣΤΟΣΕΛΙΔΑ

Στα πλαίσια της διοργάνωσης του 15<sup>ου</sup> Πανευρωπαϊκού συνεδρίου θα δημιουργηθεί μέσω του γραφείου διοργάνωσης ιστοσελίδα του Συνεδρίου, η οποία στη συνέχεια θα παραμείνει ως ιστοσελίδα της ΕΕΕΕΓΜ.

## 20. ΠΡΟΣΕΧΕΙΣ ΕΚΔΗΛΩΣΕΙΣ

Υπάρχουν σχετικές ανακοινώσεις στα «ΝΕΑ ΤΗΣ ΕΕΕΕΓΜ» τεύχος 13.

- Έχουν αρχίσει ήδη συνεννοήσεις με το ΤΕΕ για τη διοργάνωση του 6<sup>ου</sup> Πανελληνίου Συνεδρίου Γεωτεχνικής και Γεωπεριβαλλοντικής Μηχανικής το 2010. Υπάρχει πρόταση να διεξαχθεί στην Κύπρο. Εκκρεμεί σχετική απόφαση της Δ.Ε. του ΤΕΕ για τον ορισμό Οργανωτικής



## Contribution of geotechnical engineering in the rehabilitation of buildings and infrastructures

General Report  
Main Session 4 "Rehabilitation of buildings and infrastructures in urban areas"  
XIV European Conference on Soil Mechanics and Geotechnical Engineering"

Christos Tsatsanifos  
Managing Director  
PANGAEA CONSULTING ENGINEERS LTD, Athens, Greece

### ABSTRACT

The infrastructure of a country is the valuable asset which ensures its social and economic growth. However, ageing effects, operational reasons, changes in codes and standards of safety, inadequate past design practices and construction imperfections, natural disasters and war acts, as well as the recent tendency to reuse abandoned infrastructures impose their rehabilitation. In this paper examples of the contribution of geotechnical engineering for the rehabilitation of infrastructures, mainly in urban environment, are shown.

### 1 INTRODUCTION

"The quality of a nation's infrastructure is a critical index of its economic vitality. Reliable transportation, clean water, and safe disposal of wastes are basic elements of civilized society and a productive economy. Their absence or failure introduces an intolerable dimension of risk and hardship to everyday life, and a major obstacle to growth and competitiveness ... The infrastructure must rank high among our priorities. We must ensure that our highways and subways can move us swiftly and safely; that our homes, farms, and industries are supplied with ample clean water; that we reduce and safely dispose of the increasing volume of poisonous wastes our society generates; and that we provide the structural underpinning for a robust and competitive economy" (National Council on Public Works Improvement, 1988).

In 1889, 2,209 lives were lost when the South Fork Dam failed above Johnstown, Pennsylvania. The 1928 St. Francis Dam failure killed 450 persons. During the 1970s, the failures of the Buffalo Creek Dam in West Virginia, Teton Dam in Idaho and the Toccoa Falls Dam in Georgia collectively cost 175 lives and more than \$1 billion in losses. Seven people were killed in Kauai, Hawaii on March 2006 when an earth dam failed, unleashing nearly 300 million gallons of water, smashing down trees and sweeping away homes. The failures of Silver Lake Dam in Michigan in 2003 (\$100 million in damages and economic losses of \$1 million per day) and the Big Bay Lake Dam in Mississippi in March 2004 (100 homes destroyed) are current reminders of the potential consequences of unsafe dams.

At 9:15 am on Friday, October 21, 1966 a waste tip slid down a mountainside into the mining village of Aberfan, near Merthyr Tydfil in South Wales. It first destroyed a farm cottage in its path, killing all the occupants. The slide engulfed the Pantglas Junior School, just below (Figure 1), and about 20 houses in the village before coming to rest. 144 people died in the Aberfan disaster: 116 of them were school children.

A massive landslide occurred in the Las Colinas neighbourhood of Santa Tecla, El Salvador, Central America as a result of the  $M = 7.6$  earthquake of January 13, 2001. The landslide buried many houses in the neighbourhood under

tons of earth (Figure 2), leaving as many as 1,200 people dead.



Figure 1. The Pantglas Junior School, Aberfan, South Wales engulfed by the debris of the flowslide.



Figure 2. Oblique aerial view of landslide that buried Colonia Las Colinas, El Salvador.

A clogged sewer line caused a sink hole in Portland, Oregon, USA on December 2006, which swallowed a truck – which had been sent to clean the sewer. Natural gas and water lines were also ruptured in the accident. A similar accident happened in Guatemala City, Guatemala on 22<sup>nd</sup> February 2007. A hole of 30.5 m diameter and 49 m depth opened (Figure 3) swallowing five houses and killing 3 persons. The accident was the result of the leakage of a deep buried sewer pipe in tuffs (pyroclastic deposits).

A 120-ton concrete beam collapsed onto Interstate 70 in Washington County, Pennsylvania, USA, barely missing passing motorists on December 2005, while recently (2<sup>nd</sup> August 2007) the catastrophic collapse of the I-35W highway bridge over the Mississippi river in Minneapolis, Minnesota, USA, left 5 dead persons and 111 injured (Figure 4).

The above examples of infrastructures failures show clearly the need for rehabilitating ageing and imperfect structures.

Furthermore, the redevelopment and reconstruction of urban areas are essential to ensure economic development. Since the abandonment of an engineering structure, approaches to geotechnical design methods have changed. This, combined with added client requirements and changes to loadings (especially those of the earthquakes, which are of prime interest for earthquake prone countries), is another strong reason for rehabilitating infrastructures.



Figure 3. Leakage of a sewer pipe created a hole of 30.5 m diameter and 49 m depth in Guatemala City.



Figure 4. Aerial view of the collapsed bridge in Minneapolis (2<sup>nd</sup> August 2007).

Rehabilitation of old structures, particularly in urban areas, often means considering existing foundations, bridges and earthworks for reuse, and it is important to understand the impact of these old structures will have on modern geotechnical design. Existing foundations might perform satisfactorily under new loads, even though they are decades old. However, they may not satisfy current regulations.

It is common practice that in order to provide safe continuing service, engineering structures require ongoing maintenance, monitoring, and frequent inspections, to assure their safety. Moreover, based on the aforementioned examples, after some years in use, their safety is assured by their rehabilitation, which is required because of:

- Ageing
- Operational reasons (increasing demands)
- Changes in codes and standards of safety (predicted increase in extreme events)
- Inadequate past design practices and construction imperfections
- Natural disasters (earthquakes, tsunamis, hurricanes-typhoons, landslides etc.)
- War acts

The "rehabilitation" of ancient monuments could be classified in the first case, however not with the meaning that all the monuments would be again usable – habitable, but that they will be restored to a certain level which is showing off the monument and safeguarding it and its visitors.

In the latter two cases the rehabilitation required could be as large as of the scale of a city, like rehabilitation of Bam City in Iran, after the devastating earthquake of 26<sup>th</sup> December 2003, and rehabilitation of Banda Aceh in Indonesia, after the catastrophic tsunami of 26<sup>th</sup> December 2004, or of the scale of a whole country, like rehabilitation – reconstruction of Iraq in order to improve and repair the infrastructure of the country in the aftermath of the 2003 invasion.

In this paper examples of the contribution of geo-technical engineering for the rehabilitation of infrastructures will be shown, some from the authors' experience, some from the literature.

## 2 GEOTECHNICAL INVESTIGATIONS FOR THE REHABILITATION OF INFRASTRUCTURES

The practical implications of good ground condition knowledge are obvious. It can save millions of euros through informed decisions about remedial works.

Ground investigation on rehabilitation sites often means considering existing foundations, resulting in too congested ground. Investigations may involve some form of drilling adjacent to, or through, existing foundations. Poulos (2005) mentions that both forms of drilling in pile foundations may have deleterious effects on the piles being investigated. The drilling of holes adjacent to piles will generally cause vertical and lateral ground movements and these will act upon the nearby piles, inducing additional stresses and movements. These effects may be particularly severe if the ground is highly stressed. Coring through the pile itself may cause loosening or even piping of the soil beneath the pile toe when "breakthrough" is achieved and the underlying soil is soft or loose. Also, SPT testing of the soil below the pile base may cause further disturbance if it is not carried out carefully, and the SPT rods are withdrawn too quickly, thus causing suction within the soil surrounding the hole. Thus the investigation process itself may help to accentuate the problem being investigated.

Rehabilitation projects such as these are likely to see a raft of sophisticated testing techniques coming into more general use. These include the continued evolution of smarter in-situ tests, such as the use of driven pressure meters and falling weight deflectometers obtaining stiffness parameters at shallow depths, as well as other geophysical equipment as the ground penetrating radar.

In the process of the rehabilitation of the Church of Saint Peter of the Dominicans (Agios Petros Dominicanon), at Iraklion, Crete (14<sup>th</sup>-15<sup>th</sup> century building), the foundation conditions of the church were investigated in order to give reasoning to the differential settlements and the consecutive cracks, which have appeared in the monument. The

investigations consisted of three boreholes, with SPT tests on site and laboratory tests, later on, for the definition of the foundation conditions and a detailed geophysical investigation, involving seismic / acoustic tomography, for defining the details of the foundation bodies of the structure. The results of the geophysical investigation revealed that the foundation bodies of the church are resting on the bedrock, however there are some sections of the walls where either there is no foundation body, or the foundation body is resting on top of soft deposits (see Figure 5).

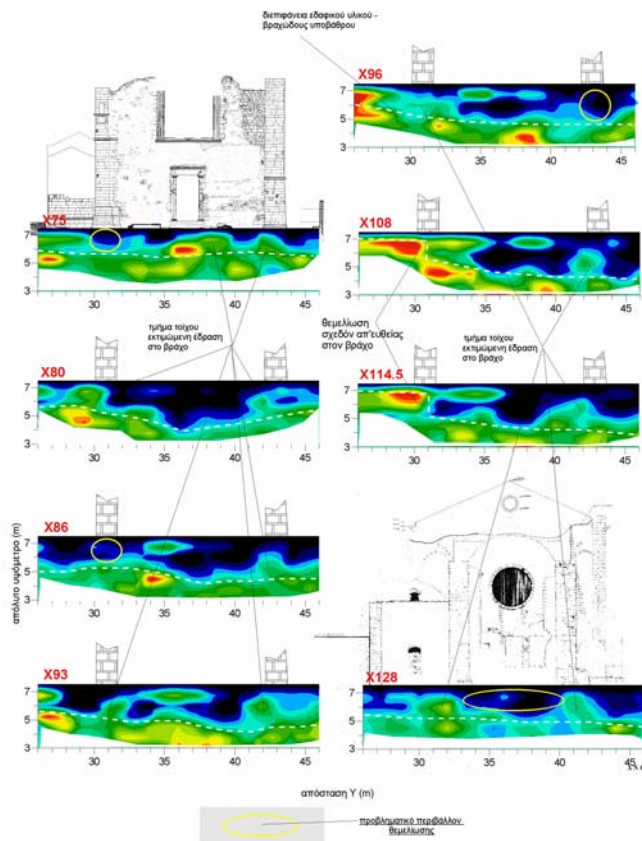


Figure 5. Vertical sections along the longitudinal axis of the Saint Peter of the Dominicans Church (Polymenakos & Tzatsanifos, 2003).

### 3 REHABILITATION OF BUILDINGS

The rehabilitation of buildings, from the geotechnical engineering point of view, refers, in the most cases, to the rehabilitation of their foundations. The main reasons for which this rehabilitation is required are either the uneven settlements, which the buildings may have presented, or the low bearing capacity of the foundations, compared to the loads which will be applied.

According to Poulos (2005), the methods for correcting the uneven settlements of buildings' foundations can be divided broadly into two categories:

- i. "Hard" methods, which rely on the application of some form of direct force to the building, like:
  - Application of force by anchor stressing
  - Application of additional loading
  - Cutting of piles, in the case of deep foundations
  - Jetting of the soil beneath the pile tips
  - Jacking of the foundation on the "low" side
  - Fracture grouting

- ii. "Soft" methods, which rely on processes which produce corrective foundation movements by inducing appropriate ground movements, like:
  - Soil extraction
  - Dewatering
  - Compensation grouting
  - Removal of soil support

On the other hand, among the options that may be considered for foundation enhancement works are:

- i. Repair of the existing foundations which contain imperfections or defects.
- ii. Strengthening of the existing foundation by its extension or addition of new footings and shear beams connecting the footings in order to strengthen and / or stiffen the existing foundation and increase the foundation bearing area.
- iii. Underpinning of the foundation by means of oscillated piles or by means of bored piles constructed through the body of the foundation.
- iv. In case of pile foundations extension of the pile caps or rafts to provide additional bearing capacity and stiffness.
- v. Increase of the footing level of the foundation.
- vi. Subsoil improvement (cementation, silication, chemical and electro - chemical strengthening, high pressure grouting capable of stabilising the soil mass, deep soil mixing, etc.).
- vii. Provision of a slab underneath the building or a box - type foundation in the underground area of the building.
- viii. In order to protect existing buildings from the uneven settlements induced by excavations or construction of new buildings in their neighbourhood, isolation or separation trenches can be constructed between the two structures

The most famous example of the contribution of geotechnical engineering in the rehabilitation of a building is that of the Leaning Tower of Pisa, where the soil extraction method has been applied. The tower is founded on weak, highly compressible soils and its inclination has been increasing inexorably over the years to the point at which it was about to reach leaning instability (about 5.5 degrees to the vertical - see Fig. 6 from Burland et al., 2003).

Any disturbance to the ground beneath the south side of the foundation was very dangerous; therefore the use of conventional geotechnical approaches at the south side, such as underpinning, grouting etc., involved unacceptable risk. Since the internationally accepted conventions for the conservation and preservation of monuments and historic sites provided that any intrusive intervention on the Tower had to be kept to an absolute minimum, permanent stabilisation schemes involving propping or visible support were unacceptable and in any case could have triggered the collapse of the fragile masonry. After a careful consideration of a number of possible approaches, the International Committee for the Safeguard and Stabilisation of the Tower of Pisa, appointed by the Italian Government, adopted a controlled removal of small volumes of soil from beneath the north side of the tower foundation (underexcavation - see Figures 7 and 8). This technique provided an ultra soft method of increasing the stability of the tower, which is completely consistent with the requirement of architectural conservation.

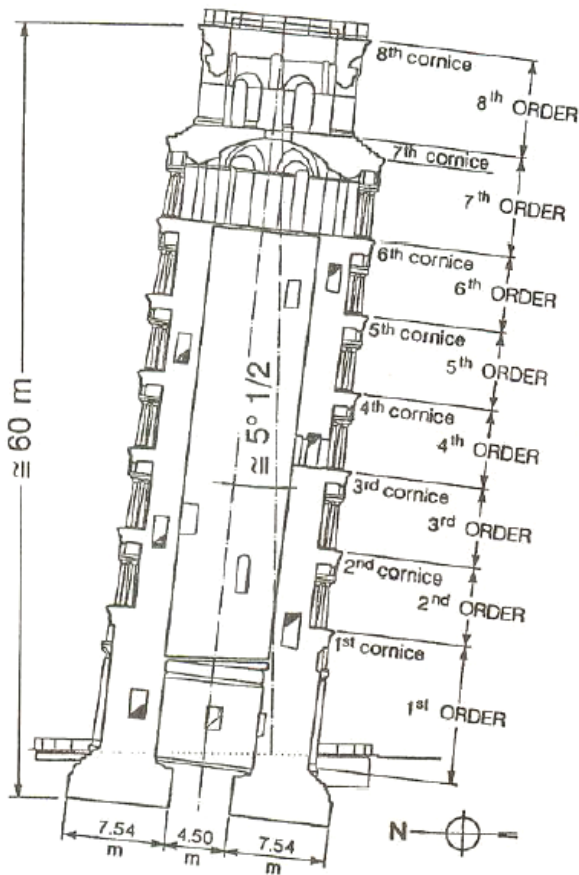


Figure 6. Cross section of the Leaning Tower of Pisa

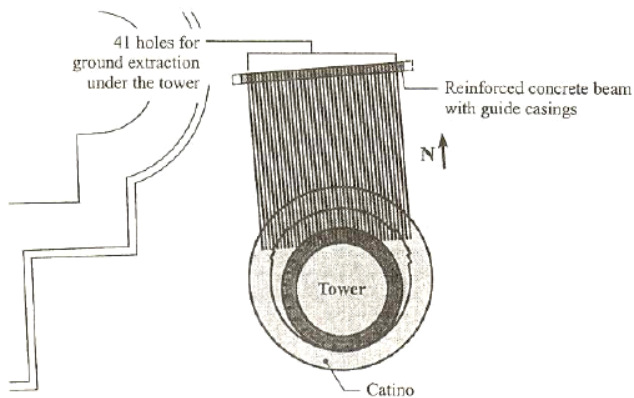


Figure 7. Pisa Tower. Holes for full ground extraction (Burland et al. 2003).

Different physical and numerical models have been employed to predict the effects of soil removal on the stability. The preliminary underexcavation intervention, only undertaken once the Commission was satisfied by comprehensive numerical and physical modelling together with a large scale trial, has demonstrated that the tower responds very positively to soil extraction. The final underexcavation has attained the target of reducing the tilt of the tower by half a degree, i.e. to bring the tower "back to future" to the time just before the excavation of the catino in 1838.

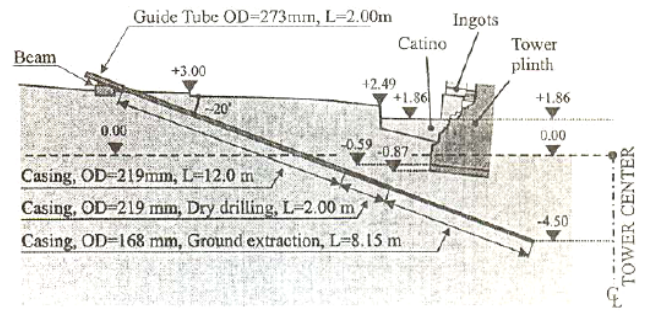


Figure 8. Pisa Tower. A hole for full ground extraction (Burland et al. 2003).

The technique of soil extraction has been used for rehabilitation of buildings longer before proposed by Terracina (1962) for Pisa. Johnston & Burland (2004) reported the application of the method as early as 1832 by James Trubshaw for the stabilization of the 15<sup>th</sup> century tower of St Chad's church in Wyburnbury, South Cheshire. Barends (2002) gives a full contemporary account of the stabilization of a leaning church tower at Nijland by means of soil extraction in 1866. In the same year it has come to light that the method of soil extraction was also used to straighten a 100 m high chimney at the Bochum Cast Steel Works in Germany. The report on the work was discovered in the journal the 'Zeitschif Bauwesen' published in 1867 and written by Haarman – the engineer who executed the work (see Figure 9, Johnston & Burland, 2004). Brandl (1989) has described the use of soil extraction to correct uneven settlement of piles supporting bridge piers, while the use of soil extraction has been widely used in Mexico City to reduce the differential settlement of a number of buildings due to regional subsidence and earthquake effects, before its application to the Pisa Tower (Tamez et al., 1997).

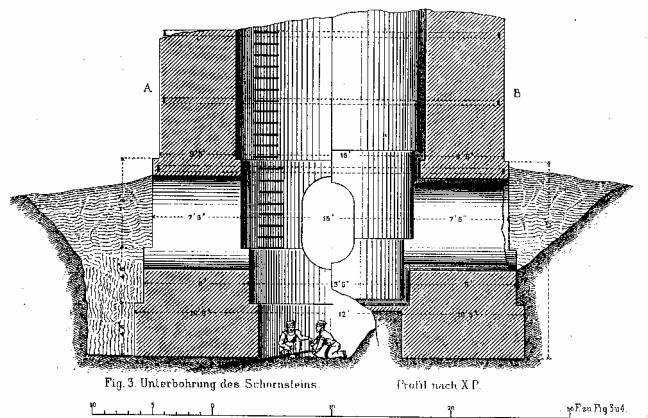


Figure 9. Vertical section at base of Bochum chimney showing the process of soil extraction (Johnston & Burland, 2004).

A similar to the soil extraction approach was proposed by Poulos et al. (2003) for the rehabilitation of buildings on piles which have undergone uneven settlements due to uneven ground conditions, or/and interaction among closely-spaced buildings, or/and faults in the foundation piling. The approach, which has been termed the "RSS" (Removal of Soil Support) method, involves the drilling of a number of boreholes on the "high side" of the building, so that restoring vertical movements will be developed within the area of the building foundation (see Fig. 10). A major advantage of the method is that it is not intrusive (i.e. it can be performed outside the building footprint) and can be controlled and adjusted via an observational approach.

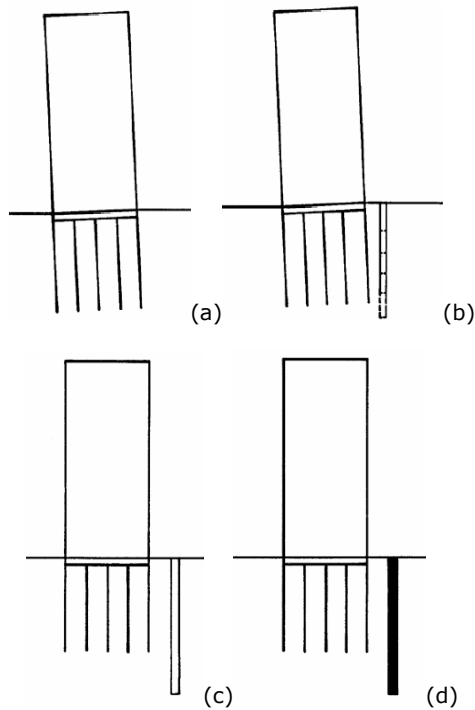


Figure 10. Principle of the RSS method: (a) Tilting of pile – supported structure (b) Progressive drilling of boreholes on the “high” side of the foundation (c) Restoration of structure tilt (d) Grouting of boreholes.

A very interesting example of underpinning for strengthening the foundation of a historical building was presented by Sata (2003). The AEB Bank chose a two-storied historic building for its headquarters in Budapest (see Fig. 11). The renewal, re-utilisation and enlargement of the building should follow the original architecture. An underground garage had also to be constructed, requiring the deepening of the foundation level.

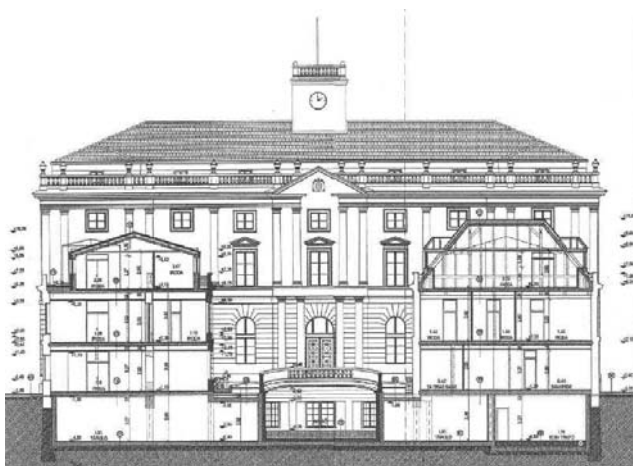


Figure 11. Architectural section of the renewed AEB Bank in Budapest.

Jet-grouting was used, and the whole intervention was executed as follows:

- i. Reinforcement of the external walls, creating a deeper definitive foundation level – by using the jet-grouting technology and CFA piling.
- ii. Creation of temporary supports for the main brick walls, by using the already mentioned jet grouting technology.
- iii. Construction of the foundation of the final supports of the brick walls.

- iv. Excavation and construction of the basement slab, construction of the final structure and removal of the temporary supports.

The loads of the internal walls were between 100 and 300 kN per meter and were transferred to the ground, temporarily, through micro piles (Figure 12).



Figure 12. The AEB Bank building “in the air”

In order to avoid any horizontal movements or / and vertical displacements of the very fragile brick-walls, jet piles were made on the two sides of the wall, and into them common steel tubes were placed. The connection between these so-called micro-pile heads and the wall is shown in Figure 13.

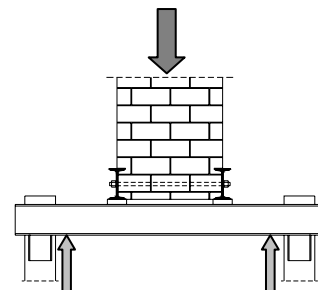


Figure 13. The connection between the micro-pile heads and the wall for the AEB Bank building.

Another very interesting case study of rehabilitation of the foundation of a building is that of the Sweden’s Parliament, the Sveriges Riksdag.

The building has been constructed on the small island of Helgeandsholmen in the centre of Stockholm, over a century ago and is founded on timber piles. Regional uplift since the Riksdag was built means that the ground surface is higher, relative to sea level, than when its piles were installed. The top 700 mm of the timber piles were exposed to the atmosphere and were beginning to rot, with considerable risk of settlement as a consequence.

Two main solutions have been considered by the Swedish Parliament. Initial plans (a solution of the problem was sought since 1980) were to underpin building with new piles. More recently efforts have focused on a novel solution which involved creating a cut-off dam downstream aiming at restoring the groundwater to the level it was when the piles were installed, re-immersing the wooden piles in the groundwater and halting their degradation.

At the Riksdag the cut-off dam runs along the north side and then cuts across in front of its main façade, creating a curved L-shape (see Figure 14) that connects to the low weir, marking the transition between the lake and the tidal Baltic Sea.

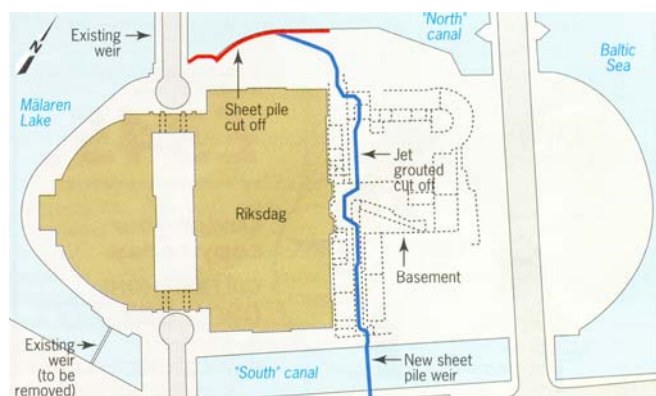


Figure 14. The cut-off dam to restore groundwater below Riksdag to the level of Lake Malaren

The dam is made up of two rows of jet grouted columns, extending from 15 m to 30 m in a sandy moraine and penetrating 150 mm into rock (European Foundations, 2004).

Madrid's Prado Museum is the largest art gallery in the world, but only has space to show a tenth of its immense collection at any one time. An expansion programme, completed in 2005, doubled the museum's capacity by constructing the spacious underground Jeronimos extension, which connects the museum's main neo-classical Villaneuva building to the existing cloister of the San Jeronimos church.

The most geotechnically demanding component of the project has been to create a 20 m deep, 46 m by 20 m hole beside these historic buildings and adjacent roads.

The ground movements were controlled with the novel use of 34 integrated hydraulic jacks that in effect reacted and pushed back the retaining walls as they started to move. The excavation was built top-down and jacks were installed to connect the two new "floating floors" to the retaining walls, incorporating a system which measured movement in the wall caused by the load of the surrounding buildings and traffic (see Figure 15).

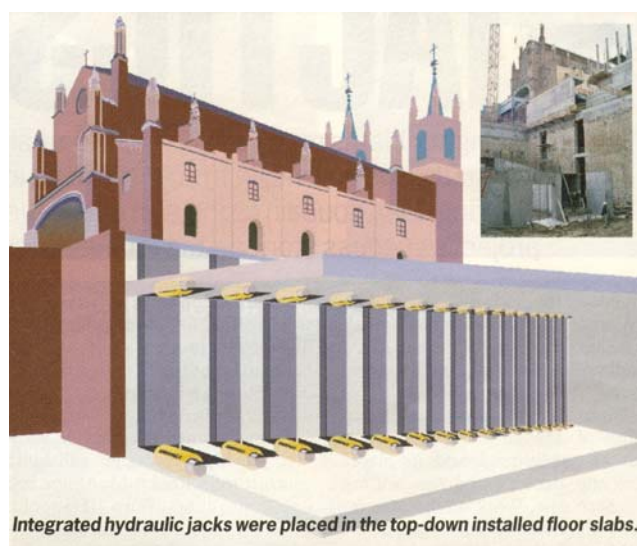


Figure 15. The retaining system for the construction of the Prado Museum's underground extension

At each of the two floor levels, separated vertically by 8 m, 17 double-acting 500 t capacity jacks were installed, each with 100 mm stroke. Individual jacks were equipped with a positioning sensor to measure movement and a tilting swivel saddle to compensate for side load caused by non-centred loads (European Foundations, 2004).

As mentioned before, in rehabilitating old structures one should consider the existing foundations, and the impact of these old structures will have on modern geotechnical design. Existing foundations might perform satisfactorily under new loads, even though they are decades old. The research project "Re-use of Foundations on Urban Sites" (RuFUS), financed by the 5<sup>th</sup> European Commission Framework, has aimed at providing ways to overcome the barriers, both technical and non-technical, to the reuse of foundations for sustainable development. The outcome of the project was presented and discussed at the RuFUS Conference (19-20 October 2006) and published at the conference proceedings as well as in A Best Practice Handbook.



Figure 16. The RuFUS rosette.

Finally, rehabilitation of buildings in urban environments could create damages to adjacent structures. Following a spell of wet weather in February 2006, several residential properties in Burgess Hill, West Sussex, experienced foul flooding. Initially it was believed that the cause was a simple blocked sewer. However, detailed survey identified that part of the downstream sewer pipe, located 100 m from the area of foul flooding, had been damaged during the installation of pile foundations for a small house extension. The piles had breached the sewer pipe, located 7 m below ground surface, resulting in the 450 mm diameter sewer pipe being filled with 6 m of structural concrete.

The only solution with minimal disruption to the properties and at a low cost was an in situ repair of the damaged sewer. The solution involved sinking a 7.5 m deep mine shaft, from which a tunnel was driven. Steel sheeting was used for retaining the wall of the 3 m<sup>2</sup> shaft. The ground was made up of stiff clay to a depth of 5 m and mudstone to 8 m. Once the tunnelers reached the sewer pipe, the heading was driven in both directions, breaking out the damaged pipe. The erroneous pile foundation was then trimmed back and supported with a steel bridge that diverted its point load to below the invert of the sewer. After removing the blockage, the sewer was structurally realigned, increasing its lifespan by at least 50 years. The excavation was then backfilled with concrete (Ground Engineering, 2007).

#### 4 REHABILITATION OF ROADS AND RAILWAYS

The continuous increase of traffic volume, as well as of the loads of the vehicles using roads and railways and the freight loadings themselves impose the need for their rehabilitation, mainly of the sub-grade – sub-base – pavement system.

Pavement rehabilitation problems may be enormously varied and range from the addition of rejuvenating surface treatment coats and simple overlays to total reconstruction. Rehabilitation due to normal traffic growth is usually solved by the use of overlays, whereas reconstruction work is necessary for pavements showing incipient failure (Rodriguez et al., 1988).

Establishing a criterion for rehabilitation is strictly a matter of reviewing the circumstances responsible for the unsatisfactory performance of the pavement. It is far more complicated than simply observing the appearance of superficial cracks. *Unsatisfactory* rarely is the result of a catastrophic failure. Rehabilitation may prove necessary in a pavement that is appropriately supporting very high volumes and loads of traffic, but for which maintenance costs are excessively high. The following are the principle criteria that are usually considered when determining the need for rehabilitation (Highway Research Board, 1972):

- i. Level of serviceability, estimated, usually, on the basis of the opinion of a group of users.
- ii. Structural condition, i.e. the capacity of the pavement to support current traffic loads and to continue to do so in the near future without progressive damage.
- iii. Surface condition (irregularities, waves, ruts, and cracks, not necessarily associated with structural capacity).
- iv. Safety usually assessed on the basis of accident statistics.
- v. Cost, referring not only to the expenditure required for rehabilitation, but also to continuing maintenance and operational costs.

On top of these some less tangible factors, as the anticipated increase in traffic volume and vehicle loads to which the pavement will be subjected, the cost of rehabilitation work and the availability of funds for its execution, the service life anticipated or desired for the rehabilitation work and the cost of the pavement maintenance, must be considered.

The usual pavement reinforcement consists of an overlay of asphaltic concrete or a combination of asphalt concrete and layers of a granular material that can be stabilised or treated with asphalt, cement or lime. Geosynthetics can also be used.

## 5 REHABILITATION OF SLOPES

The Egnatia Odos project comprises the construction of a 680 km motorway from the port of Igoumenitsa, at the NW coast of Greece, through Macedonia and Thrace, to Alexandroupolis, a city situated near the border with Turkey. A big part of the motorway "cuts" through the mountains of Pindus and its "wild flysch" formations (melange type formations consisting of fractured siltstones with sandstone, limestone and clayey schist fragments, of variable size, in a siltstone matrix), resulted from the thrust of the Pindus geotectonic zone over the Ionian zone (Tsatsanifos & Pandis, 2005).

Near the village of Anthochori and the town of Metsovo the alignment of the motorway called for the construction of a 190 m long embankment. The geomorphology of the greater area as well as the "geological history" of that region of Greece, which is well known for frequent natural slope failures, were showing up the existence of old landslides, but were not taken into consideration when firstly designing the embankment. The first indications of the reactivation of an old landslide were revealed in the form of embankment settlement and culverts' cracking, in an early phase of the project (1994). The works stopped at that

time, due to change in the alignment of the highway, and restarted in 2000, when the temporary placement of excavation materials from a nearby cut reactivated again the pre-existing landslide. Well defined cracks started showing on the ground surface "shortly" after the excavation material from the cut was placed. These cracks kept on propagating, quite rapidly, upslope at a point at which the boundaries of the whole landslide could be clearly identified.

Detailed geological and geotechnical investigations were carried out in order to define the geometry of the slip surface and the geomechanical properties of the soil layers above, below and along the slip surface itself. The geotechnical investigation program was carried out, in a step-by-step approach following evaluation of all data available as being acquired.

The sliding mass geomaterial comprised of "completely to highly weathered siltstone" and "old landslide debris", in the form of low plasticity clay with sandstone – siltstone gravels, underlain by "moderately sheared" siltstone. The bedrock is in form of slightly sheared siltstone and fractured sandstone.

The inclinometer measurements revealed that the failure surface develops between the "highly weathered" and the "moderately sheared" siltstone at a depth ranging from 20 m to 28 m, approximately, with a rate of movement ranging between  $7.9 \times 10^{-5}$  mm/min and  $6.3 \times 10^{-4}$  mm/min (see Figure 17).

Back analyses yielded a factor of safety equal to  $FS = 1.114$ , well above 1.00, meaning that the placement of the excavations' materials was adding to the stability of the slope! The picture changed when excess pore water pressures were considered to have been developed within the low permeability clay formations underlying the fill area.

Back analyses yielded a factor of safety equal to  $FS = 1.114$ , well above 1.00, meaning that the placement of the excavations' materials was adding to the stability of the slope! The picture changed when excess pore water pressures were considered to have been developed within the low permeability clay formations underlying the fill area.

It was found that the rapid ("undrained") placement of the excavation material and a raise in excess pore water pressures of the order of 70% ( $\bar{A} = 0.70$ ) of the total fill weight, along the part of the failure surface underlying the area where fill material had been placed, was sufficient to reinitiate the slide ( $FS = 0.993$ )(Tsatsanifos et al., 2006).

The stabilization measures selected comprised the construction of a berm at the toe of the landslide - a large retaining structure constructed by gabions along the bank of the Metsovitikos River - combined with a net of drainage ditches behind the embankment and a drainage blanket under the embankment. Also, on two ravine beds, passing through the area of the landslide, Armco tubes, able to accept differential settlements without being cracked, were placed under the stabilization fill. Finally, the slopes of the toe weight were vegetated for preventing their erosion. Figure 18 shows a general view of the landslide area after the construction of the embankment and of the remedial measures.

## 6 REHABILITATION OF RETAINING STRUCTURES

In 2003, a condition assessment of the retaining wall at Gibbon Falls, Yellowstone National Park, USA, established that it was losing its foundation and was in danger of failing. In addition to conducting a further investigation to better understand the condition of the wall and failure mechanism, it was decided to conduct a pilot micropile program. A micropile was drilled through the face rock of the stone masonry wall, which added strength and ductility to the

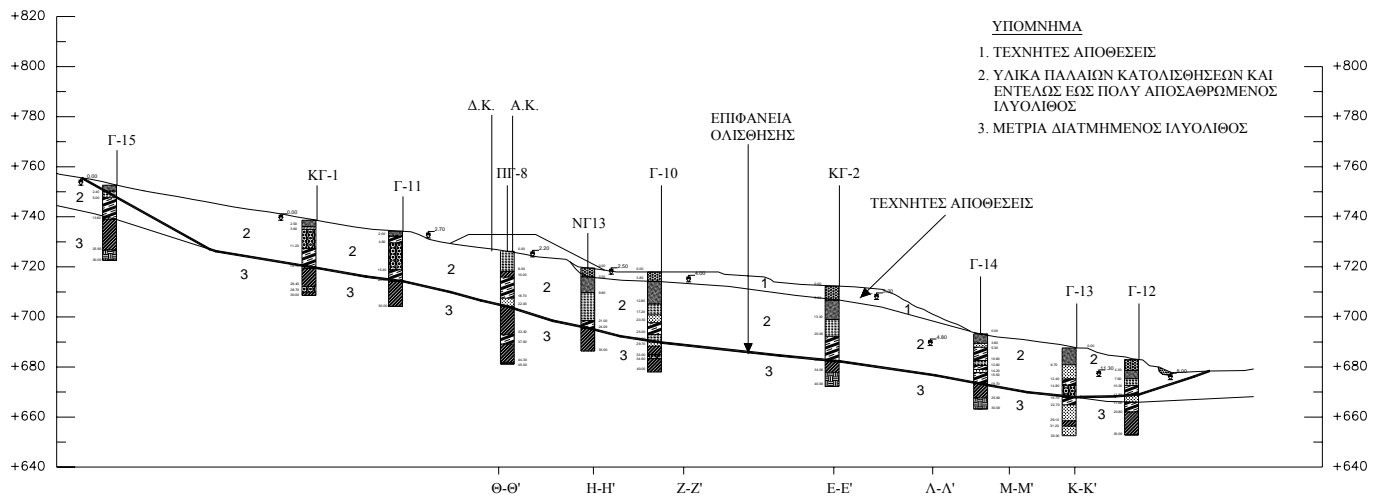


Figure 17. Slope section of the Anthochori Landslide with the assumed failure surface and the applied external loadings.



Figure 18. The Anthochori Embankment on the Landslide Area after the Construction of the Remedial Measures.

wall, and also provided underpinning several meters into the wall foundation. The layer of “face rock” averaged 430 mm wide, with the narrowest measured point measuring approximately 300 mm. The mortar condition in the wall was unknown, yet anticipated to be highly variable. The contractor had to comply with several restrictions: no new grout could be visible, drill rods could not come through the outer wall face, the casing and bar could not be visible after completion, and the drill could not sit on, push against, or vibrate the wall during drilling.

The contractor drilled the micropile on the same batter as the wall face using high rotational speed (1,000 rpm), and low down pressure to help maintain the batter (Figure 19). Drilling progressed without problems through the 8.5 m wall, through 5 m of gravel and cobbles, and through 3 m of highly to moderately weathered rhyolitic tuff. Casing was installed and a 25 mm threadbar was grouted into the hole through perforations in the casing below the toe of the wall, under 3 MPa of pressure. When the work was completed, there were no visible signs to indicate that any significant disturbance had occurred. The pile added reinforcement and bearing capacity and preserved the historic structure without impacting the natural resources around the wall (Barrows et al., 2005).

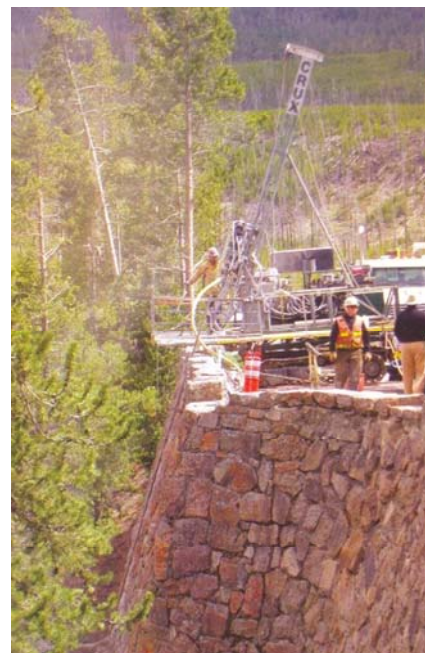


Figure 19. Micropile installation at Gibbon Falls Retaining Wall (Barrows et al., 2005).

## 7 REHABILITATION OF BRIDGES

The differential settlements, which were presented by the two central piers of a bridge over the Athens – Corinth Highway, is a classical example of required rehabilitation of a structure because of lack of geotechnical information combined with inadequate design practice (Stefanides & Tsatsanifos, 1995).

The design of the pile foundations of the bridge was based on the results of boreholes performed for a series of neighbouring structures, however at a distance of about 100 m (see Figure 20).

The pile tips reached a depth of about 10.5 m below ground surface, according to the design, where a layer of dense gravels with sand has been foreseen. However, the design did not take into account that through that area a small stream was passing, having created, through its old meanders, different subsoil conditions within short distances. Thus, while the piles at the north pier reached the gravel layer, those of the south pier did not and after 15 months from the beginning of the measurements of the settlements



Figure 20. Location of bridge with differential pier settlements and of boreholes, on which the design was based.

the south pier had settled by 83 cm compared to the settlement of 16 cm of the north pier (see Figure 21).

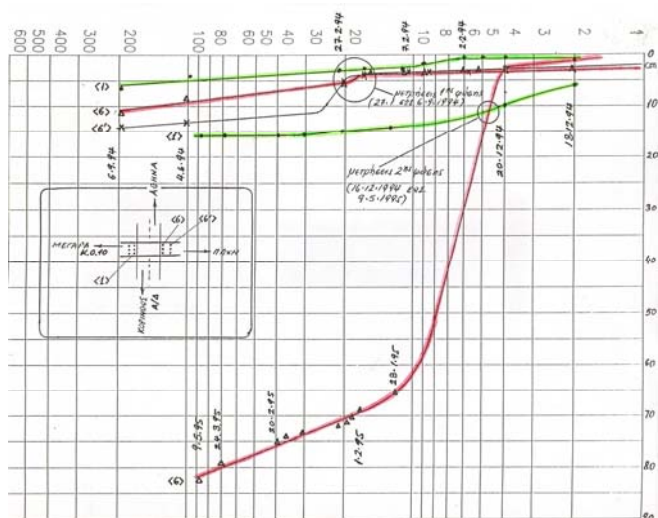


Figure 21. Settlements of the central piers of the bridge (red: south pier, green: north pier).

Five alternative methods were proposed for the rehabilitation of the bridge, taking into account that the motorway under the bridge should be in continuous use:

- i. Use of small diameter piles and reconstruction of the pile cap.
- ii. Construction of two series of small diameter piles at both sides of the pile cap and connection of them with the pile cap.
- iii. Construction of diaphragm walls at both sides of the pile cap and connection of them with the pile cap.
- iv. Extension of the pile cap and addition of new piles.

- v. Use of jet grouting to improve the soil over and beneath the pile tips.

Finally, the decision was made to apply the last method and the bridge presents no settlements since then.

Nez Perce Creek Bridge in Yellowstone National Park USA (see Figure 22) was widened in 1996 to allow for increased traffic and larger vehicles, and to comply with current safety standards. It has been determined that the stone masonry piers would not sustain the design seismic loads but it was important to retain the look of the original work. One of the steps taken to accommodate these new design loads was to add steel reinforcement to the piers to make them more ductile and self-stable, and to isolate them from the bridge deck. This technique involved placing micropiles through each pier at 1.5 m spacing, and extending those 3 m into bedrock. The deck isolation was achieved by elastomeric/steel bearing pads which allowed the pier masonry to remain untouched. The bridge abutments were widened by deconstruction of the stone masonry and constructing new concrete core walls for the additional width. To retain the same masonry look, the walls were faced with original stones as well as stones conserved from roadway excavation (Barrows et al., 2005).



Figure 22. Nez Perce Creek Bridge at the Yellowstone National Park, USA (Barrows et al., 2005).

The Million Dollar Bridge carries the Copper River Highway across the Copper River near Cordova, Alaska, approximately 240 km east of Anchorage. The 478.5 m long bridge consists of four Pratt truss spans that, from south to north, measure 122 m, 92 m, 137 m and 122 m. The bridge is supported in the river on three immense concrete piers. The structure was built in 1909 and 1910. Its name comes from its construction cost, which exceeded \$1.4 million.

In 1964 the structure was severely damaged during Alaska's "Good Friday" earthquake (March 27, M = 9.2). During the quake the southern end of span 4 separated from pier 3 and fell into the river. Span 3 shifted several feet on top of pier 3; the pier itself tilted several degrees from the vertical, and its top part sheared several feet relative to the bottom part (see Figure 23). Because of this heavy damage, the authorities closed the structure to traffic.

On March 31, 2000, the Million Dollar Bridge was added to the National Register of Historic Places, prompting officials to rehabilitate the bridge and perform a seismic retrofit to give it the ability to withstand a future earthquake.

The first major repair to the bridge involved raising the fallen span 4. This was accomplished by erecting temporary support towers upstream and downstream of the fallen span.

The other major facet of the bridge's rehabilitation involved replacing the damaged pier 3, which appears to have been

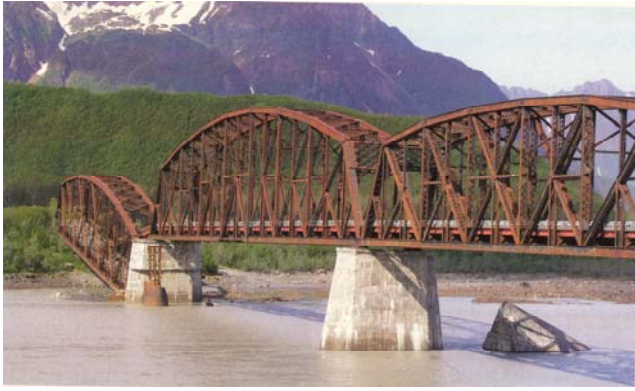


Figure 23. The Million Dollar Bridge after the Alaska's 1964 earthquake.

constructed in a zone of liquefiable river sands. Liquefaction of the sands beneath pier 3 is believed to have been the main cause of the bridge's failure during the earthquake. Such liquefaction would explain the observed 5 degree tilt of the pier and the inferred tilt of the caisson supporting it. Indeed, span 4 may have fallen off the pier because of that tilt. As the span fell, it struck the pier and broke that structure along a construction joint.

To prevent a similar problem in future earthquakes, the solution seen as most cost effective was to replace the damaged pier with a hollow pier supported on piles that would extend 46 m below the riverbed, that is, below the zone of liquefiable sands (see Figure 24). The new foundation is supported on five piles, each a 1.8 m diameter steel pipe filled with concrete.

The seismic retrofit will involve installing friction pendulum isolation bearings, as well as strengthening piers 1 and 2 (massive structures of unreinforced concrete). At these piers, bundles of three high-strength steel rods – each rod 32 mm in diameter – will be grouted into 140 mm diameter holes cored through the piers and extending into the caissons below. The rods will increase the flexural strength of the piers and prevent rocking on the caissons that might damage the friction pendulum bearings (Ingham et al., 2007).

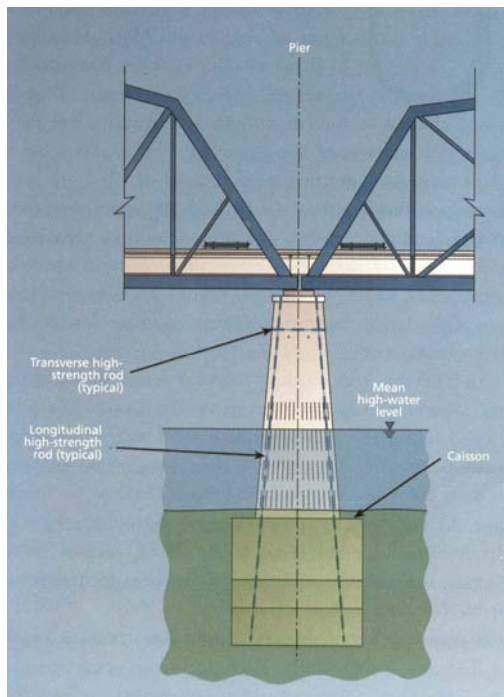


Figure 24. Pier 3 replacement at the Million Dollar Bridge, Alaska.

## 8 REHABILITATION OF TUNNELS

The 45 years old 619 m long George Massey Tunnel carries four lanes of traffic under the Fraser River to the south west of Vancouver, Canada. Built in an era when little consideration was given to seismic concerns, the tunnel is made of six 350 m long precast sections in a trench underlain by almost 600 m of loose saturated sediments.

Upgrading the tunnel is vital as it is designated lifeline structure on Vancouver's Disaster Response Route (a network of land and water transportation routes that will be open to emergency vehicles only in a post disaster situation).

Though the quality of the precast concrete was good, there was only about half the reinforcing that would be used today. This made the structure incapable of handling any relative movement produced by the new design earthquake.

Structural upgrade involved adding reinforcement to ensure that an earthquake would induce many well distributed cracks as opposed to a few large ones. The biggest challenge was finding space where to add steel. Trucks already "scrape" the ceiling so only the ceiling corners, the floors and the walls were reinforced, as well as the wind tubes and the air ducts (see Figure 25).



Figure 25. Crews prepare the main joint between tunnel sections for structural repair and strengthening of George Massey Tunnel.

Once the structural upgrades are complete the tunnel will be able to withstand the rigors of a separate contract to complete geotechnical upgrade. Earlier concerns of the tunnel floating during an earthquake resulted in rock and concrete being placed over the tunnel, which add to the challenge of underwater ground improvement. The plan is to improve by densifying a 50 ft wide strip along both sides of the tunnel (65 ft wide near the river bank) and to 30-45 ft below the mudline using stone columns or timber piles. Other measures to prevent movement include careful monitoring, and alternating the densification between both sides of the tunnel. (Jurbin, 2006).

The Tymfristos Tunnel has been constructed along the Lamia – Karpenissi (East – West) Road Axis of Central Greece. The 1,365 m long tunnel is passing through the flysch formation of the Pindos geotectonic unit, which consists, mainly, of claystones and slickensided argillaceous schists. It was designed to be excavated in two phases: top head and bench, without any provision for the distance between the top head and the bench excavation. Sprayed concrete (shotcrete), with wire mesh, steel frames and rockbolts were considered for the primary lining and a cast in place, steel reinforced, inner concrete lining.

Due to contractual problems and lack of funding the project has proceeded intermittently in three different contracts, with a halt of more than two years (from September 1995 to October 1997) between the second and third contract. During this period a 531 m long section of the top head, already excavated along the whole length of the tunnel, in an area with a rock mass of poor strength and deformation characteristics, suffered from excessive deformations, which destroyed the primary support and led to substantial closure of the opening (see Figure 26).



Figure 26. The maximum squeezing deformation of the Tymfristost Tunnel was as much as of 2 m.

In the process of rehabilitating the tunnel, a series of forth and back analyses were performed taking into account the new ground conditions. The analyses revealed that the deformation of the tunnel was due to the squeezing behaviour of the rock mass (Tsatsanifos et al., 2000) which could be tackled effectively through the "immediate" closure of the primary lining ring (Tsatsanifos, 1995). The excavation of the tunnel cross section along this part (130 m<sup>2</sup>) was subdivided into top heading, bench and invert drifts, while three support classes were specified. Shotcrete (0.30 ÷ 0.40 m thick), with two layers of T131 wire mesh, lattice girders Pantex 70/30/D30 and systematic rockbolting (13/ 14 6 ÷ 9 m fully grouted bolts at each excavation step) were used for the primary lining. The excavation step of the top heading was 1 m and the complete closure of the primary lining ring was done every 2 m.

An extensive convergence - monitoring program has been adopted, providing for measuring sections every 15 m. Furthermore, a number of convergence stations have been installed in several sections ahead of the advancing face of the excavation, which greatly contributed to the adjustment of the support measures to the anticipated rock mass conditions.

## 9 REHABILITATION OF AIRPORTS

Airport operators face growing pressure to keep traffic moving on the ground while maintaining runways, taxiways and aprons. An added complexity is the need to assess and upgrade pavements for increased loadings from bigger planes. In this case one can apply the same methods already described for the rehabilitation of highway pavements.

Figure 27 shows a location of the geotechnical investigations performed for the design of the rehabilitation of the Tanagra Airport Runway Pavement. The results of the investigations and the subsequent preliminary design revealed that it was more economic to reconstruct the whole pavement instead of rehabilitating it (Magrioti et al., 2003). The tricky think in this case was that, since Tanagra airport is a military airport in a 24 hours operation, the time allocated for the investigations was only one day, hence all the boreholes and trial pits had to be drilled / excavated and

the pavement reinstated within this one day. To tackle this problem, special materials for the local rehabilitation of the pavement were used.



Figure 27. Geotechnical investigations for the rehabilitation of Tanagra airport runway pavement.

## 10 REHABILITATION OF PORTS

The Flour Mills of Nigeria, Inc. port installations at the Apapa Bay, Lagos, Nigeria consist of a pier of 435 m length, hosting docks and several storage houses and other installations necessary for cargo handling. Docking bollards are developed along the whole length of a 210 m long gravity wall, built with reinforced concrete, and a 225 m long Larssen sheet-pile wall. The average sea depth, in front of the dock, is of the order of 9.80 m, thus limiting the ship classes the port can accommodate to those with relative small sinking depth.

The rehabilitation of the whole port installations was found to be necessary on the basis of the increasing future needs. In that context, the installations should get modified in a way that the port will become capable of docking ships of 75,000 DWT in size. In order to do so, it was imperative to increase sea depth in front of the dock from 9.80 m to 14.50 m. However, given the geotechnical conditions prevailing in the area (soft silty - clayey deposits), such an increase of the sea bottom depth without taking special retaining measures could result in severe instability problems of the existing piers, because of the loss of the passive resistance that the soil exerts on the "foot" and the embedded length of the gravity walls and the sheet piles, respectively. There was a possibility of a deep circular failure developing underneath the foundation of the gravity wall, whereas in the case of the sheet pile walls such an action could result in excessive deformations at the top of the wall and / or at its embedded part.

In order to make possible the excavation of the sea bottom, a row of bored piles, to be placed prior to the excavation, was proposed, ensuring the stability of the existing walls. These piles were constructed in front of the gravity wall, whereas in the case of the sheet pile wall the initial proposal was to place bored piles on both sides of the wall, in order to achieve alignment of the pier face. However, unsurpassed difficulties were encountered behind the sheet pile wall during the construction of the bored piles. So, in order to overcome these difficulties, an alternative was proposed consisting mainly of stabilizing the soil, behind the existing diaphragm, by "soil-grout" piles, using the Jet Grouting method.

The single bored piles wall consist of piles of 1.50 m diameter, placed at 2.52 m, distance (from centre to centre), whereas along the transitional section of the pier, where

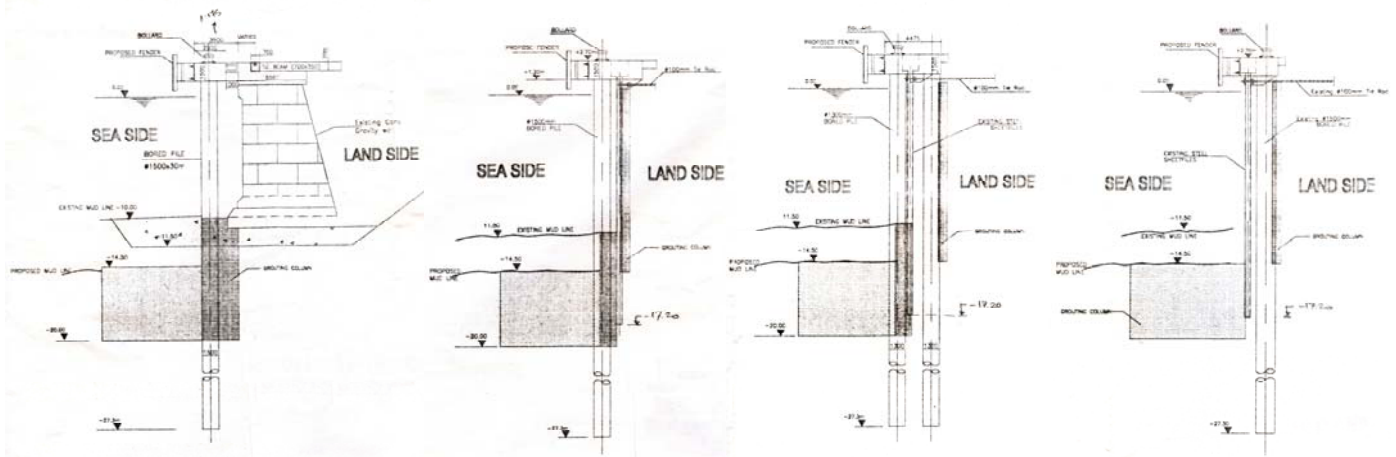


Figure 28. Different sections along the Apapa Bay, Lagos, Nigeria quay wall: (a) Gravity wall area, (b) Steel sheet-pile A area, (c) Steel sheet-pile B area, (d) Steel sheet-pile C area

two rows of bored piles wall were constructed, these have a diameter of 1.30 m, placed at 2.52 m, distance (from centre to centre). All piles reached the depth of -27.30.

In addition, a special arrangement for the pile cap was foreseen, in order to accomplish cooperation of the existing pier wall with the additional retaining measures, as well as anchoring, so that a part of the horizontal loading (caused by the waves, the wind etc.) is transferred to the ground.

According to the alternative proposal, two rows of "soil-grout" piles were constructed, behind the sheet pile wall, in contact with each other from level +1.20 (bottom side of the pile cap) down to level -22.00 (coincides with the foundation level of the external "box" of "soil-grout" piles) and a pile cap, on top of which the bollards were placed. Existing anchors were connected to the "new" pile cap as suggested in the initial proposal. Bollard load is primarily borne by the existing anchors and secondarily by shearing between the pile cap and the subsequent two rows of "soil grout" piles, which were ensured through placement of HE steel sections or steel tubes.

Behind the aforementioned two rows of piles, another group of "soil-grout" piles were placed, forming a square pattern cell, of 4.80 x 4.80 m<sup>2</sup>, from level -2.00 down to -20.00.

Finally, a row of "struts" was constructed in 4.80 m distances, consisting of three tangential bored piles each, from -10.00 down to -20.00.

A jet grouting scheme was also foreseen in order to improve soil properties in front of the pier down to -20.00 m, so that the minimum accepted value of 1.50, for the factor of safety against general failure of the "soil-pier" system, is achieved

## 11 REHABILITATION OF WATERWAYS

The Corinth Canal is a junction of international sea transport and serves ships coming from the Western Mediterranean and Adriatic en route to Eastern Mediterranean and Black Sea ports and vice versa (see Figure 28). The Corinth Canal intersects the Isthmus of Corinth and has a length of 6.343 m. The minimum width of the canal at sea level is 24.6 m and bottom width of 21 m at 8 m depth.

The ancient seafarers, in order to avoid the circumnavigation of Peloponnesus, had to transport their entire ships and precious cargo intact across land from shore to shore, sliding them on a masonry trail known by the name of Diolkos.

Since early times, a number of spirited souls entertained thoughts of constructing a canal through the Isthmus. In

602 B.C., Periander, Tyrant of Corinth and one of the Seven Sages of Antiquity, was the first man to seriously consider the possibility of opening a canal through the Isthmus. Periander is said to have given up on his plans fearing the wrath of the gods. In 307 B.C., Demetrios Poliorketes made up his mind to cut a naval passage through the Isthmus. He actually began excavations before he was talked out of continuing with it by Egyptian engineers, who predicted that the different sea levels between the Corinthian and the Saronic Gulfs would inundate Aegina and nearby islands with the sea. In Roman times Julius Caesar in 44 B.C. and Caligula, in 37 B.C. again courted with the idea. In 66 A.D., Nero reconsidered earlier plans and, a year later, he set teams of war prisoners from the Aegean islands and six thousand slave Jews to work on the canal. They dug out a ditch 3,300 m in length and 40 m wide, before Nero had to rush back to Rome to quell the Galva mutiny. The next historic personality to be associated with the canal of Corinth was Herod of Atticus. He tried, as also did the Byzantines, but to no avail. The Venetians were next in line. They commenced digging from the shore on the Corinthian Gulf but the enormity of the task made them give up overnight.

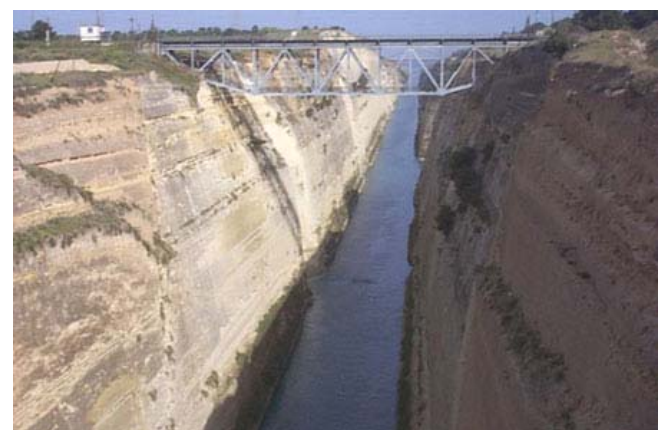


Figure 28. The Corinth Canal and its location.

In the nineteenth century, Capodistrias, the first Governor of the Hellenic State, commissioned a special study on the

canal project. The conclusions of that study made Capodistrias abandon further consideration. However, a final push of sufficient threshold energy came to rescue: Another mammoth-scale canal project, the Suez Canal opened its gates to naval traffic in 1869. In view of that event, in November 1869 the Hellenic Administration assigned the project to two French contractors, who, however, never started it. Twelve years later, in 1881, another contractor, a Hungarian general by the name of Stefan Tyrr took over the project. Construction of the canal began on April 23, 1882 and was completed in 1893. By then, the initial contractor had run dry of funds and was replaced by a Greek Company under Andreas Singros. Naval traffic in the Corinth Canal was inaugurated in a brilliant ceremony held on July 25th, 1893. It was indeed a vindication of a dream first conceived some 2495 years ago.

The rock formations in the flanks of the Corinth Canal consist of Neocene deposits of marls and sandstones. There are several faults running in east-west direction at a perpendicular angle to the canal axis, some of them seismically active. These geologic features were responsible for a number of major landslides into the Canal at several instances. On account of these landfalls, the Canal often had to be closed for repairs. The most serious such incident happened in 1923, when the Canal remained closed to traffic for 2 years on account of 41,000 m<sup>3</sup> of earth which had fallen in. Another major interruption of operation occurred in 1944, when the retreating German Army set explosives to the flanks of the Canal and caused 60,000 m<sup>3</sup> of earth to cave in. To make repairs even more difficult, the Germans also sunk railroad cars into the canal. It took 5 years to clear the Canal for traffic then.

In all these cases major rehabilitation works had been required for the re-opening of the Canal. Currently, in order to safeguard the passage of the ships through the Canal, continuous rehabilitation of the slopes is required, as shown in Figure 29.



Figure 29. Rehabilitation works on the slopes of the Corinth Canal

## 12 REHABILITATION OF DAMS

Public safety demands that earth dams either retain their reservoirs in the event of an earthquake or at worst release their reservoirs in a manner that does not pose a threat to life. Existing dams, especially older ones, are now being re-

examined using more severe earthquakes that their designers envisioned with evaluation methods unavailable to the original designers. Some of these re-examinations result in the determination that a seismic hazard exists (Marcusson III et al., 1996).

In order to rehabilitate an earth dam to prevent potential seismic instability, one must either change the engineering properties of the dam and / or foundation, modify the geometry of the existing dam, or both.

Upstream and downstream berms and buttresses are used to increase the effective overburden pressure on the problem material and thus decrease its liquefaction potential, or to increase the failure surface, provide a counterweight to limit movement and maintain a remnant section.

In some cases excavation and replacement of the problem material is used, as well as in-situ densification or strengthening. Both cases result in the decrease of the liquefaction potential of the problem material involved. Similarly, drainage to relieve of seismically induced pore-water pressures decreases the liquefaction potential.

Finally, an increase in freeboard may, also, be used for rehabilitating old dams or various combinations of the aforementioned approaches. Nevertheless, there are cases where removal of the dam from service or replacement with a new one was the only feasible solution.

The Saluda Dam is a hydroelectric dam located approximately 10 miles west of Columbia, South Carolina, USA. It was built during the late 1920s (completed in 1930) on the Saluda River. It has been determined that a recurrence of the 1886 Charleston Earthquake (magnitude 7.3-7.5) would cause the Saluda dam to liquefy and fail. Such an earthquake is expected once every 450 years. The Lake Murray reservoir, behind the Saluda Dam, contains 2,200,000 acre-feet of water. Failure of the Saluda Dam would cause major flooding for many miles downstream, including the city of Columbia, flooding a population of over 100,000, with an expected significant loss of life.

The Saluda Dam Remediation Project required the construction of a new back-up dam, or an additional berm at the downstream toe of the dam to add stability. The new berm involved a 4 million cubic yard rock berm section and a 1.3 million cubic yard roller-compacted concrete section (Figures 29 and 30).

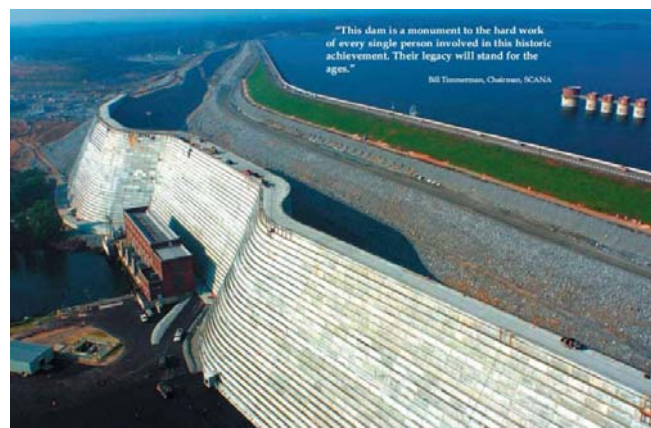


Figure 29. The Saluda Dam after its rehabilitation.

During the inspection in the process of the rehabilitation of the City of Baltimore's Loch Raven Dam, Maryland, USA, one of the main safety issues concerned was the need to inspect conditions of the dam's downstream toe to determine if excessive scouring and undermining of the structure had occurred.

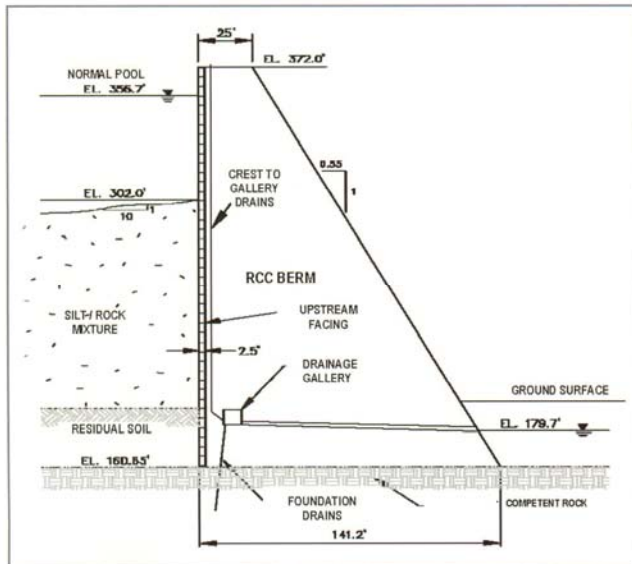


Figure 30. Saluda Dam's typical RCC berm section (Bair and Koleber, 2006).

To allow construction of the required stilling basin, significant excavation was required at the toe of the original (1912) structure. As this excavation would have decreased the dam's overall stability during construction, 57 high-capacity post tensioned rock anchors were designed to pin the dam to the underlying bedrock. Installed to resist potential loads created during construction, the anchors also act in combination with the RCC buttress section to stabilize the dam against the extreme loading condition that would occur in the event of a Probable Maximum Flood.

The anchors were installed within the spillway and a portion of the dam's nonoverflow sections. Typically they were installed through the dam's face and angled down at 45 degrees to penetrate the bedrock. Drilled holes were 300 to 350 mm in diameter and up to 49 m long. Total anchor lengths, including boded and unbonded sections, vary between 21 m and 48 m, the longest anchors being situated within the spillway (Bingham & Holderbaum, 2007).

The Forest Lake Reservoir supplies recycled irrigation water to seven Californian golf courses. The reservoir was originally constructed in 1887, and had operated as an unlined reservoir until the early 1990s. The rehabilitation of the project was commissioned by the authorities, because if water saturated the reservoir embankments, the stability of the embankments could be affected in an earthquake. The rehabilitation of the reservoir consisted in the application of a Hypalon liner (DiAntonio, 2007).

Standley Lake Dam and Reservoir in the north-western greater Denver Metropolitan area, Colorado, USA, is an earth embankment with a height of 33.5 m and a crest length of 2,012 m. The reservoir stores 51.8 Mm<sup>3</sup> of raw water that cannot be drained without causing a major interruption to Denver's water service. The dam was constructed in 1908 using soil from railroad trestles and "puddling" in a clay core on a foundation of weak expansive and slickensided claystone bedrock (Coss, 2006).

Given these factors, the dam was plagued with slope failures from the beginning. Recently, the old pressurized outlet works constructed through the maximum section of the dam, experienced separation problems at the joints due to creep and sliding of the embankment and foundation.

The rehabilitation of the dam included constructing outlet works tunnelled, using microtunnelling techniques, in the abutment (separate from the embankment), a new spill-

way, and placement of additional stability berms (see Figure 31).

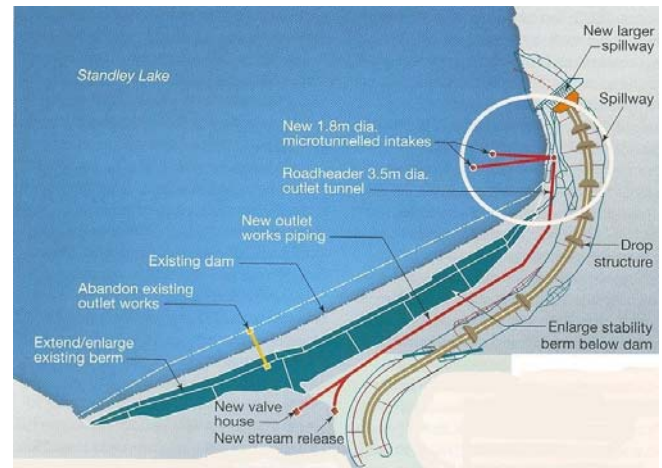


Figure 31. The Standley Dam Rehabilitation project (Coss, 2006).

Finally, sometimes it is not worth to rehabilitate an old dam, as in the case of the Calaveras Dam near San Francisco, USA. In 2001 the safety inspectors concluded that the dam (a hydraulic fill dam, with slopes buttressed with rockfill, completed in 1925) would probably collapse during an earthquake. The engineers considered a variety of alternatives, from rehabilitating the old dam to constructing a new one with the aid of such materials as roller-compacted concrete and earth and rock fill. They finally decided that the best and most economical solution would be to build a new earth dam just downstream of the existing dam (see Figure 32) that will be able to withstand forces from a large earthquake from the nearby Calaveras Fault (Hansen, 2005).

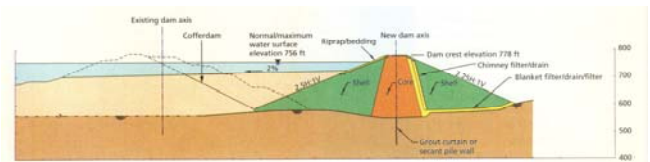


Figure 32. The Calaveras Old and New Dam, San Francisco (Hansen, 2005).

### 13 LAND REHABILITATION

Land rehabilitation is the process of returning the land in a given area to some degree of its former self, after some process (business, industry, natural disaster etc.) has damaged it. Many projects and developments will result in the land becoming degraded, for example industry, mining, farming and forestry. Reusing brownfield sites is also a key to building the homes and commercial developments we need for the future.

While it is rarely possible to restore the land to its original condition, the rehabilitation process usually attempts to bring some degree of restoration. Modern methods have in many cases not only restored degraded land but actually improved it, depending on what criteria are used to measure "improvement".

Mine rehabilitation aims to minimize and mitigate the environmental effects of modern mining, which may in the case of open pit mining involve movement of significant volumes of rock. Rehabilitation management is an ongoing process, often resulting in open pit mines being backfilled.

After mining finishes, the mine area must undergo rehabilitation:

- Waste dumps are contoured to flatten them out, to further stabilise them against erosion.
- If the ore contains sulphides, it is usually covered with a layer of clay to prevent access of rain and oxygen from the air, which can oxidise the sulphides to produce sulphuric acid.
- If the ore contains asbestos, it is also covered with a layer of clay to avoid spread of asbestos fibres in the air.
- Waste dumps are covered with topsoil, and vegetation is planted to help consolidate the material.
- Dumps are usually fenced off to prevent livestock denuding them of vegetation.
- The open pit is then surrounded with a fence, to prevent access, and it generally eventually fills up with ground water.
- Tailings dams are left to evaporate, then covered with waste rock, clay if need be, and soil, which is planted to stabilise it.

For underground mines, rehabilitation is not always a significant problem or cost. This is because of the higher grade of the ore and lower volumes of waste rock and tailings. In some situations, stops are backfilled with concrete slurry using waste, so that minimal waste is left at surface.

The removal of plant and infrastructure is not always part of a rehabilitation programme, as many old mine plants have cultural heritage and cultural value. Often in gold mines, rehabilitation is performed by scavenger operations, which treat the soil within the plant area for spilled gold using modified placer mining gravity collection plants.

Another form of land rehabilitation is the restoration of ecosystems and landscapes, which have been altered because of infrastructure works. They are designed not only for the geotechnical stabilization but mainly to integrate the infrastructure in the local ecological context. Ecological restoration at the sides of a highway, for example, would lead to biodiversity, landscape and natural heritage conservation.

The rowing events of the Athens 2004 Olympic Games were held at the Olympic Rowing and Canoe Centre at Shiniias, Marathon, in an area that used to be an airfield for light aircrafts and a military base for the last 40 years. However, before the construction of the airfield, the area used to be a marshland, very rich in wild life, which was drained in the late 1920s to create cultivatable land.

The design of the Olympic Centre (see Figure 33) presented some very interesting geotechnical problems to deal with and provided all the necessary works in order to reinstate the old marshland through the water overflow from the rowing ponds to the marshland (Tsatsanifos, 2004).

A similar story has been reported for a wetland in California. Before 1932, when it became the site of a military base, the land now occupied by the Hamilton Army Airfield, on the shore of San Pablo Bay near Novato, California, was strictly agricultural. But before it was reclaimed for agriculture at the beginning of the 20<sup>th</sup> century, the 1,000 acre parcel of land supported an array of tidal and seasonal wetlands. Now, more than 100 years later, the site is to be returned to its original state. The airfield's runway will remain in place, but its presence will not be noted as it will repose beneath several million cubic meters of dredged material that will be placed there (Landers, 2005).



Figure 33. The Athens 2004 Olympic Games Rowing and Canoe Centre at Shiniias, Marathon.

## 14 CONCLUSIONS

An attempt to show the contribution of geotechnical engineering in the rehabilitation of buildings and infrastructures is made in this paper through the presentation of recent relative case histories. It is easily foreseen that rehabilitation initiatives are a key growth area for geotechnical innovation.

## ACKNOWLEDGEMENTS

The author expresses his thanks to Prof. Harry Poulos for his valuable suggestions in the early stages of the preparation of the paper.

## REFERENCES

- Bair, J.M. & Koleber, M.L. 2006. Seismic Rehabilitation of Salduda Dam. *Geo-Strata*. Geo-Institut, American Society of Civil Engineers, Vol.7, No.6, November/December, pp.12-17.
- Barends, F.B.J. 2002. A Dutch leaning tower saved in 1866 by the same method used for the Pisa tower. *Geotechnique*, Vol.52, No2, pp.141-142.
- Barrows, R.J., Anderson, S.A. & Williams Clark, E. 2005. Preservation in a Setting of Change. *Geo-Strata*. Geo-Institute, American Society of Civil Engineers, July/August, pp. 15-18.
- Bingham, W.B. & Holderbaum, R.E. 2007. Renovating Loch Raven Dam. *Civil Engineering*. Vol.77, No.2, February, p.46-51.
- Brandl, H. 1989. Underpinning. *Special Lecture D. Proceedings 12<sup>th</sup> International Conference on Soil Mechanics & Foundation Engineering*, Vol.4, pp.2227-2258.
- Burland, J.B, Jamiolkovsky, M. & Viggiani, C. 2003. The Stabilisation of the Leaning Tower of Pisa. *Soils and Foundations*, Vol.43, No.5, pp.63-80.
- DiAntonio, P. 2007. Quake-proof liner stabilises US reservoir. *World Water and Environmental Engineering*, Vol.30, No.1, pp.20-21.
- European Foundations. 2004. *Open the Sluice Gates*. Vol.37, No.23, Summer, pp.22-25.
- European Foundations. 2004. *Jack Plug*. Vol.37, No.23, Summer, p.17.
- Goss, C. 2006. Rehabilitation at Standley Lake. *Tunnels & Tunnelling International*, March, pp. 25-27.

- Ground Engineering. 2007. A Smell Too Far. *Ground Engineering*, Vol. 40, No.2, p.10.
- Hansen B. 2005. Calaveras Dam to Be Replaced. *Civil Engineering*. Vol.75, No.10, October, p.16-27.
- Highway Research Board. 1972. *Pavements Rehabilitation. Materials and Techniques*. NCHRP Synthesis 9.
- Ingham, T.J., Fristoe, B. & Hollingsworth, R. 2007. An Uplifting Experience. *Civil Engineering*, ASCE, Vol. 77, No.1, January, pp.56-61.
- Johnston, G. & Burland, J.B. 2004. Some Historic Examples of Underexcavation. *Advances in geotechnical engineering, The Skempton Conference*. London, Vol.2, pp.1068-1079.
- Jurbin, T. 2006. Seismic upgrade for Massey Tunnel. *Tunnels & Tunneling North America*, Vol.X, March, pp.12-15.
- Landers, J. 2005. Airfield to be buried under dredged sediment to restore wetlands. *Civil Engineering*, ASCE, Vol.75, No.10, pp.21-22.
- Magrioti, A., Zarkadoulas, V. & Tsatsanifos, C. 2003. *Geotechnical investigation for the rehabilitation of the Tanagra airport runway. Design of runway and taxiways pavements*. Pangaea Consulting Engineers Ltd (in Greek).
- Marcusson III, W.F., Hadala, P.F. & Ledbetter, R. H. 1996. Seismic Rehabilitation of Earth Dams. *Journal Geotechnical and Geoenvironmental Engineering*, ASCE, Vol. 122, No.1, pp.7-20.
- National Council on Public Works Improvement. 1988. *Fragile Foundations: A Report on America's Public Works*. American Society of Civil Engineers, Final Report to the President and Congress.
- Pandis, C. & Tsatsanifos, C. 2002. *Evaluation of the Design Modification for the Rehabilitation of Cement Off Loading Jetty at Apapa Bay, Lagos, Nigeria*. Report for the Atlantic Bulk Carriers Ltd.
- Polymenakos, L. & Tsatsanifos, C. 2003. *Holy Church of Agios Petros of Dominicans at Iraklion, Crete. Geotechnical and Geophysical Investigation*. Pangaea Consulting Engineers Ltd. (in Greek).
- Poulos, H.G. 2005. Pile Behavior – Consequences of Geological and Construction Imperfections. *Journal Geotechnical and Geoenvironmental Engineering*, ASCE, Vol. 131, No.5, pp.538-563 (Terzaghi Lecture).
- Poulos, H.G., Badelow, F. & Powell, G.E. 2003. A Theoretical Study of Constructive Application of Excavation for Foundation Correction. *Proceedings International Conference on Response of Buildings to Excavation – Induced Ground Movements*, London, CIRIA Spec. Pub. 199, F.M. Jardine, ed., pp.469-484.
- Rico Rodriguez, A., del Castillo, H. & Sowers, G.F. 1988. *Soil Mechanics in Highway Engineering*. Clausthal-Zellerfeld: Trans Tech Publications.
- Sata, L. 2003. Foundation strengthening of a historic building. *Proceedings 2nd International Young Geotechnical Engineers Conference*, Mamaia, Romania.
- Stefanides, C. & Tsatsanifos, C. 1995. *Geotechnical Investigation for the Structure T16 (Overpass of Perpendicular Road 10) at the Chainage 8+178 of the Section Giorgos Stream – Megara of the Athens – Corinth Highway*. Pangaea Consulting Engineers Ltd. (in Greek).
- Tamez, E., Ovando-Shelley, E. & Santoyo, E. 1997. Underexcavation of Mexico City's Metropolitan Cathedral and Sagrario Church. *Proceedings 14<sup>th</sup> International Conference on Soil Mechanics & Foundation Engineering*, Vol.4, pp.2105-2126.
- Terracina, F. 1962. Foundation of the leaning tower of Pisa. *Géotechnique*, Vol.12, No.4, pp. 336-339.
- Tsatsanifos, C. 1995. Tymfristos Road Tunnel – Rock mass properties for design purposes. *Internal Report*, Special Service for Road Tunnels and Underground Works, Ministry of the Environment, Planning & Public Works of Greece.
- Tsatsanifos, C. 2004. Geotechnical Investigations and Designs for the Construction of the Olympic Rowing and Canoe Centre at Shinias, Marathon. *Proceedings one Day Conference "The Foundations of the Athens 2004 Olympic Games*, April 20<sup>th</sup>.
- Tsatsanifos, C.P., Mantziaras, P.M. & Georgiou, D. 2000. Squeezing rock response to NATM tunneling: A case study. *Proceedings of the International Symposium on Geotechnical Aspects of Underground Construction in Soft Ground – IS – Tokyo'99*, pp.167-172, A.A.Balkema.
- Tsatsanifos, C. & Pandis, C. 2005. Egnatia Odos / Anthochori (Northern Greece): Estimating the Geomechanical Characteristics of a Sliding Slope in a Thrust Zone. *Proceedings 16<sup>th</sup> International Conference on Soil Mechanics & Foundation Engineering*, Osaka.
- Tsatsanifos, C., Pandis, C. & Melekis, G. 2006. Investigation of the Causes of the Reactivation of a Pre-existing Landslide at Egnatia Motorway. *Proceedings 5<sup>th</sup> Panellenic Conference on Geotechnical and Geoenvironmental Engineering*, Vol.3, pp.117-122 (in Greek).

## Integration of geotechnical and structural design in tunneling

The 2008 Kersten Lecture

Evert Hoek

Consulting Engineer, Vancouver, British Columbia, Canada

Carlos Carranza-Torres

CCT Rock Engineering, Minneapolis, Minnesota USA

Mark Diederichs

Geological Sciences and Geological Engineering, Queen's University, Kingston, Ontario, Canada

Brent Corkum

Rocscience Inc., Toronto, Canada

Proceedings University of Minnesota 56<sup>th</sup> Annual Geotechnical Engineering Conference. Minneapolis, 29 February 2008

### ABSTRACT

In the majority of modern rock tunnels the deformation and hence the stability of the tunnel is controlled by a combination of reinforcement and support systems. The reinforcement consists of rockbolts or cables which modify the properties of the rock mass in much the same way as reinforcement does in concrete. The support systems generally involve steel sets or lattice girders fully embedded in shotcrete and these provide resistance to control the convergence of the tunnel. This paper describes the methods that can be used to optimize the design of tunnels using a combination of reinforcement and support methods. Particular attention is given to tunnels in very weak rock or soil in which large deformations can occur. Two case histories are presented to illustrate the integration of geotechnical and structural design methods. The first is a 12 m span two lane highway tunnel, excavated by top heading and benching in a very weak rock mass and the second involves a 25 km long, 5.5 m diameter water supply tunnel through the Andes in Venezuela.

### 1 INTRODUCTION

Current practice in tunnel reinforcement and lining design tends to vary a great deal, depending upon national or owner imposed design requirements, local tradition and practice and the experience of the tunnel designer. There are no universally accepted guidelines on how to assess the safety of a tunnel or the acceptability of a design and this means that engineering judgment and experience play a very large role in the design of tunnel reinforcement and linings.

There is a general desire to define a factor of safety for tunnel design but this has proved to be an extremely difficult task and there are very few methods that are considered acceptable. One of these methods, described by Kaiser (1985), and Sauer et al (1994), involves the use of support capacity diagrams and, indeed, there are a few tunnel design companies that use this methodology. However, the available papers are generally lacking in detail and there is no mention of this method in design guidelines such as the Tunnel Lining Design Guide published by the British Tunneling Society (2004). Consequently, the average tunnel designer is left with few options other than the use of tunnel classification systems (Barton et al, 1974, Bieniawski, 1973), general empirical guidelines and the advice of experienced tunnel consultants. The main difficulty with this approach is to decide when the design is acceptable (Hoek, 1992).

In an effort to remedy some of these problems, the authors have set out to present two relatively complex case histo-

ries in sufficient detail that tunnel designers can follow the use of support capacity diagrams as a tunnel design tool. Based on a paper by Carranza-Torres and Diederichs (2008), the derivation of the equations used to define these support capacity curves are presented in an appendix and it is relatively simple to program these equations in a spreadsheet.

The support capacity diagrams presented in this paper are based on elastic analyses and the authors recognize that this is a simplification compared to much more sophisticated non-linear models that are used in structural engineering. However, given the uncertainties associated with the loads imposed on tunnel linings, this simplification is considered to be justified. These loads depend upon the adequacy of the geological model, the properties of the rock mass surrounding the tunnel, the in situ stresses and the groundwater conditions. All of these contributing factors are open to a wide range of interpretations, particularly during the design stages in a tunnelling project. Consequently, the aim in developing the elastic support capacity diagrams presented in this paper is to provide the tunnel designer with a set of tools of comparable accuracy to the input data.

### 2 CASE HISTORY 1 – A SHALLOW TUNNEL AND ADJACENT OPEN CUT

This case history, assembled from a number of actual tunnel designs, involves a 12 m span highway tunnel excavated by drill and blast methods using a top heading and bench approach.

Once the tunnel has been excavated and a final concrete lining has been cast in place, an open cut is excavated close to and downhill from the tunnel to accommodate a second carriageway.

The overall geometry of the slope, the tunnel and the adjacent cut is shown in Figure 1. The rock mass is a gently dipping interbedded sedimentary sequence of jointed sandstone, bedded sandstone and a series of shear zones parallel to bedding. The properties of the individual rock units, based on a nearby tunnel in a similar rock mass, are listed in Table 1 and the corresponding Mohr envelopes are plotted in Figure 2.

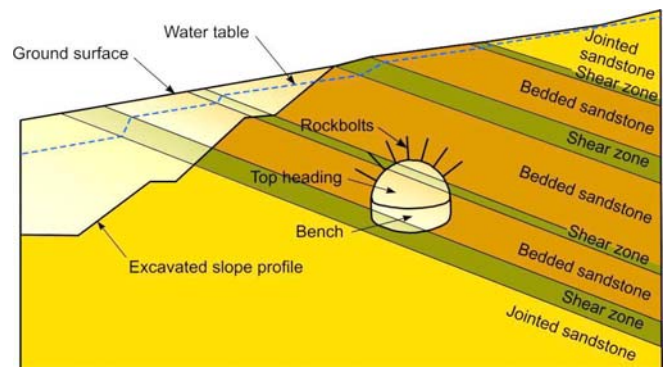


Figure 1. Geometry of the original slope showing the rock layers, the location and geometry of the tunnel and slope excavations and the original water table.

Note that the friction angles shown in Table 1 may appear to be unusually high, particularly to soil mechanics readers. This is because the tunnel is very shallow and the average confining stress in the rock mass surrounding the tunnel is only about 1 MPa. Under these conditions the Mohr failure envelopes are strongly curved, as shown by the dashed lines in Figure 2 (Hoek et al, 2002) and the Mohr Coulomb parameters are estimated from tangents to the curved envelopes.

Table 1. Rock mass properties

Property	Jointed Sandstone		Bedded Sandstone		Shear Zones	
	Peak	Residual	Peak	Residual	Peak	Residual
Cohesive strength $c$ - MPa	2.0	1.5	1.4	1.2	0.8	0.8
Friction angle $I$ - degrees	52	50	50	47	40	40
Rock mass modulus $E$ - Mpa	9500		4000		650	
Poisson's ratio	0.25		0.25		0.3	
Permeability - m/sec	$1 \times 10^{-6}$		$1 \times 10^{-6}$		$1 \times 10^{-7}$	

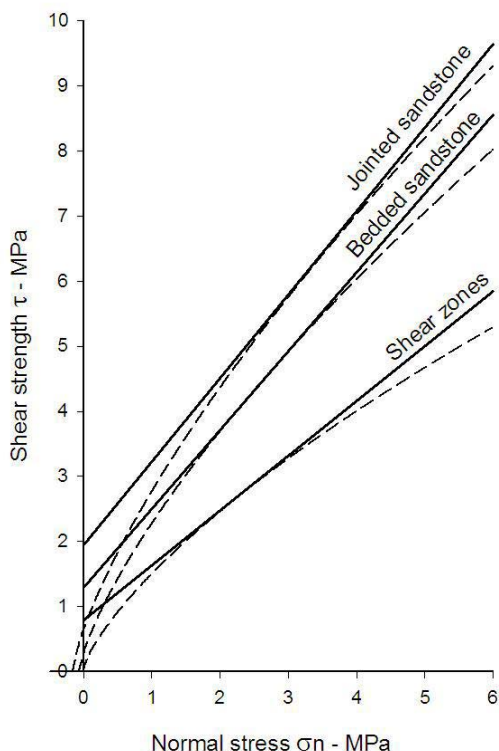


Figure 2. Mohr failure envelopes for individual rock units.

**2.1 In situ stress conditions**

The vertical stress acting on the rock mass in which this tunnel will be excavated is given by the product of the depth below surface and the unit weight of the rock. Horizontal stress magnitudes and directions can vary greatly, depending upon the tectonic history of the area, the variation in stiffness of different rock units in the rock mass and the local topography. As a starting point for this analysis it has been assumed that the ratio of vertical to horizontal stresses parallel to the tunnel axis is 2:1 and that the ratio normal to the tunnel axis is 1.5:1.

If no in situ stress measurements are available in the vicinity of the tunnel then it is prudent for the tunnel designer to check the sensitivity of the design to variations in these ratios between 0.5:1 and 2:1. If the design proves to be sensitive to horizontal stress variations then steps should be taken to have in situ stress measurements made before the design proceeds to completion. An alternative is to leave sufficient flexibility in the contract to allow design changes during construction and to rely on the back analysis of tunnel convergence measurements to determine the in situ stresses acting on the tunnel.

**2.2 Groundwater conditions**

The excavation of the tunnel and the slope for the adjacent carriageway result in changes in the groundwater conditions in the slope. These changes have a significant impact on the effective stresses in the rock mass surrounding the tunnel. Consequently, a full analysis of these groundwater conditions is a starting point for this analysis of the tunnel stability.

Assuming a permeability of  $1 \times 10^{-7}$  m/sec for the shear zones and  $1 \times 10^{-6}$  m/sec for the jointed and bedded sandstones (see Table 1), a finite element analysis of the groundwater conditions in the slope was carried out. The resulting water tables, for different stages of tunnel and slope excavation, are shown in Figure 3. In this analysis it was assumed that the tunnel acts as a drain except for an extreme long term condition in which the tunnel drains are blocked.

In the finite element analysis of the tunnel lining that follows the pore water pressures and the resulting effective stresses, from the groundwater analysis described above, have been incorporated into the tunnel stability model.

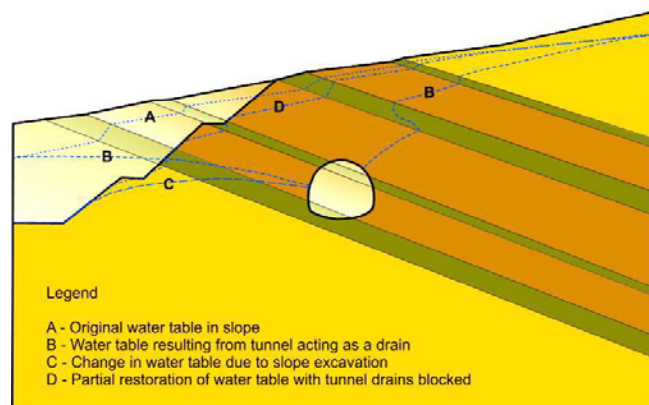


Figure 3. Water tables at different stages of tunnel and slope excavation and assuming long term blockage of the tunnel drains.

**2.3 Lining requirements**

The client's requirements for the lining of the tunnel are as follows:

- i. An initial lining consisting of steel sets or lattice girders embedded in shotcrete, with the addition of rockbolts if required, sufficient to stabilize the tunnel during construction and until the final lining is placed.
- ii. A drainage layer consisting of porous geotextile fabric, connected to drainage pipes in the final tunnel invert.
- iii. A waterproof membrane to prevent water entering into the space behind the final concrete lining.

- iv. A cast in place concrete lining and invert capable of resisting loads imposed by the surrounding rock mass for both short and long term operation of the tunnel. The factor of safety of the final reinforced concrete lining should exceed 2.0 for normal operating loads and 1.5 for unusual and long term loads.

A typical tunnel lining, designed to meet such requirements, is illustrated in Figure 4.

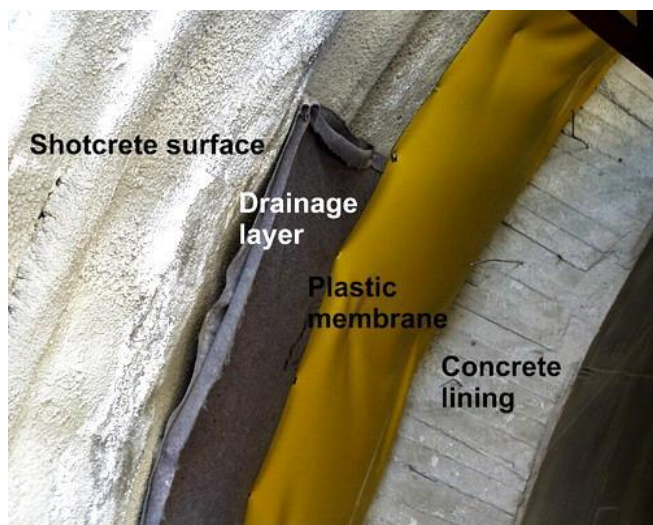


Figure 4. Construction of a complete tunnel lining consisting of an initial lining of lattice girders embedded in shotcrete, a geotextile drainage layer, a waterproof plastic membrane and a cast-in-place concrete final lining.

#### 2.4 Top heading versus full face excavation

An important issue that has to be considered by any drill and blast tunnel designer is whether to specify excavation of the tunnel using a top heading and bench approach or a full face excavation method. Small diameter tunnels, less than say 6 m span, are invariably driven by full face methods since stabilization of the face, if required, is relatively simple. At the other end of the spectrum, large underground caverns are almost always excavated in multiple stages from a top heading or from side drifts. The 12 m span transportation tunnel considered in this example falls in the range where either top heading and bench or full face excavation can be used. Full face excavation has many advantages in terms of geometrical simplicity and, in ground of adequate strength, greater rates of tunnel excavation. Consequently, where possible it is the preferred method of tunneling.

One of the technical factors that controls the choice of which method to use is the stability of the tunnel face. When the stresses in the rock mass surrounding a tunnel exceed the strength of the rock mass a zone of failure or a "plastic" zone is formed around the tunnel. As shown in the derivation of longitudinal displacement profiles for tunnels in Appendix 1, when the radius of the plastic zone around a tunnel exceeds twice the radius of the tunnel, the zone of failure around the tunnel interacts with the failed rock ahead of the tunnel face to form a continuous bullet shaped plastic zone. This three-dimensional plastic zone becomes increasingly difficult to stabilize as the ratio of stress to available rock mass strength increases.

Stabilizing the plastic zone ahead of the tunnel face is generally achieved by means of fully grouted fiberglass dowels parallel to the tunnel axis. The reason for using fiberglass dowels is that they can be cut off as the tunnel advances and they do not damage conveyor belts in the muck disposal system. These dowels are typically placed in a grid pattern of 1 m x 1 m and their total length is approximately

equal to the span of the tunnel. For 12 m long dowels an overlap of 3 to 4 m is generally used to ensure that there is continuous support of the face.

Lunardi (2000) discusses the action of face reinforcement in considerable detail and the authors have no disagreement with his statement that "... In order to prevent instability of the face, and therefore the cavity (tunnel), preconditioning measures must be adopted, appropriately balanced between the face and the cavity, of an intensity adequate to the actual stress conditions relative to the strength and deformation properties of the medium". The preconditioning to which he refers includes the placement of fiberglass dowels, forepoles and other devices that control the deformation of the rock mass ahead of the tunnel face. Achieving an appropriate balance between the face and the tunnel cavity requires a three dimensional analysis of the bullet shaped plastic zone discussed above.

In addition to the stability of the face, consideration has also to be given to the deformations that control the stability of the tunnel itself. Depending upon the in situ stress field and the characteristics of the rock mass surrounding the tunnel, these deformations may be more important than those in the rock ahead of the face. In such cases, the control of the tunnel deformations will determine the choice between top heading and bench and full face excavation.

Practical considerations related to the size of the tunnel, availability of specialized equipment required for the installation of pre-reinforcement, local contracting experience and the preference of the owner can also play an important role in choosing between top heading and bench and full face excavation methods.

In the tunnel under consideration in this model (Figure 1), the owner considered that the risk of losing control of the face due to the presence of the weak shear zones is unacceptably high. Consequently the use of a top heading and bench approach has been specified, in spite of the fact that it may have been possible to drive this tunnel by full face excavation.

#### 2.5 Analysis of face stability

The analysis of the stability of a top heading or a full face tunnel face requires a three dimensional analysis. In simple cases this can be done by means of an axi-symmetric application of a two-dimensional numerical analysis (see Figure A1.3 in Appendix 1). In more complex cases, such as that under consideration in this example, a full three-dimensional analysis is required.

The purpose of the three-dimensional analysis is to simulate in the most realistic possible way the mechanical process of excavation and support and reinforcement installation behind the face and, if applicable, on the face itself to investigate whether the face shows signs of instability. In these three-dimensional models, face instability normally manifests itself as caving of the face resulting in a plastic failure zone that extends ahead of the face or, if the tunnel is relatively shallow as in this example, towards the ground surface. Excessively large displacements can occur and the numerical model tends not to converge (i.e., reach an asymptotic value) as the excavation sequence progresses.

Figure 5 shows the three-dimensional numerical model used to analyze the stability of the face in this example. Note that only half of the model, as defined by a vertical plane cutting through the tunnel axis, is represented in this figure. The model considers excavation of the top heading through the interbedded sedimentary sequence introduced in Figure 1. Mechanical properties of the different rock types are those indicated in Figure 2 and Table 1. The in situ stress conditions prior to excavation assumed for the model are those discussed in Section 2.1, while the

groundwater conditions correspond to the worst case scenario, that of the original water table (configuration A) in Figure 3.

As indicated in Figure 5, the three-dimensional model simulates the mechanical process of advancing the top heading in increments of 2 meters, corresponding to the design blast round length of 2 m, and installing shotcrete and rockbolts at a distance of 2 meters behind the face, corresponding to the design length of installation of support and reinforcement behind the face.

The geometrical and mechanical characteristics of the support and reinforcement used are the same considered in the two-dimensional numerical analyses to be discussed in later sections. In addition, the model simulates the process of installation of a set of 60 fiberglass dowels in a circumferential pattern at the face, with an approximate spacing of 1 meter between dowel heads.

In this case, the dowels are installed at intervals of 8 meters on the face, leading to a minimum overlap length of 4 meters between two sets of dowels. The geometrical and mechanical properties of fiberglass dowels are normally provided by the manufacturer; this example considers dowels of 18 mm diameter, with a Young's modulus of 40,000 MPa and a tensile strength of 1000 MPa.

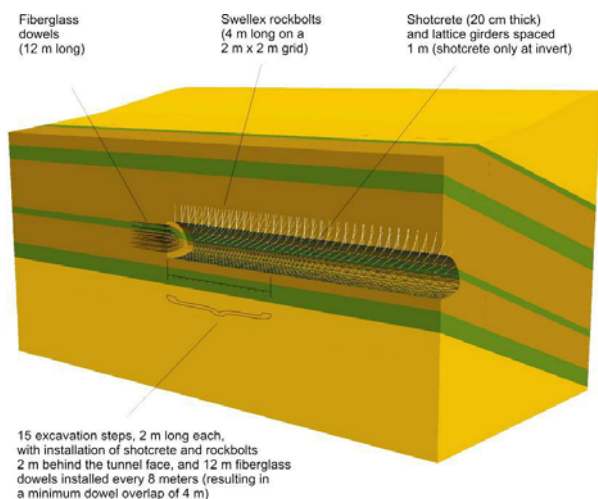


Figure 5. View of the three-dimensional numerical model used to analyze stability of the tunnel face.

A total of 15 excavation stages have been considered in this example leading to a total length of sequential advance of 30 meters. For the last stage (indicated in Figure 5) the stability conditions at the face have been inspected. Figure 6 represents contours of resulting magnitude of displacements at this stage. Displacements at the face are below one millimeter. The resulting plastic failure zone is also of limited extent of less than 50 centimeters and does not show any tendency to develop into a caving zone towards the ground surface. Comparison of equivalent results from a model without fiberglass dowels installed at the face reveals that these dowels do indeed make a mechanical contribution to the stability of the tunnel face. Both the extent of plastic zone and resulting displacements at the face, when no fiberglass dowels are considered, are at least twice the values shown in Figure 6.

It is doubtful whether fiberglass dowel reinforcement is actually required in this example and it is probable that the top heading could be advanced safely without reinforcement or with a simpler restraint in the form of a face buttress (Hoek, 2001). However, the calculations presented in Figures 5 and 6 demonstrate the procedure that can be used to analyze the need for face reinforcement and the stabilization that can be achieved by the installation of such

reinforcement.

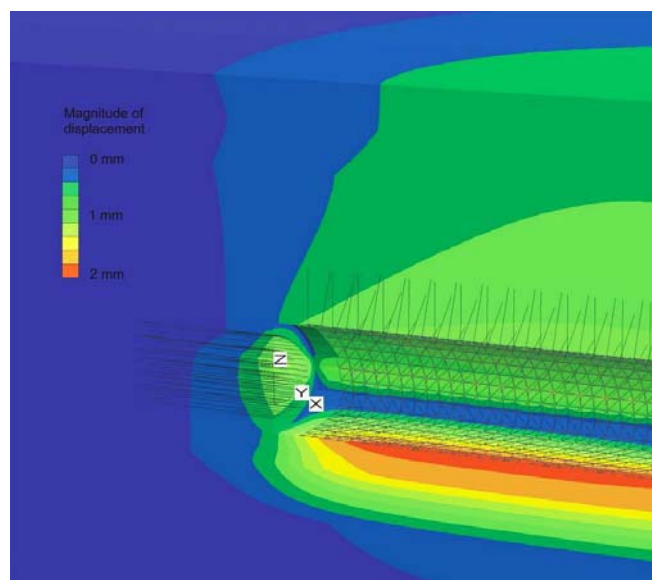


Figure 6. Representation of contours of magnitude of displacements for the last stage of excavation in the three-dimensional model of Figure 5.

## 2.6 Characteristic curve and longitudinal deformation profile

The next step in the design procedure is to determine the point at which the support in the tunnel is installed and activated. In a 12 m span tunnel this would normally be at a distance of between 2 and 4 m behind the face and a distance of 2 m has been chosen for this analysis.

In using a two dimensional analysis of the rock-support interaction it is necessary to simulate the three-dimensional tunnel advance by means of some deformation control process. This means that the deformation that takes place at a distance of 2 m behind the face must be known and controlled to allow the support to be installed and activated. This can be done by calculating the characteristic curve for the rock mass surrounding the tunnel by progressively reducing either an internal support pressure or by progressively decreasing the deformation modulus of an inclusion in the tunnel. In complex situations, such as that under consideration here, the modulus reduction method is preferred since it automatically accommodates variations in the surrounding stress field due to a non-circular tunnel shape and progressive failure in the rock mass as the tunnel deforms.

Figure 7 shows the characteristic curve for this tunnel and the stepwise reduction of the modulus of the inclusion in the tunnel. The analysis required to generate the characteristic curve also shows the extent of failure around the tunnel and this is important in calculating the longitudinal deformation profile in the next stage of the analysis.

Figure 8 gives a plot for the longitudinal deformation profile for the tunnel in this example. As shown in Appendix 1, this profile depends upon the ratio of the radius of the plastic zone to the radius of the tunnel and, for this example, this ratio is approximately 2:1. Figure A1.5 in Appendix 1 shows that the tunnel closure at the face is approximately one quarter of the final closure at many meters behind the face. The deformation profiles are calculated from equations A1.6 and A1.7.

From Figure 8 it can be seen that installation and activation of the support at a distance of 2 m behind the advancing face corresponds to a deformation of 0.011 m. Using this value in Figure 7, the modulus of the inclusion required to

limit the tunnel deformation to this value is approximately 100 MPa. Hence, in constructing the two dimensional model to simulate the three-dimensional effects of the advancing face, an inclusion with a modulus of 100 MPa has been used for the first stage of the calculation. Excavation of this inclusion activates the installed support system and allows it to react to the additional deformation that occurs as the tunnel advances.

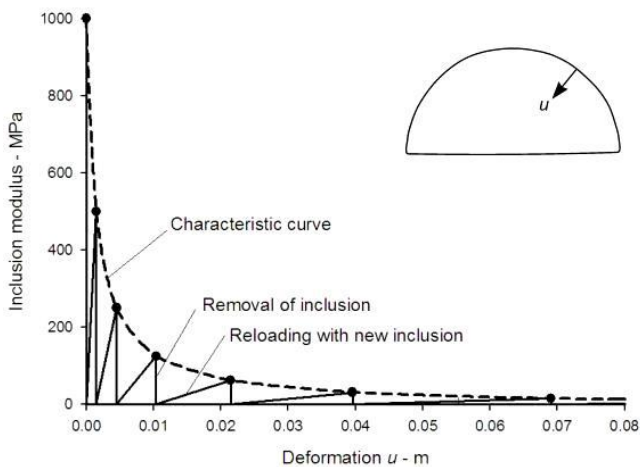


Figure 7. Characteristic curve for the unsupported, undrained tunnel excavated by a full face method. Note that any monitoring point can be chosen on the tunnel boundary since, although the magnitude of the deformations will vary, the shape of the excavation curve will remain constant.

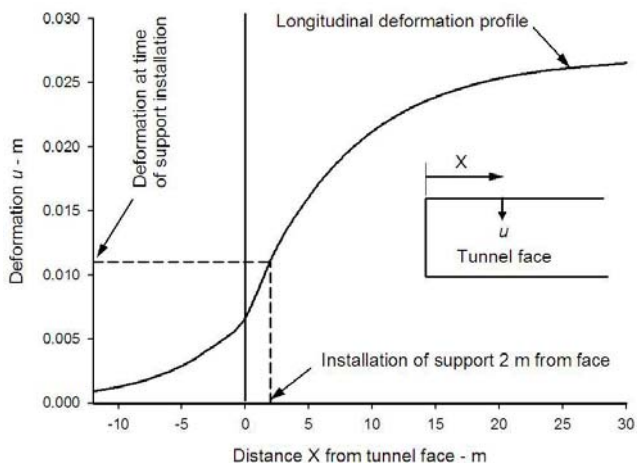


Figure 8. Longitudinal deformation profile for a 12 m span tunnel where the radius of the plastic zone is less than twice the radius of the tunnel.

## 2.7 Analysis of top heading with a flat floor

For large span tunnels the top heading shape preferred by contractors is illustrated in Figure 9. This consists of an arched roof and a flat floor. The flat floor is simple to excavate and it provides an excellent road base for construction traffic. In good rock at low to moderate stress levels, this top heading shape is acceptable. The suitability of this top heading profile for this example is investigated below.

Figure 10 gives a cross section through a typical support system used for the initial support of a large span tunnel. This consists of 3 bar lattice girders embedded in a 20 cm thick shotcrete layer. The lattice girders are spaced at 1 m intervals along the tunnel and rockbolts are installed between every second girder at a spacing of 2 m. In this case the rockbolts are 4 m long standard Swellex bolts on a 2 m x 2 m grid spacing.



Figure 9. A simple top heading shape in good quality interbedded sandstones and siltstones. The tunnel arch is supported by means of rockbolts and a layer of shotcrete and no face support is required. The flat floor requires no special treatment other than good drainage of surface water accumulations.

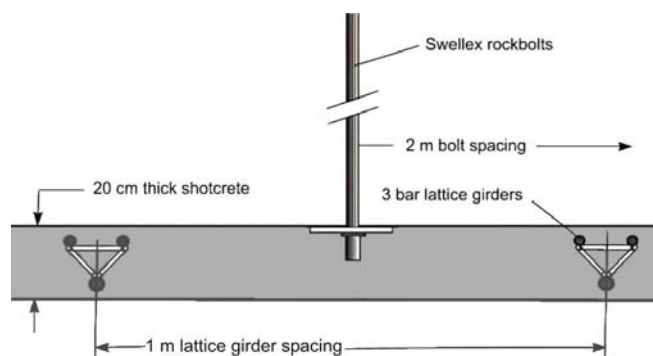


Figure 10. Reinforcement and support for the top heading arch consisting of standard Swellex rockbolts on a 2 m x 2 m grid and 3 bar lattice girders spaced at 1 m centers and embedded in a 20 cm thick shotcrete lining (Not to scale).

An important issue that has to be considered in the design of this support system is the time-dependent properties of the shotcrete layer. As described above, the support system is installed 2 m behind the face and activated immediately. The rockbolts and lattice girders respond to the deformation of the rock mass surrounding the tunnel as soon as the tunnel advances but the shotcrete is only 1 day old at this stage and it has not yet developed its full capacity. While it does not carry its full share of the load, because its stiffness is low, this load may be sufficient to induce failure in the shotcrete.

Choosing the shotcrete properties is not quite as simple as one would think. Many tunnel designers turn to structural codes such as the American Concrete Code (ACI 318 - Building Code and Commentary) and follow the recommendations set out in these documents. However, in their Guidelines for Tunnel Lining Design the Technical Committee on Tunnel Lining Design of the Underground Technology Research Council states the following:

“Structural codes should be used with caution. Most codes have been written for above ground structures on the basis of assumptions that do not consider ground-lining interaction. Accordingly, the blind application of structural design codes is likely to produce limits on the capacity of linings that are not warranted in the light of the substantial contributions from the ground and the important influence of construction method on both the capacity and cost of linings.

Specific load factors are not recommended in these guide-

lines. The loading conditions should be evaluated by a careful, systematic review of the geologic and construction influences. It is important that the evaluation of ground loads and structural details be coordinated to select a factor of safety."

In the support capacity calculations given in this paper the authors have adopted a policy of using the ultimate uniaxial compressive and tensile strengths of shotcrete and concrete and calculating a range of factors of safety. This eliminates the complication of hidden or unknown load factors or safety factors and, by including a family of factor of safety plots in the support capacity diagrams, the user is presented with a clear picture of performance of the lining being designed.

Melbye and Garshol (2000) give shotcrete mix designs and uniaxial strength results, many from in situ cores, for 35 tunneling projects around the world. These results are plotted in Figure 11 and it can be seen that the 28 day strength varies from 25 to 86 MPa. This variation depends upon the mix design, whether the wet or dry shotcrete method was used, whether the shotcrete was applied manually or by robot and upon local factors such as haulage distance between the batch plant and the face. It is the responsibility of the tunnel designer to discuss all of these issues with the shotcrete supplier in order to determine the optimum shotcrete product for a particular site.

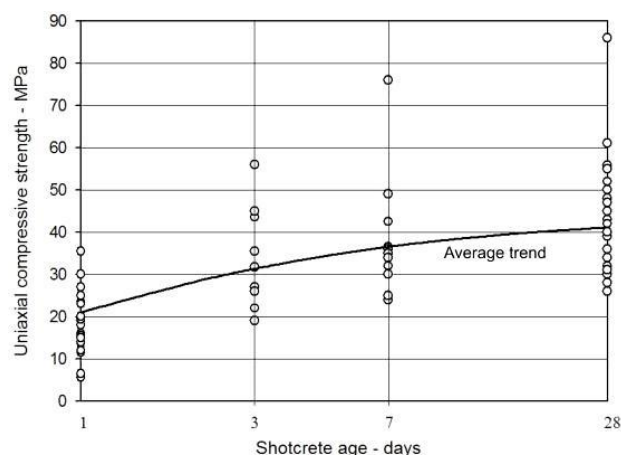


Figure 11. Uniaxial compressive strength development with time for shotcrete linings in tunnels around the world. After Melbye and Garshol (2000).

For the model under consideration the sequence of loading and the corresponding shotcrete properties are defined in Figure 12 and Table 2 in which the age dependent properties have been assembled from a number of tunnel case histories. In constructing the numerical model used to analyze this case these properties have been incorporated into the shotcrete lining at the stages of excavation shown.

In the case of the top heading with an unsupported and unreinforced flat floor, as illustrated in Figure 13, the heave of the floor induces bending in the lower parts of the lining arch. These bending moments can overload the 3 day old shotcrete and they can also permit deformations sufficient to allow failure propagation in the adjacent rock mass. This failure may have a detrimental influence on the loading of the lower legs of the arch when the bench is excavated.

In order to study the response of the support system to the excavation sequence and consequent tunnel deformations, a set of support capacity diagrams have been plotted in Figure 14. Note that the rockbolts are not part of the support system since they act as reinforcement and alter the properties of the rock mass surrounding the tunnel. Nevertheless these bolts play an important role in stabilizing the tunnel arch and in supporting the shotcrete shell.

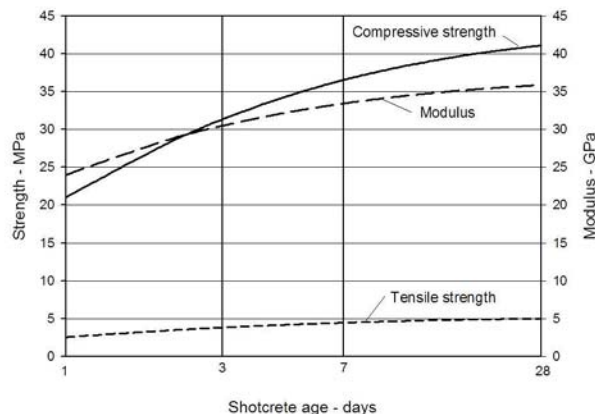


Figure 12. Assumed time dependent properties for shotcrete.

Table 2. Excavation sequence and shotcrete properties

Property	Compressive Strength $\sigma_{csh}$	Tensile Strength $\sigma_{tsh}$	Deformation Modulus $E_{sh}$
Day 1 - installation and activation of support	21.0 MPa	- 2.6 MPa	24,000 MPa
Day 3 - top heading convergence at about 10 m behind the face	31.0 MPa	- 4.0 MPa	30,000 MPa
Day 28+ - excavation of bench which may be as much as 1 year after top heading excavation	41.4 MPa	- 5.0 MPa	36,000 MPa

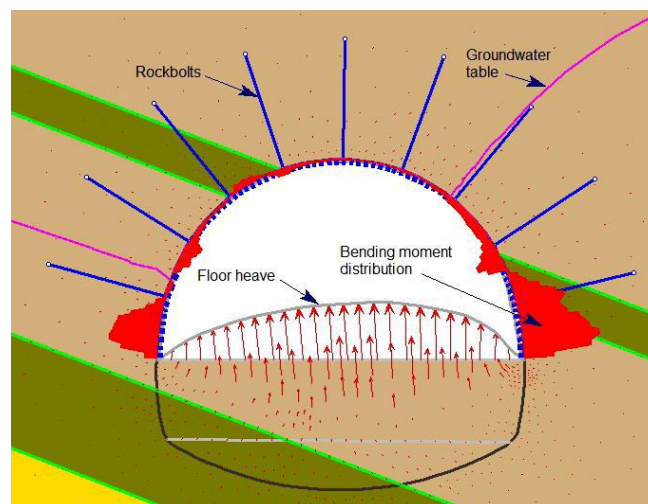


Figure 13. Bending moment distribution in the lining of the top heading with a flat unsupported floor on day 3 after installation of the support.

The derivation of the equations required to calculate these figures is given in Appendix 2. The calculation process results in a set of moment versus axial thrust and moment versus shear force diagrams for the lattice girders and the shotcrete. In the case of the shotcrete, the diagrams are calculated for 1 day, 3 day and 28 day strengths as defined in Table 2. From the numerical analysis, the axial forces, bending moments and shear forces in the installed top heading arch support are distributed onto the lattice girders and the shotcrete shell by means of equations A2.24 to

A2.29 in Appendix 2. The resulting values, for the 1 day and 3 day loading conditions, are plotted as points in Figure 14.

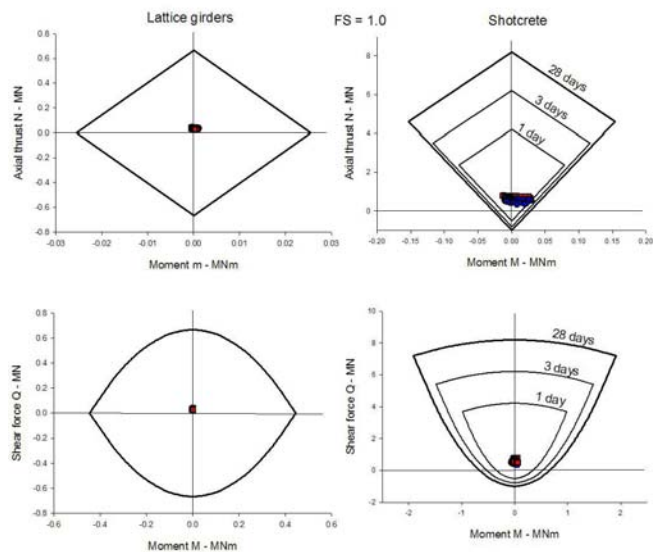


Figure 14. Support capacity diagrams for a 20 cm shotcrete lining, reinforced with 3 bar lattice girders, placed in a top heading excavation with a flat floor (see Figure 9).

Because of the shallow depth of the tunnel the axial loads carried by the support system are very low. Similarly, bending moments and shear forces in the lattice girders are small. However, the bending moments in the shotcrete lining are sufficient to exceed the capacity of the shotcrete at ages of 1 day and 3 days, as shown in the moment versus axial thrust diagram for the shotcrete, assuming a factor of safety of 1. This analysis illustrates that, for the in situ stresses, rock mass properties, excavation sequence and lining properties chosen, a top heading with a flat unreinforced and unsupported floor is not an appropriate choice.

The excessive bending moments in the lower portions of the top heading arch can be addressed in a number of ways including the installation of stressed anchors to limit the bending of the upper arch legs, increasing the thickness of the shotcrete shell, placing additional reinforcement in the lower arch legs or placing a temporary invert to limit the floor heave and the "pinching" of the arch. In this example, the placement of a temporary shotcrete invert will be investigated.

Examining Figure 14 may suggest to the reader that, since the loads carried by the lattice girders are so small, the shotcrete could be dispensed with and the lattice girders used on their own to carry the loads. This would be a serious mistake since these capacity plots are only valid when the lattice girders and the shotcrete act as a composite structure. The shotcrete, even when very young, provides lateral confinement for the lattice girders and this is essential to prevent buckling failure of these slender structures in the wide span tunnel.

### 2.8 Analysis of top heading with a curved shotcrete invert

A temporary shotcrete invert, such as that illustrated in Figure 15, is generally constructed from unreinforced shotcrete, typically 20 cm thick, so that it can be broken easily during benching. Backfill is placed over this invert in order to form a road surface for construction traffic.

It is important that a smooth connection is provided between this invert and the top heading arch legs in order to prevent the formation of stress concentration points. The shear capacity of the connection between the arch legs and

the shotcrete invert can be deficient if the shotcrete is



Figure 15. Top heading and bench excavation in a weak rock tunnel where a temporary shotcrete invert was used to control floor heave.

placed at different times. This problem can be overcome by adding reinforcement, such as that illustrated in Figure 16, to ensure that the loads in the arch are transferred into the invert. This reinforcement should be designed so that it can either be cut off or bent downward and incorporated into the lower arch legs when the temporary shotcrete invert is excavated.

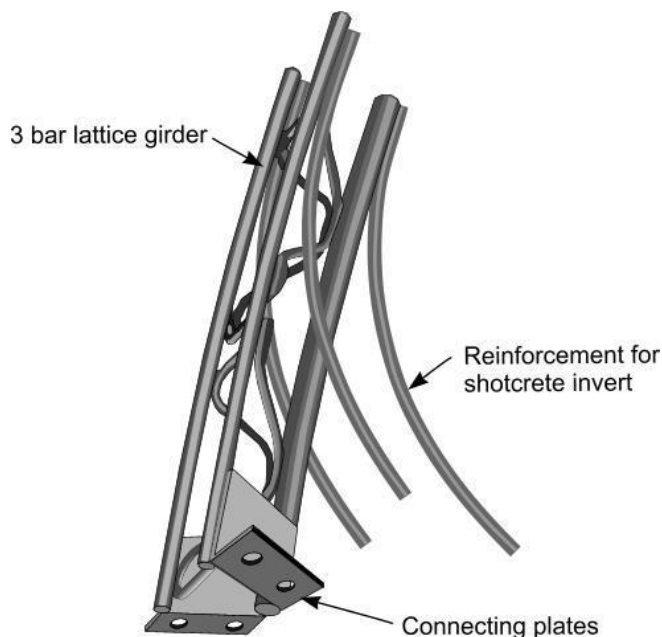


Figure 16. Additional reinforcement at the junction between the top heading arch legs and the temporary shotcrete invert.

A numerical analysis of top heading lining with a curved shotcrete invert covered by backfill results in the bending moment shown in Figure 17 and the corresponding support capacity plots given in Figure 18. In this case the analysis has been extended to include the removal of the bench and the placement and activation of the lower arch legs and the tunnel bottom invert.

Since the structure of the arch legs is identical to the top heading arch it is permissible to plot the points for these two components on the same support capacity diagrams.

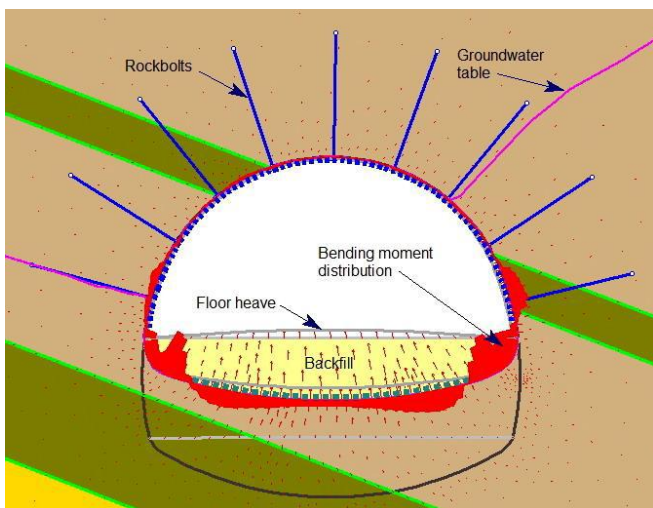


Figure 17. Bending moment distribution in a top heading lining with a curved shotcrete invert covered by backfill (see Figure 15).

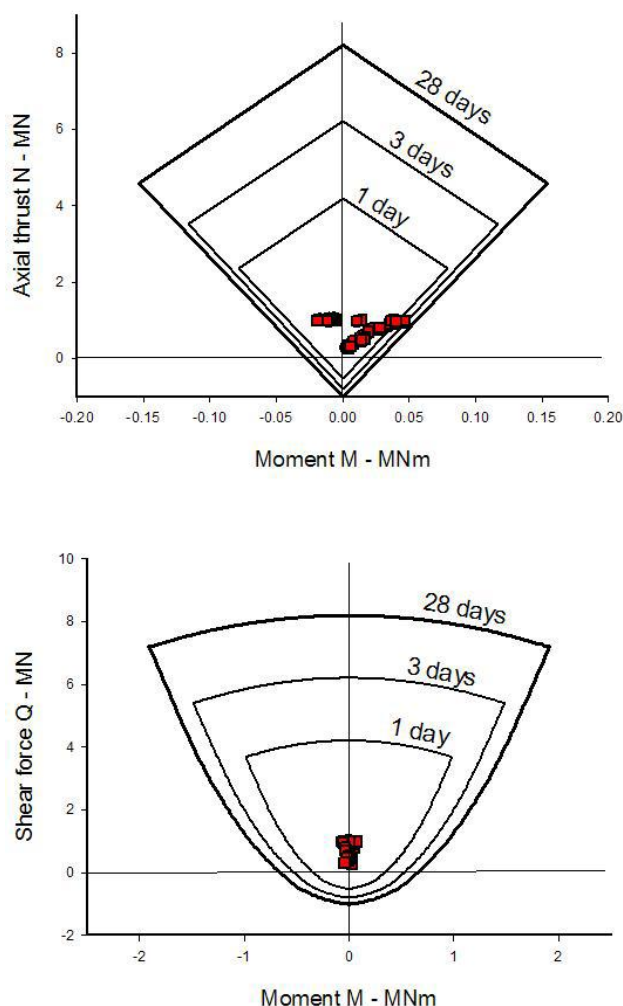


Figure 18. Support capacity plots for the 20 cm thick unreinforced shotcrete invert in Figure 17.

Figure 17 shows that the results of this analysis of the top heading arch are similar to those for the top heading with the flat floor, shown in Figure 13, except that the bending moments in the arch are reduced by the placement of the shotcrete invert. The support capacity plots for the unreinforced invert, given in Figure 18, show that the bending moments induced in the invert are just sufficient to induce

tensile cracking in the 1 day and 3 day old shotcrete. While this would be a problem elsewhere it is considered to be acceptable here since the shotcrete invert is constrained by the overlying backfill and some minor cracking will be of little consequence. However, if the designer is uneasy about this cracking or if the client is reluctant to accept any indication of failure, the invert can be made thicker or it can be reinforced with polypropylene fibers to increase its capacity.

The support capacity plots for the shotcrete arch and lower legs for the case of the curved shotcrete invert are shown in Figure 19. The Moment-Axial thrust points for the shotcrete all fall well within the capacity curves for the corresponding age of shotcrete. This confirms that the use of the shotcrete invert has reduced the bending moments that resulted in problems in the top heading excavated with a flat floor (Figure 14).

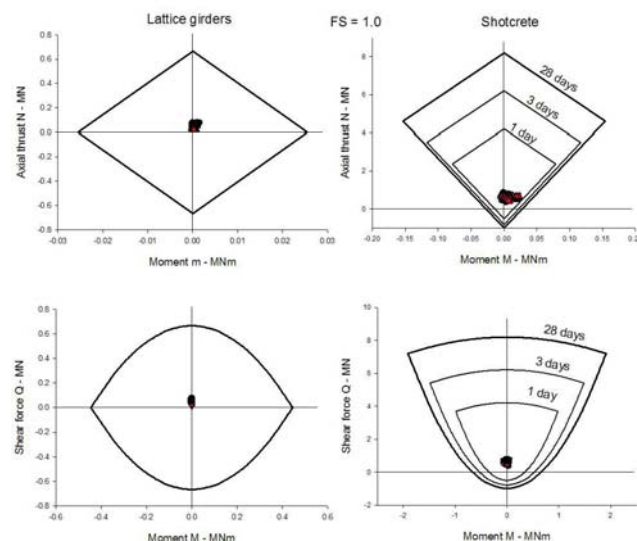


Figure 19. Support capacity diagrams for a 20 cm shotcrete lining, reinforced with 3 bar lattice girders, placed in a top heading excavation with a curved shotcrete invert (see Figure 15).

A check on the invert on the bottom of the tunnel shows no overstressing and, hence, the complete lining is stable and the design can proceed to the installation of the final lining. Note that, if there is a large time delay (say for more than 1 year) between the excavation of the tunnel and the installation of the final lining, it may be necessary to recalculate the lining forces for a reduced rock mass strength to allow for time-dependent deterioration.

## 2.9 Final lining design

The next step after the excavation and stabilization of the full tunnel profile is the installation of a final lining. The typical geometry of this lining was shown in Figure 4 and it is given in detail in Figure 20. In this example it is assumed that the final lining itself consists of 30 cm thick cast-in-place concrete reinforced by means of 20 mm diameter steel reinforcing rods spaced at 18 cm x 22 cm apart.

For simplicity the properties of the cast in place concrete final lining are assumed to be the same as those of the initial shotcrete lining, as defined in Table 2. Because the final lining is installed in a stable tunnel it carries no initial load except for its self-weight. Hence, only the 28 day properties are relevant in the following calculations. Loads are imposed on the final lining as a result of stress changes, changes in the groundwater conditions, changes in the characteristics of the initial support system or deterioration of the rock mass surrounding the tunnel. All of these changes are assumed to occur in this example and the consequences will be examined in the analysis that follows.

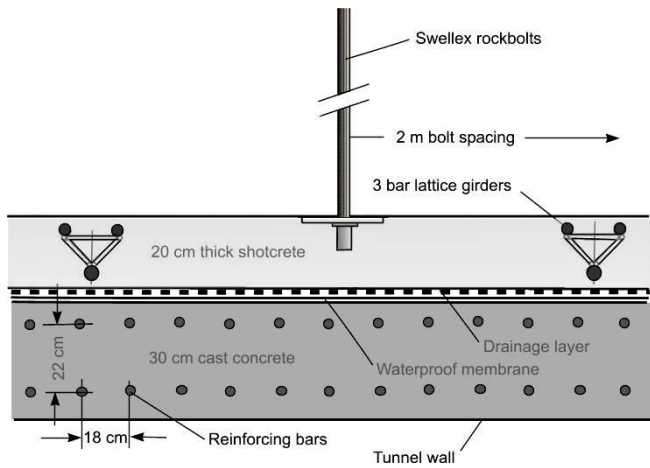


Figure 20. Geometry of composite final lining consisting of a 20 cm thick initial shotcrete lining, a drainage layer, a waterproof membrane and a 30 cm thick cast concrete lining (Not to scale).

After the installation of the final lining the open cut for the adjacent highway carriageway is excavated as defined in Figure 1. This results not only in changes in the stress field surrounding the tunnel but also changes in the groundwater conditions as defined by curve C in Figure 3. In designing the final lining these changes have to be accommodated and a factor of safety in excess of 2.0 has to be provided by the lining for these "normal" loading conditions.

The long term loading conditions, for which a factor of safety of 1.5 has been specified for this example, include corrosion of all the rockbolts, blockage of the tunnel drains and deterioration of the rock mass surrounding the tunnel. Other extraordinary long term-loading conditions may apply in specific cases and these should also be included. Basically, the aim of the designer should be to ensure that the tunnel will remain stable and operational under all possible conditions that could occur during its service life.

The participation of the initial shotcrete lining has been a matter of contention for many years. Until relatively recently tunnel designers in some countries were required to ignore the contribution of all initial reinforcement and shotcrete linings in calculating the support capacity of the final lining. However, this very conservative approach has changed and the International Tunnelling Association's Guidelines for the Design of Tunnels (1988) gives the following recommendation: "An initial lining of shotcrete may be considered to participate in providing stability to the tunnel only when the long-term durability of the shotcrete is preserved. Requirements for achieving long-term durability include the absence of aggressive water, the limitation of concrete additives for accelerating the setting (liquid accelerators), and avoiding shotcrete shadows behind steel reinforcement".

The extent of rock mass failure surrounding the tunnel, after installation of the final lining and excavation of the adjacent open cut is shown in Figure 21. Note that some rock mass failure of the surface occurs as a result of surface subsidence and stress relief due to the open cut excavation. While this is not significant in the design of the tunnel lining it does highlight the need for the designer to check on surface subsidence and slope stability issues. In shallow tunnel such as this one, caving to surface can be a critical issue and it has to be checked very carefully during the sequential excavation of the tunnel.

The bending moments and the deformations induced in the final lining are shown in Figure 22. Note that the presence of the two shear zones has a significant influence of these distributions, particularly on the right hand side of the tunnel arch. As shown in the support capacity plots in Figure

23, these bending moments are the most significant forces to be considered in the lining design since all other forces are very low.

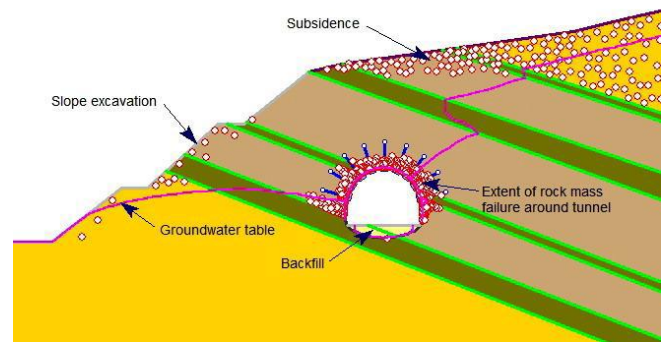


Figure 21. Changes in stress and groundwater conditions as a result of excavation of the open cut for an adjacent carriageway can result in propagation of failure zones in the rock mass.

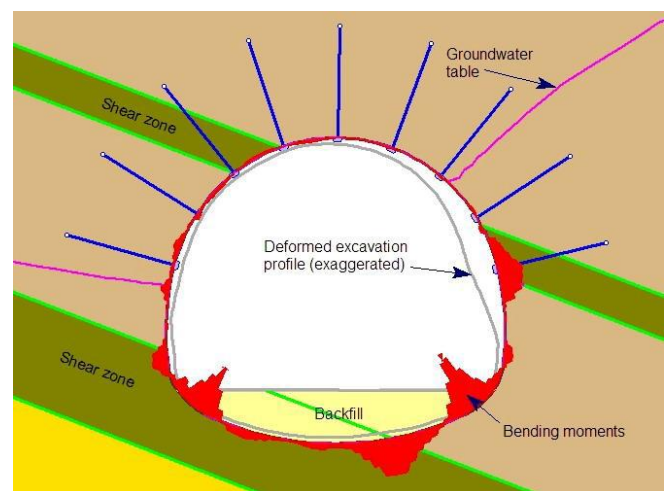


Figure 22. Distribution of bending moments and deformations of the final tunnel profile after installation of the final lining and excavation of the adjacent cut.

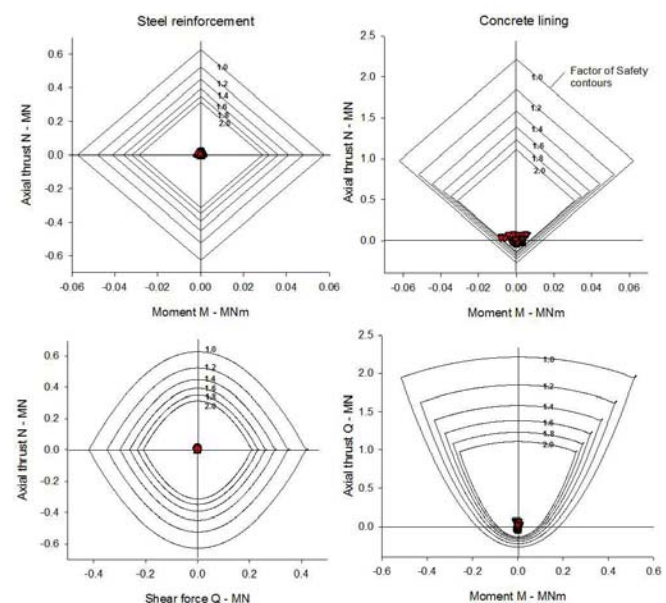


Figure 23. Support capacity plots for the final concrete lining.

Detailed plots of the moment-thrust relationships for the

final lining for three model stages are given in Figure 24. These show that the lining carries practically no load at the time of installation. The forces in the lining change slightly when the adjacent open cut is excavated and they change by a significant amount when the long term loads are applied. These loads are induced by a reduction of the residual strength of the failed rock surrounding the tunnel, an elimination of all rockbolts and changes in the groundwater conditions as a result of blockage of the drains. The factor of safety for the lining for these long term loads is approximately 2.0.

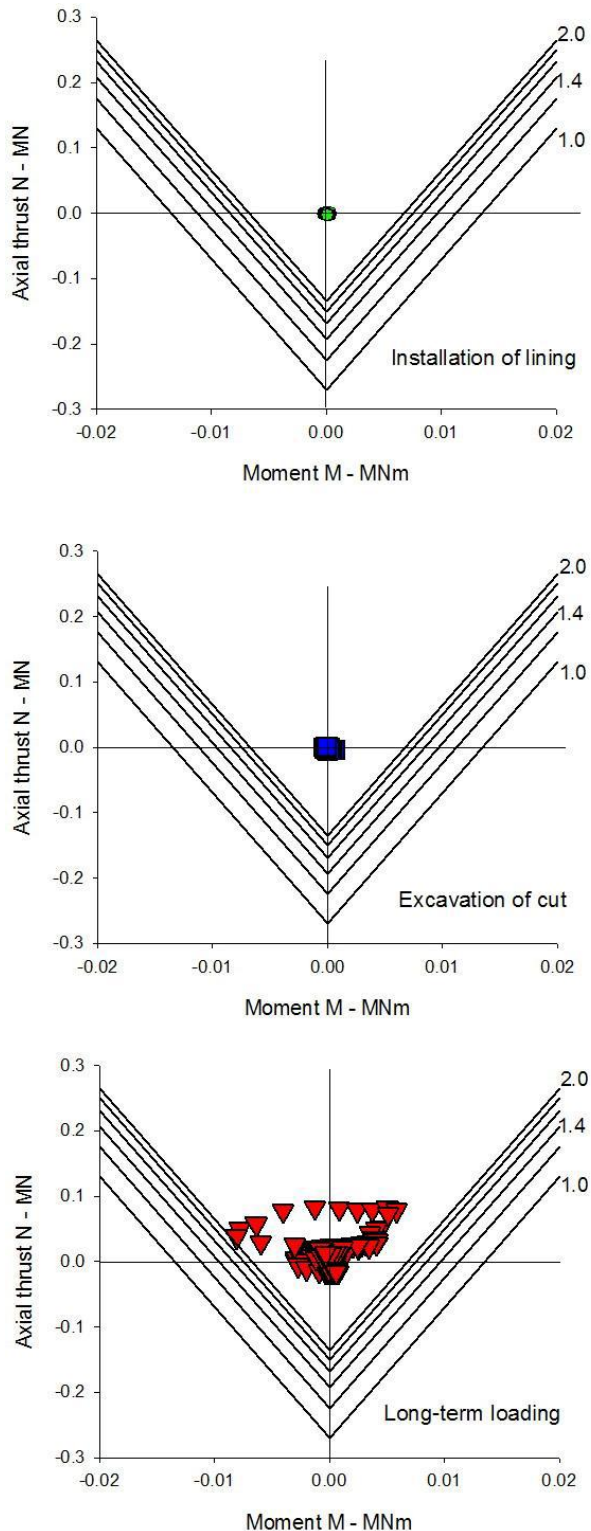


Figure 24. Detail of moment versus axial thrust development in the final concrete lining from the installation of the lining, the excavation of the open cut and long-term loading conditions.

Figure 25 gives a minimum moment-thrust capacity diagram for the reinforced final lining for a factor of safety of 2.0, generated using the structural program Response 2000 (Bentz, 2000).

This is a sectional analysis program that will calculate the strength and ductility of a reinforced concrete cross-section subjected to shear, moment, and axial load. All three loads are considered simultaneously to find the full load-deformation response using the modified compression field theory (Vecchio and Collins, 1986).

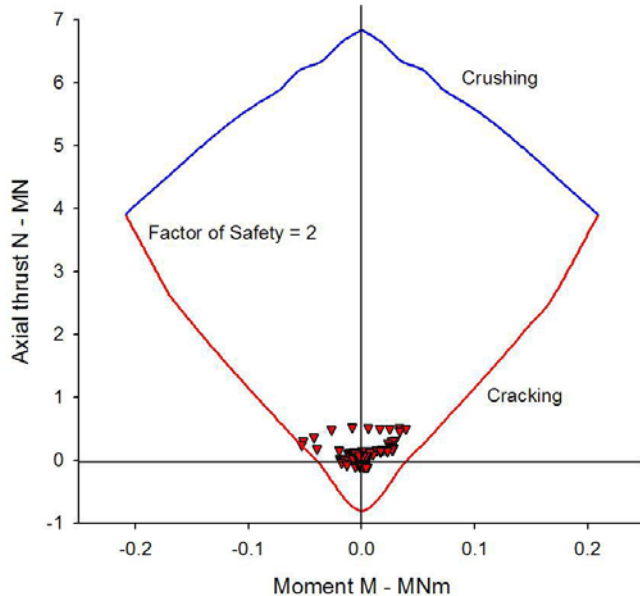


Figure 25. Minimum Moment-Thrust capacity for the reinforced concrete final lining calculated by the structural program Response 2000 (Bentz, 2000) for a factor of safety of 2.0.

The total moment-thrust points for the final lining under long-term loading conditions are also plotted in Figure 25. The relationship of these points to the capacity curve, defined by cracking of the concrete, is similar to that illustrated in Figure 24 for the concrete component of the lining. This comparison serves as a confirmation that, at least for the low load considered in this example, the elastic support capacity plots derived in Appendix 2 are an appropriate tool to use for reinforced concrete lining design.

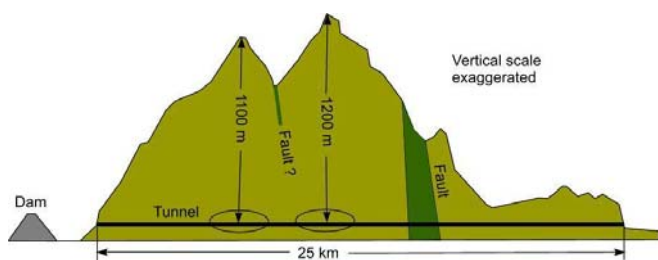
The separation of the forces in the concrete (or shotcrete) and the steel reinforcement, as has been done in Figures 19 and 23, gives information on the contribution made by each of these components and on the combination of forces that control the design process. In this example the bending moments in the concrete are by far the most important forces and, when combined with the relative low tensile strength of concrete, they determine the performance of the lining.

### 3 CASE HISTORY 2 – A DEEP TUNNEL IN WEAK GROUND

This case history is based on the Yacambi-Quibor tunnel currently under construction in the Northern Andes in Venezuela. Aspects of this project are described by Guevara (2004). Design and construction details are simplified for the purposes of this example. This analysis involves new construction within the central portion of a 25 km tunnel, 5.2 m in diameter, in highly variable metamorphic rock at depths of up to 1200 m below surface (Figure 26).

The tunnel is designed for water transport, under moderate velocity and head, from a rainforest region in the south to an agricultural centre to the north. The tunnel will include

the facilities to drain and inspect the tunnel with vehicle access after construction and during service life.



a) longitudinal topographic profile (north to the right)



b) tunnel wall side view (to scale—tunnel diameter is 5.2m)

Figure 26. a) Longitudinal topographical profile along tunnel alignment. Major regional faults are shown. Ellipses indicate zones of interest for this case study. b) Two typical tunnel wall maps showing high variability in geological structure and fabric alignment.

The design problem discussed here relates to a typical tunnel profile in highly deformed graphitic phyllite (Figure 27). The deformation in the rock mass is the result of the tectonic processes inherent in the Andes Mountains and is also the result of the proximity of the tunnel to a large regional fault related to the intersection of three major crustal plates. The fault passes through the tunnel as seen in Figure 26. A second fault has been identified on surface but it is not known whether this will be intersected at tunnel depth. This analysis is related to the section of tunnel identified in this figure where the average depth of overburden is approximately 1150 m. The in situ stresses at depth are assumed to be approximately equal (30 MPa) in all directions as a result of the low shear resistance due to the fact that the tectonic history of the rock mass has reduced its properties to their residual values.

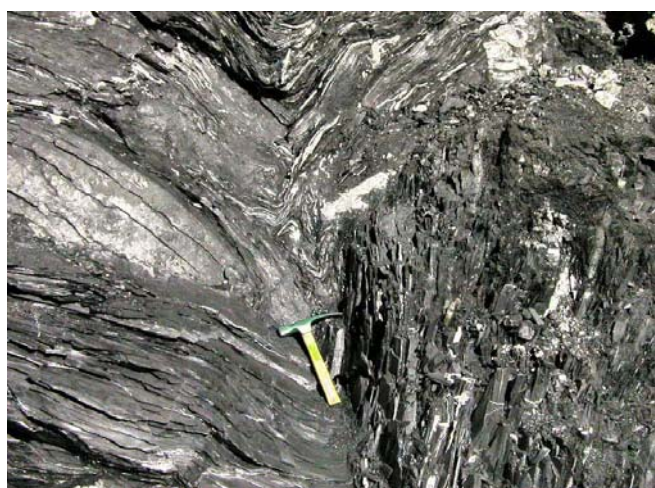


Figure 27. Graphitic phyllite in the tunnel face. Note the tight secondary folding and high variability of fabric orientation – rock hammer in center is 45cm long.

Tests on intact core samples of this rock gave uniaxial compressive strength values of 15 MPa to 110 MPa (Salcedo, 1983). The high variability in results is due to the orientation of the phyllitic foliation with respect to the loading direction. As seen in Figure 27, the rock mass in the tunnel is tightly folded and no particular orientation of fabric presents itself over a significant portion of the tunnel

profile. On the scale of the tunnel, therefore, isotropic rock mass strength can be assumed. Back analyses of monitored sections of the excavated tunnel confirm that the average uniaxial compressive strength of the intact graphitic phyllite is approximately 50 MPa and this value has been assumed for this analysis.

The rock mass was assessed using the Geological Strength Index (GSI) system (Marinos and Hoek, 2001) and rock mass strength parameters, according to Hoek et al. (2002), are shown in Figure 28. A GSI value of 25 is assigned to the rock mass over this section of the tunnel. As the rock mass is already in a deformed (residual) state, it is assumed to act plastically in response to stress change and deformation. The long term strength of the rock mass is assumed to correspond to moderate disturbance according to the GSI system with a Disturbance factor  $D = 0.2$ .

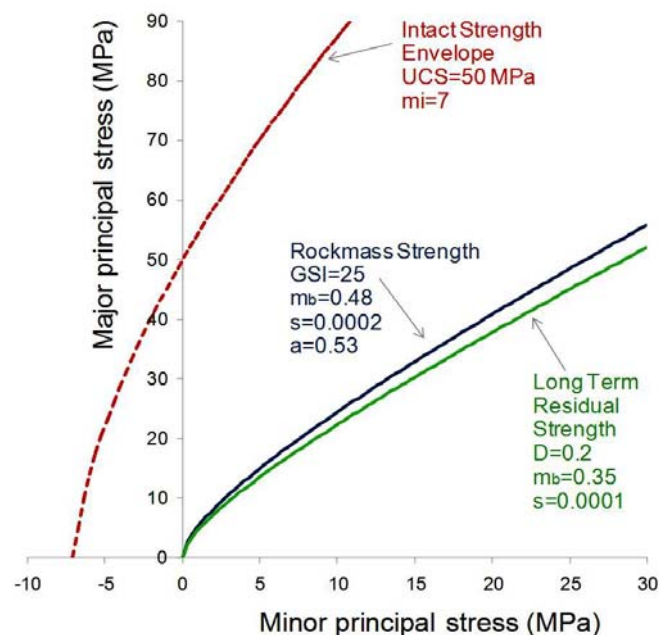


Figure 28: Rock mass strength parameters for Case 2 analysis. In situ stress = 28MPa.

The deformation modulus of the rock mass is estimated to be 1650 MPa, based on the methodology of Hoek and Diederichs (2006).

Tunnelling in these conditions is extremely difficult (Hoek and Marinos, 2000). Preliminary analysis of an unsupported tunnel in this rock mass at this depth indicates closure in excess of 50%. The key to liner design is to sequence the installation of support to avoid overload while still maintaining a safe working environment at and near the face.

Numerous challenges have been encountered over the long history of this construction project (a complete history of which is beyond the scope of this paper) and, due to the high cost of an additional concrete lining, it has been decided that the support system installed during construction will act as the final lining. In addition to resisting cracking and spalling this liner must control displacements to preserve the minimum tunnel size required for vehicular access during operation.

After several iterations in liner design over the years, each with its own lessons, the current design was adopted. A circular profile with steel arches (W6 X 20) at 1 m intervals, embedded in 60 cm of shotcrete applied in two passes of 20 cm and 40 cm thickness, is specified. There is a requirement to install support early to provide a safe working space at the face. Activation of the full lining, however, has to be delayed to prevent an unacceptable build-up of inter-

nal loads due to the high closure rates near the tunnel face. Premature installation of the final lining could result in buckling of the primary support system, associated expansion of the plastic zone and increase in final closure.

Specifications for the support were based, in part, on analytical convergence-confinement calculations (Carranza-Torres and Fairhurst, 2000). In this analysis, illustrated in Figure 29, the liner is treated as a single 60 cm thick concrete shell enclosing one W6 x 20 steel set per metre.

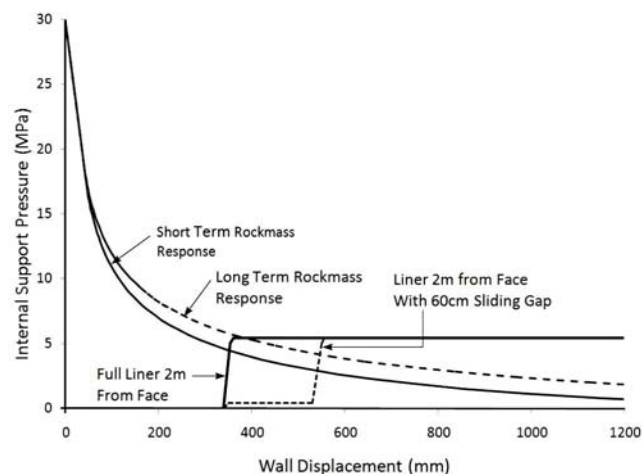


Figure 29. Convergence confinement analysis (according to method of Carranza-Torres and Fairhurst, 2000) for short and long term ground response (unsupported). Liner load development for 60 cm shotcrete section with W6 x 20 steel section. Dashed support load curve represents delayed loading due to sliding joint.

The relationship between wall displacement and location along the tunnel (the linear displacement profile) is estimated based on the methodology described in Appendix 1 for a normalized plastic zone radius  $P_r$  of 6.5. Installation of the full liner near the face results in a low short term factor of safety and an unacceptable long term factor of safety of approximately 1.0. This long-term factor of safety is increased to approximately 1.4 with the installation of sliding joints. This prediction for the supported tunnel is conservative as it ignores the overall displacement reduction due to rock-support interaction.

Sliding joints, shown in Figure 30, allow controlled convergence (closure) of the steel sets without excessive loading of the steel. These joints provide resistance against moments but allow slip at low axial loads until the gap is closed. At this time the liner builds up load as a closed circle. The sliding joint is fabricated on site using two heavy steel plates constraining the set flanges through the tensioning of bolts as shown in the inset in Figure 30. The opposing steel sections are clamped by this device with a controlled gap (in this case 25 to 30 cm). This technique has proved to be very effective at Yacambi-Quibor. Alternative yielding support systems have also been widely used in squeezing ground conditions in Europe (Schubert, 1996).

The original design called for the complete steel set to be erected near the face and a 20 cm layer of shotcrete sprayed over the sets with 1 m gaps left over the sliding joints as shown in Figure 31. The two sliding joints are installed just below the spring line for a total circumferential closure of 60 cm (2 x 30 cm). Once the gap is closed by tunnel deformation, the gap is filled with shotcrete and an additional 40 cm of shotcrete, reinforced by means of circumferential rebar, is applied to the inside of the liner. The effect of the sliding gap is illustrated by the dashed support response line in Figure 29. This simple convergence-confinement analysis does not consider moments and neglects the interaction between support layers. In

addition the stabilizing effect of the liner and the resultant reduction in rock mass displacement are not considered. Nevertheless, this analysis correctly indicates the need for delayed loading of the liner.



Figure 30. Circular steel arches (W6 X 20) with two sliding joints (detail in inset).



Figure 31. Initial Liner composed of circular steel arch and 20 cm of shotcrete. Inset shows detail of sliding joint with shotcrete gap. Note rebar in place to reinforce final shotcrete layer.

Due do difficulties with face instability, the contractor found it necessary to implement the support system in two stages with a short 1.5 m bench (from floor to springline) maintained to buttress the face. The upper semicircular section of the steel set is installed at the face to provide a primary safety system. The arch sections rest on the bench and are covered in shotcrete. The bench is then excavated approximately 1.5 m from the face and the circular arch, including the pair of sliding joints, is completed. The first 20 cm shotcrete layer is completed at this stage (Figure 32a).

A reinforcement cage is assembled adjacent to the initial shotcrete lining as seen in Figure 31. Once joint closure is achieved (within 5 to 15m of the face) the gap is closed with shotcrete to complete the final 40 cm thick final lining. The final lining section is illustrated in Figure 32b.

The following analysis represents a more rigorous consideration of the interactions between the liner components and the construction sequence. The first step in the design process is to determine the normalized maximum unsupported failure radius via a simple plane strain analysis of the unsupported tunnel. In this case, the ratio of maximum plastic radius to tunnel radius is 6.5.

Next, the longitudinal deformation profile can be calculated using the methodology given in Appendix 1. Alternatively, since the stresses are isotropic and the tunnel is circular, an axisymmetric model (Figure 33b) can be used for this pur-

pose. A longitudinal deformation profile for the unsupported tunnel is shown as a dashed line ("Disp. vs Distance") in Figure 33a. An estimate of the displacement profile for the supported tunnel (with liner and sliding joints) is presented in Figure 33a as a dotted line for comparison.

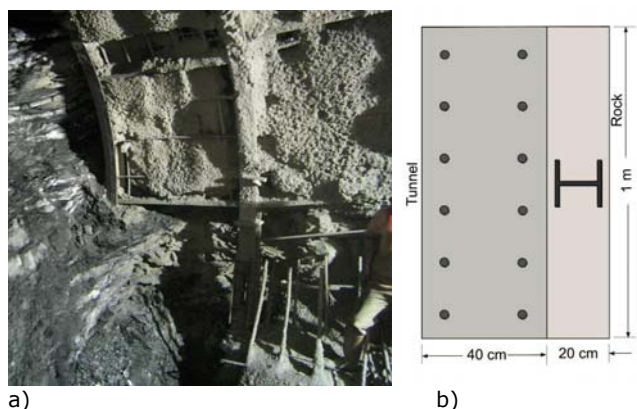


Figure 32. a) Configuration of mid-height bench (partially disintegrated in this photograph) and upper steel arch installed ahead of lower section and sliding joint. b) Final 60 cm section with outer shotcrete and steel set composite section and inner reinforced shotcrete section. The tunnel is to the left and rock mass is to the right of the section.

A 2D finite element plane strain analysis is then applied to the full face construction sequence (unsupported). The technique of progressive face replacement described in the previous section (Figure 7) is used here. The resulting points on the ground reaction curve (white diamonds on "Disp. vs Support Pressure" curve in Figure 33a) can be assigned locations along the tunnel (filled diamonds in Figure 33a) using the (dashed) longitudinal deformation profile.

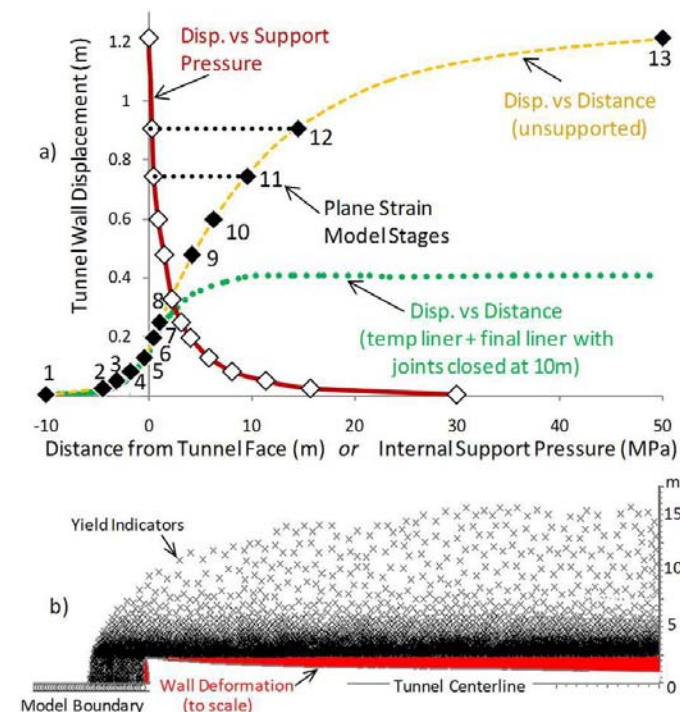


Figure 33 a) Ground reaction curve "Disp. vs Support Pressure" and corresponding longitudinal displacement profile "Disp vs Distance (unsupported)" for a axisymmetric model. Normalized plastic radius = 6.5. Longitudinal displacement profile function fitted based on Appendix 1. Point symbols and number ID's represent corresponding stages in plane strain model (related symbols are linked between two curves as shown for stage 11 and 12 by dotted lines). Sup-

ported longitudinal deformation profile (dashed line without symbols) shown for comparison. b) Axisymmetric model used for calibration showing yield indicators (x's) and wall displacement profile along tunnel.

The same correlation of model stage to tunnel location can be used for the benched tunnel model with offset stages of bench excavation and with appropriate installation of support (remember that the model support is installed at the beginning of the stage while the displacements are reported at the end of the stage). The benched tunnel model is illustrated in Figure 34.

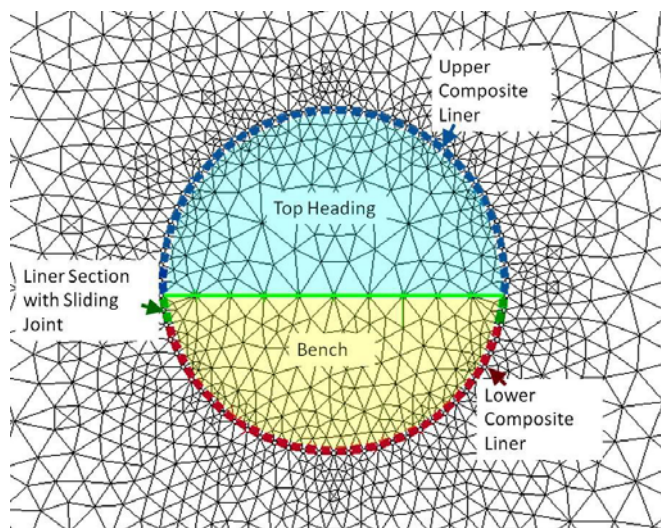


Figure 34. Finite element mesh, geometry of excavation stages and liner segments for 2D plane strain analysis of sequenced excavation and support.

It is anticipated that the steel sets and the initial 20 cm shotcrete layer will undergo some limited yielding after the sliding joints close. The upper half of the arch, installed in the bench, may also yield prior to this due to the moments induced by a reduction in the arch radius. This partial arch and the complete arch, with sliding joints, are modeled as separate but joined layers with appropriate material and section properties. They are assumed to act plastically with yield in the steel and a 33% reduction in residual uniaxial compressive strength of the shotcrete after yield.

Following the geometry in Figure 34, the bench excavation sequence lags behind the top heading by 2 stages. The upper composite liner is installed immediately behind the face (start of stage 7 in Figure 33). The lower composite liner and the sliding joints are installed approximately 1 m behind the bench (beginning of stage 9), and the filler sections of 20 cm shotcrete are installed and assumed to set by the beginning of stage 10. In this analysis the sliding joint gap closes automatically two stages later (within stage 11) between 6 and 10 m from the face.

The final lining is applied behind the gap closure, beginning of stage 12 (10 m from the face) for this analysis. This final lining is applied as an elastic composite according to the methodology in Appendix 2. For the purposes of this analysis, a symmetrical reinforcement array of 6 x 25 mm rebar per metre, 75 mm from each surface is used. The moment of inertia, section depth and total area are calculated for the rebar arrangement. The procedure is then similar as that described in Appendix 2 for steel sets. The relevant properties are given in Table 3.

The aging of shotcrete is neglected here as the excavation rate is very slow (approximately 1 m per day). The shotcrete used at the site was of very high quality and 7 day strength and stiffness values are used.

The short- and long-term liner loads are shown in Figure 35 for the full face excavation and for the top heading and bench option. The compromise required to provide a bench for face support results in a less uniform loading of the two halves of the arch and the build-up of moments in the sliding joint area. This effect is exaggerated dramatically if the final lining is installed before the sliding gap has closed.

To analyze the loadings within the steel and concrete components of the final inside lining layer, the equations in Appendix 2 are used to partition the loads and moments and to generate elastic capacity envelopes for comparison as shown for the full face options in Figure 36.

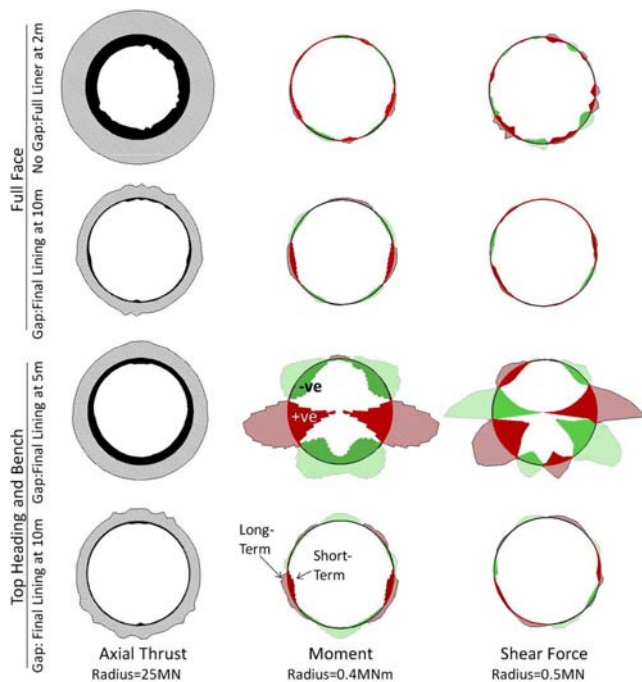


Figure 35. Relative magnitudes and distribution of total axial load, moment and shear load in the final 40 cm thick reinforced layer. Values plotted inside tunnel as solid represent short term loading conditions. Hatched values outside of tunnel represent long term conditions. Red shading indicates positive values for moment and shear, Green shading indicates negative values. This inner final liner layer is modeled elastically. This plot does not include residual loadings in the plastic outer lining layer (steel sets embedded in 20 cm shotcrete).

Table 3. Liner properties for reinforced 40 cm inner liner (for use with Appendix 2).

Tunnel Radius	2.52 m
Rebar Properties	
Number of Pairs per Section	6
Height of Rebar Section	0.25 m
Area of Section	0.005985 m <sup>2</sup>
Moment of Inertia	9.40E-05 m <sup>4</sup>
Young's Modulus	200000 MPa
Poisson's Ratio	0.3
Compressive Strength	400 MPa
Tensile Strength	-400 MPa
Width of Section	
	1 m
Shotcrete Properties	
Height of Section	0.4 m
Young's Modulus	30000 MPa
Poisson's Ratio	0.2
Compressive Strength	40 MPa
Tensile Strength	-4 MPa
Number of sets n	1

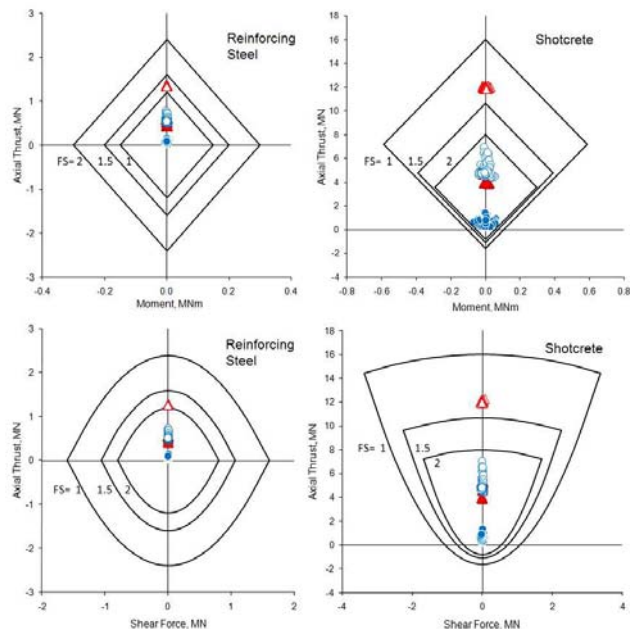


Figure 36. Partitioned liner loads compared to component capacity envelopes for full face tunnel option. Circles represent a full 60 cm lining, as per Figure 32b, installed in one step 2 m from the face. Triangles represent the option involving W 6x 20 sets installed at the face with a sliding gap in combination with 20 cm of shotcrete, followed at 10 m distance by a filled gap and 40 cm of reinforce shotcrete. These plots are for the inner 40 cm of reinforced shotcrete only. Filled symbols represent short term loading while open symbols are for long term loading.

The most obvious result from Figure 36 is the large axial thrust predicted in the full lining installed near the face with no sliding joints. This confirms the conclusion from Figure 29 and points to the definite requirement to allow deformation prior to full lining installation. For the full face excavation, the liner with a sliding joint and with the final reinforced layer applied at 10 m from the face performs well, giving a factor of safety for long term loading greater than 2 for all loading combinations. The limiting state is the short term moment in the shotcrete component (FS = 2). In this case the gap closed automatically in response to loading, between 5 and 10 m from the face, well before final lining installation.

As discussed, logistical and safety issues related to deformation and deterioration of the face mandated the adoption of a top heading and short bench sequence. This required the lining to be installed as an immediate top and slightly delayed bottom section. The partitioned capacity plots for top heading and bench excavation are shown in Figure 37.

For the top heading and bench option, the predicted performance is adequate in short and long term loading provided that the gap (sliding joint) is filled and the final lining completed after the joint has fully closed or the deformations have stabilized. The penalty for delaying liner completion will be unacceptable degradation and yielding of the initial 20 cm lining and the steel sets resulting in service and safety problems. While this initial composite layer is expected to yield to some degree, excessive yielding should be avoided. In addition, a long delay in the installation of the final liner could lead to loss of wall control.

The ideal condition is to fill the gap with shotcrete immediately upon joint closure to complete the lining. In this example, the joint or gap closes between 6 m and 10 m from the face. The triangles in Figure 37 represent completion of the final liner at 10 m. The limiting state in this case is the short term moment in the shotcrete (FS > 2). The open

circles in Figure 37 represent the case of premature completion of the final lining at 5 m from the face.

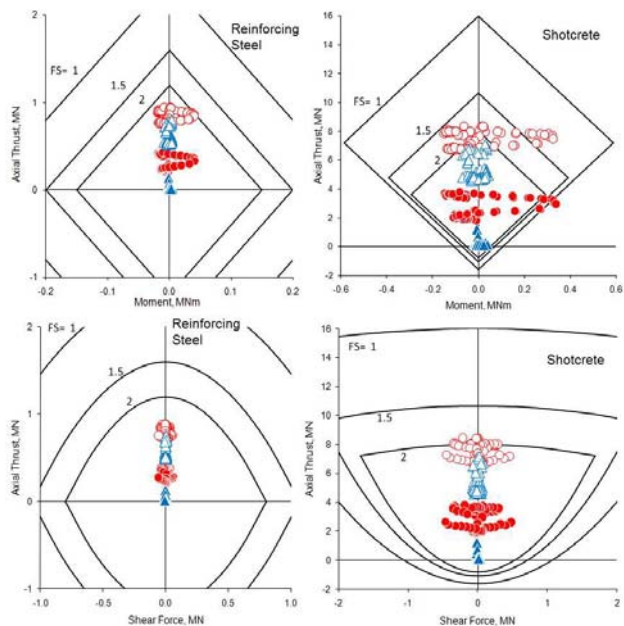


Figure 37. Partitioned liner loads compared to component capacity envelopes for top heading and bench options. In these analyses, the sliding joint (gap) closes automatically under load between 5 and 10 m. Circles represent completion of the final lining at 5 m from the face (before gap closure). Triangles represent the completion of the final lining at 10 m from the face (after gap closure). These plots are for the inner 40 cm of reinforced shotcrete only. Filled symbols represent short term loading while open symbols represent long term loading.

This design requires careful construction monitoring and management. If the gap is filled with shotcrete and the final lining completed before the joints are allowed to close or before deformations have stabilized, the penalty is increased axial, shear and moment loading throughout the liner. In the case shown here, cracking will be induced due to high moments for short term loading and the factor of safety for all loading combinations drops for long term loading.

Even with excellent construction management, however, it is possible that liner completion could take place too soon for some individual segments or rounds within the tunnel. From a hazard mitigation perspective it is important to understand the consequences of this possibility. The factors of safety illustrated in Figures 36 and 37 refer to initial cracking of the liner. Figure 38 illustrates an alternative analysis of the results in which the non-partitioned liner loadings and capacity envelopes are calculated in a non-linear fashion, using the program Response 2000 (Bentz, 2000) that allows plastic (cracked) moments.

Figure 38 shows that the critical loading, in the case of premature completion of the liner, is the short term moment. This is indicated by the calculated values falling outside the capacity envelopes for cracking. These envelopes are equivalent to the elastic envelopes for the partitioned liner, presented in the previous figures. This case still falls within the solid capacity envelopes representing the ultimate load capacity of the liner with tension cracks fully developed and internal loading redistributed. This indicates that the prematurely installed final lining will not collapse catastrophically in compression or bending. Instead, cracks would become visible during the construction phase of the tunnel and repairs can be made.

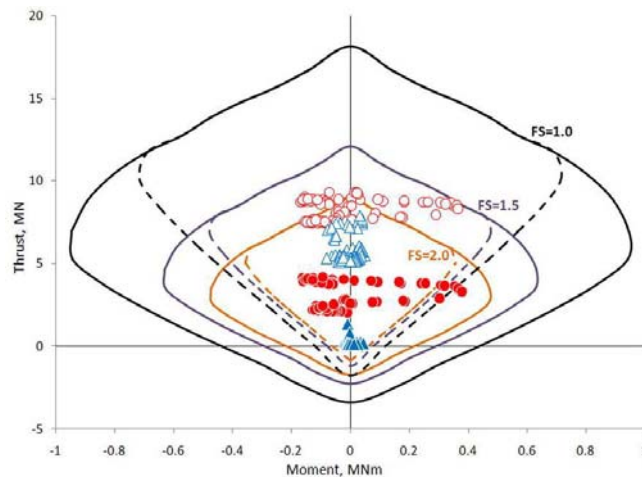


Figure 38. Total (non-partitioned) thrusts and moments from modeled inner liner of 40 cm reinforced shotcrete. Dashed envelopes represent limits for initial cracking of shotcrete. Solid envelopes represent capacity limits accounting for the development of additional moment capacity in the cracked liner as well as accounting for the tensile strength of the reinforcement (Vecchio and Collins, 1986). Triangles represent installation of the final lining at 10 m; circles represent completion at 5 m. Filled symbols indicate short term loading; open symbols indicate long term loading. Sliding joint closes automatically between 5 and 10 m from the face.

The ultimate result is a reduced long term factor of safety for all loading conditions, again reinforcing the need for good construction management to ensure the correct installation sequence for potentially variable rock mass conditions and deformation rates.

The appearance of the tunnel, constructed as described in this example, is shown in Figure 39.



Figure 39. Completed section of tunnel with a 60 cm thick reinforced shotcrete lining, placed in two layers as described above.

#### 4 CONCLUSIONS

A methodology for the design of tunnel linings has been presented. While this approach has been used by specialist tunnel designers for many years, it has never been described comprehensively in a single document that allows the reader to follow all the derivations and the step by step calculations. To make this process as easy as possible to follow, the authors have included two case history based examples, one for a very shallow tunnel and the other for a very deep tunnel. These examples have been chosen to

highlight the complex loading conditions that can occur under different geological and topographic conditions and how these complexities can be incorporated into a rational lining design.

The support capacity diagrams are based on elastic analysis of the support elements and this implies that no tensile cracking or compressive crushing of the shotcrete or concrete elements is acceptable. These simplified calculations allow the user to optimize the design of the lining components relatively quickly and efficiently. It has been demonstrated that, where tensile cracking becomes an important consideration, more sophisticated non-linear structural design approaches, which allow for crack development, can be used.

## 5 ACKNOWLEDGEMENTS

The authors wish to acknowledge the important contribution made by Professor Evan Bentz of the University of Toronto who, by making his structural program *Response 2000* available, provided the means for the early development of the procedures described in this paper.

Ing Rafael Guevara Bricepo, consultant on the Yacambi-Quibor project in Venezuela, has worked with Dr Evert Hoek for many years and has also cooperated with all the authors in the development of many of the ideas presented in this paper. He has taught all of us a great deal about the reality of very difficult tunnelling.

The permission of Sistema Hidraulico Yacambi-Quibor C.A. (<http://www.yacambu-quibor.com.ve/>) to use information on the Yacambi-Quibor tunnel is acknowledged.

## 6 SOFTWARE

The methodologies described in this paper can be used with any modern numerical package provided the input and verification of results are done according to equations and procedures presented. The three-dimensional analyses were carried out using FLAC3D, developed and sold by Itasca ([www.itascacg.com](http://www.itascacg.com)) while all other calculations were performed using Phase2, developed and sold by Rocscience ([www.rocscience.com](http://www.rocscience.com)).

The structural program *Response 2000*, developed by Professor Bentz, can be downloaded (free) from (<http://www.ecf.utoronto.ca/~bentz/home.shtml>).

## 7 REFERENCES

- American Concrete Institute (2005). ACI 318-05. *Building Code Requirements for Structural Concrete*. Farmington Hills, Michigan.
- Barton, N.R., Lien, R. and Lunde, J. 1974. Engineering classification of rock masses for the design of tunnel support. *Rock Mech.* **6**(4), 189-239.
- Bentz, E.C., Sectional Analysis of Reinforced Concrete, *PhD Thesis*, Department of Civil Engineering, University of Toronto, 2000.
- Bieniawski, Z.T. 1973. Engineering classification of jointed rock masses. *Trans S. Afr.Inst.Civ.Engrs* **15**, 335-344.
- British Tunnelling Society, 2004. *Tunnel lining design guide*. Thomas Telford, London.
- Carranza-Torres, C., Fairhurst, C., 2000. Application of the convergence-confinement method of tunnel design to rock masses that satisfy the Hoek-Brown failure criterion. *Tunnelling Underground Space Technology* **15**(2), 187-213
- Carranza-Torres, C. and Diederichs, M.S. (2008) Mechanical analysis of a circular liner with particular reference to composite supports –e.g., liners consisting of shotcrete and steel sets, Submitted for review and publication to *Tunnelling and Underground Space Technology* (December 2007).
- Chern, J.C., Shiao, F.Y., Yu, C.W. 1998. An empirical safety criterion for tunnel construction. *Proceedings of the Regional Symposium on Sedimentary Rock Engineering*, Taipei, Taiwan, 222-227.
- Duddeck, H. 1988. Guidelines for the Design of Tunnels. Prepared by the International Tunnelling Association Working Group on General Approaches to the Design of Tunnels. *Tunnelling and Underground Space Technology*, **3**(3). 237-249.
- Guevara Bricepo, R. 2004a. Túnel Yacambú-Quibor, Experiencia de Construcción – Reparación Tramo entre las Progresivas 12+800 a 12+950. In Sociedad Venezolana de Geotecnia (Ed.), *Actas del XVII Seminario Venezolano de Geotecnia. Geoinfraestructura: la Geotecnia en el Desarrollo Nacional*. Caracas, Venezuela. Noviembre, 2004.
- Guevara Bricepo, R. 2004b. Aspectos sobre diseño y construcción de los últimos 4.6 km del túnel de Yacambú. In Sociedad Venezolana de Geotecnia (Ed.), *Actas del XVII Seminario Venezolano de Geotecnia. Geoinfraestructura: la Geotecnia en el Desarrollo Nacional*. Caracas, Venezuela. Noviembre, 2004.
- Hoek, E, 2001. Big tunnels in bad rock, 2000 Terzaghi lecture. *ASCE Journal of Geotechnical and Geoenvironmental Engineering*, **127**(9), 726-740.
- Hoek, E. and Marinos, P. 2000 Predicting Tunnel Squeezing. *Tunnels and Tunnelling International*. Part 1 – November 2000, Part 2 – December, 2000.
- Hoek E., Carranza-Torres C., Corkum B. 2002 Hoek-Brown criterion – 2002 edition. *Proc.NARMS-TAC Conference*, Toronto, 2002, 267-273.
- Hoek, E. 1992. When is a design in rock engineering acceptable ? - 1991 Möller lecture. *Proc. 7th Congress Intl. Soc. Rock Mech.*, Aachen. Rotterdam : A.A. Balkema.
- Hoek, E. and Diederichs, M. S. 2006. Empirical estimation of rock mass modulus. *Int. J. Rock Mech. Min. Sci.* **43**(2), 203-215.
- Kaiser, P.K. 1985. Rational assessment of tunnel liner capacity. *Proc. 5<sup>th</sup> Canadian Tunnelling Conference*. Montreal.
- Lunardi, P. 2000. The design and construction of tunnels using the approach based on the analysis of controlled deformation in rocks and soils. *Tunnels and Tunnelling International special supplement*, ADECO-RS approach, May 2000.
- Marinos, P and Hoek, E. (2000) GSI – A geologically friendly tool for rock mass strength estimation. *Proc. GeoEng2000 Conference*, Melbourne. 1422-1442.
- Melbye, T. and Garshol, K.F. 2000. *Spayed shotcrete for rock support*. Master Builders Technologies.
- O'Rourke, T.D. 1984. *Guidelines for tunnel lining design*. Prepared by Technical Committee on Tunnel Lining Design of the Underground Technology Research Council, ACSE, New York.
- Panet M. 1995. *Calcul des Tunnels par la Méthode de Convergence-Confinement*. Presses de l'Ecole Nationale des Ponts et Chaussées. Paris. 178p
- Panet, M. 1993. Understanding deformations in tunnels. In: Hudson, J.A., Brown, E.T., Fairhurst, C., Hoek, E. (Eds.),

Panet, M. and Guenot, A. 1982. Analysis of convergence behind the face of a tunnel. *Proceedings, International Symposium Tunnelling'82*, IMM, London, 197-204.

Salcedo, D. 1983. Macizos Rocosos: Caracterización, Resistencia al Corte y Mecanismo de Rotura. *Proc. 25. Aniversario Conferencia Soc. Venezolana de Mecanica de Suelos e Ingenierva de Fundaciones*, Caracas. 143-172.

Sánchez Fernandez, J.L. and Terán Benítez, C.E. 1994. Túnel de Trasvase Yacambú-Quibor. Avance Actual de los Trabajos de Excavación Mediante la Utilización de Soportes Flexibles Aplicados a Rocas con Grandes Deformaciones. *Proc. IV Congreso Sudamericano de Mecanica de Rocas*, Santiago 1, 489-497.

Schubert, W. 1996. Dealing with squeezing conditions in Alpine tunnels. *Rock Mech. Rock Engrg.* **29**(3), 145-153.

Sauer, G., Gall, V. Bauer, E and Dietmaier, P. 1994. Design of tunnel concrete linings using limit capacity curves. in *Computer Methods and Advances in Geomechanics*, Eds.: Siriwardane & Zaman, Rotterdam, NL. 2621 - 2626.

Unlu, T. and Gercek, H. 2003. Effect of Poisson's ratio on the normalized radial displacements occurring around the face of a circular tunnel. *Tunnelling and Underground Space Technology.* **18**. 547-553

Vecchio, F.J., and Collins, M.P., 1986. The Modified Compression Field Theory for Reinforced Concrete Elements Subjected to Shear, *ACI Journal*, **83**(2), 219-231

Vlachopoulos, N. and Diederichs, M.S. 2008. Comparison of 2D and 3D analysis methods for single and paired tunnels in weak highly stressed ground. Paper in preparation - to be submitted to *Tunnels and Underground Space Technology*. 40 manuscript pages.

## 8 APPENDIX 1 – CALCULATION OF LONGITUDINAL DISPLACEMENT PROFILES

In order to design the appropriate timing for the installation of stiff support or when optimizing the installation of support with specific displacement capacity, it is important to determine the longitudinal closure profile for the tunnel. A portion of the maximum radial displacements at the tunnel boundary will take place before the face advances past a specific point. The tunnel boundary will continue to displace inwards as the tunnel advances further beyond the point in question. This longitudinal profile of closure or displacement versus distance from the tunnel face is called the longitudinal displacement profile and can be calculated using three-dimensional models for complex loading and geometric conditions or with axisymmetric models for uniform or isotropic initial stress conditions and circular tunnel cross sections. This profile can be used to establish a distance-convergence relationship for 2D modeling or for analytical solutions (as in Carranza-Torres and Fairhurst, 2000). The following discussion of longitudinal displacement profile estimation is excerpted from Vlachopoulos and Diederichs (2008).

In order to facilitate analytical calculations of ground response (convergence-confinement) Panet (1995) derived a relationship for the longitudinal displacement profile based on elastic analysis:

$$\frac{u_r}{u_{max}} = \frac{1}{4} + \frac{3}{4} \left( 1 - \left( \frac{3}{3 + 4d_t} \right)^2 \right) \quad (A1.1)$$

where  $dt = X / R_t$ ,  $u_r$  is the average radial displacement at

a specified longitudinal position,  $X$ , and  $u_{max}$  is the maximum short term radial displacement distant from the face and corresponding to plane strain analysis of a tunnel cross section.  $R_t$  is the tunnel radius and  $X$  is positive into the tunnel away from the face ( $X = 0$ ). The position  $X$  is negative into the rock ahead of the face and is specified along the tunnel centerline.

Numerous other authors have suggested alternative expressions for the elastic longitudinal displacement profile including Unlu and Gercek (2003) who noted that the curve in front of the face and the curve behind the face do not follow a single continuous functional relationship with  $X$ . The radial deformation profile with respect to distance from the face is accurately predicted for the elastic case to be:

$$\text{for } X < 0 \quad \frac{u_r}{u_{max}} = \frac{u_0}{u_{max}} + A_a \left( 1 - e^{B_a d_t} \right) \quad (A1.2)$$

$$\text{for } X > 0 \quad \frac{u_r}{u_{max}} = \frac{u_0}{u_{max}} + A_b \left( 1 - (B_b / (A_b + d_t))^2 \right)$$

where  $u_0$  is the radial displacement at the face location ( $X=0$ ) and  $A_a$ ,  $A_b$ ,  $B_a$ ,  $B_b$  are functions of Poisson's Ratio:

$$\begin{aligned} \frac{u_0}{u_{max}} &= 0.22\nu + 0.19; \\ A_a &= -0.22\nu - 0.19; B_a = 0.73\nu + 0.81 \\ A_b &= -0.22\nu + 0.81; B_b = 0.39\nu + 0.65 \end{aligned} \quad (A1.3)$$

These preceding equations are for elastic deformation. Panet (1993, 1995), Panet and Guenot (1982), Chern et al. (1998) and other have proposed empirical solutions for longitudinal displacement profiles based on plastic modeled deformation of varying intensity (correlated to various indices such as the ratio between insitu stress and undrained cohesive strength, for example).

Alternatively, an empirical best fit to actual measured closure data can be used (for example based on data from Chern et al, 1998):

$$\frac{u_r}{u_{max}} = \left( 1 + e^{\left( \frac{-d_t}{1.10} \right)^{-1.7}} \right) \quad (A1.4)$$

These relationships are summarized in Figure A1.1.

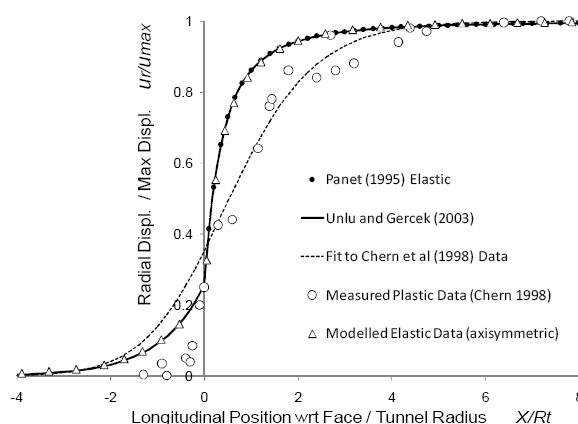


Figure A1.1: Longitudinal displacement profile functions from various researchers and example data from Chern et al.(1998).

The development of radial deformation, however, is directly linked to the development of the plastic zone as the tunnel

advances. Studies by the authors have shown that the longitudinal displacement profile function proposed by Panet (1995) and by Unlu and Gercek (2003) is reasonable for plastic analysis provided that the radius of the plastic zone does not exceed 2 tunnel radii and provided that the yielding zone in the tunnel face does not interact with the developing yield zone around the tunnel walls as illustrated in Figure A1.2.

The advancing front of plastic yielding is bullet shaped in three dimensions and for large plastic zones (radius of plastic zone  $R_p \gg 2$ ) the shape of this developing yield zone is geometrically similar for increasing maximum plastic radii. There is no reason, therefore to expect that a single longitudinal displacement profile will suffice for these conditions. In order to account for the influence of increased overall yielding on the shape of the normalized longitudinal displacement profile, the most logical index to relate to the longitudinal displacement profile function is the ultimate radius of the normalized plastic zone radius,  $R_p/R_t$ .

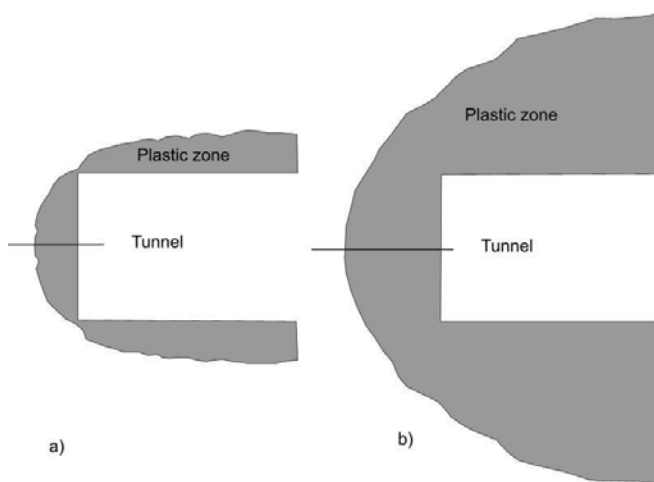


Figure A1.2: a) Plastic yield zone developing as tunnel advances to the left. Maximum plastic zone radius is less than twice the tunnel radius and the wall yield zone does not interact with the face yield zone (Panet's 1995 longitudinal displacement profile is valid); b) wall yield zone more than double the tunnel radius and interacts with face yield zone (Panet's longitudinal displacement profile is not valid).

To illustrate this problem, one series of analyses were performed involving a radial tunnel section and an axisymmetric analysis along the tunnel axis. The first suite of analyses is based on a typical rock mass at 1100m depth in graphitic phyllite found in the Yacambu-Quibor Tunnel in Venezuela. This is case  $A_1$  in the table below. In this case the initial insitu stress is approximately 10 times the estimated rock mass uniaxial strength. 5 other rock masses are investigated with increasing strength (increasing intact strength and/or GSI) giving a series of representative cases with varying  $P_0/V_{crn}$  (in situ stress/rock mass strength). The rock mass parameters are summarized in Table A1.1.

The rock mass strengths are estimated as per Hoek et al (2002) and the elastic moduli are estimated based on Hoek and Diederichs (2007). A second set of analyses were performed based on rock mass  $A_1$  (plastic) and  $G_1$  (elastic) in Table A1.1 the stress levels listed in Table A1.2:

The tunnels were analyzed (with Phase2) in plane strain cross section to determine the extent of the plastic zone and the maximum radial deformation in each case. In addition, the cases were analyzed, using axisymmetric models, with 1 m incremental advance to determine the longitudinal displacement profile in each case as shown in Figure A1.3. The maximum displacements and sizes of plastic zone were comparable between the radial and longitudinal models. These summary results are presented in Table A1.3 and the

resultant normalized longitudinal displacement profiles are presented in Figure A1.4.

Table A1.1: Rockmass parameters for longitudinal displacement profile analysis using PHASE2 (constant  $P_0 = 28$  MPa)

	$A_1$	$B_1$	$C_1$	$D_1$	$E_1$	$F_1$	$G_1$
$P_0/\sigma_{cm}$	10	8	6	4	2	1	Elastic
$\sigma_{ci}$ (MPa)	35	35	35	50	75	100	
$m_i$	7	7	7	7	7	7	
$\nu$	0.25	0.25	0.25	0.25	0.25	0.25	
GSI	25	35	45	48	60	74	
$m$	0.481	0.687	0.982	1.093	1.678	2.766	
$s$	0.0002	0.0007	0.0022	0.0031	0.0117	0.0536	
$a$	0.531	0.516	0.508	0.507	0.503	0.501	
$E_m$ (MPa)	1150	2183	4305	7500	11215	27647	1150
$\sigma_{cm}$ (MPa)	2.8	3.5	4.7	7	14	28	
$P_0$ (MPa)	28	28	28	28	28	28	28
Radius, m	2.5	2.5	2.5	2.5	2.5	2.5	2.5

Table A1.2: Rockmass parameters for longitudinal displacement profile analysis using PHASE2 (constant  $\sigma_{cm} = 2.8$  MPa)

	$A_2$	$B_2$	$C_2$	$D_2$	$E_2$	$F_2$	$G_2$
$P_0/\sigma_{cm}$	10	8	6	4	2	1	elastic
$P_0$ (MPa)	28	22.4	16.8	11.2	5.6	2.8	28

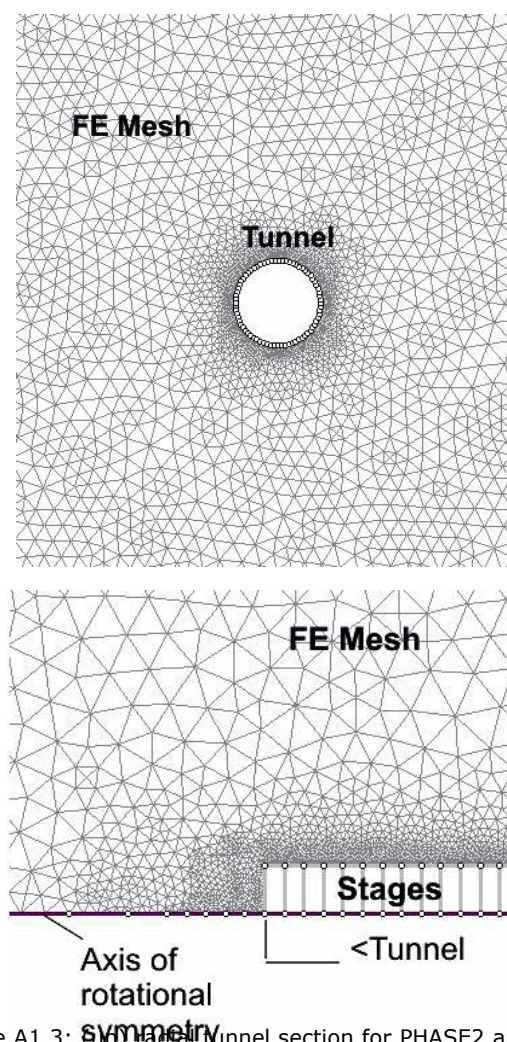


Figure A1.3: (top) radial tunnel section for PHASE2 analysis; (down) axisymmetric model with 1 m excavation stages (tunnel advances to the left).

Table A1.3: Summary results from radial and longitudinal (axisymmetric) analysis

$P_0/\sigma_{cm}$	10	8	6	4	2	1	Elastic
Constant $P_0$	$A_1$	$B_1$	$C_1$	$D_1$	$E_1$	$F_1$	$G$
Plastic $R_p$	7.5	5.1	3.5	2.3	1.5	1.2	1
Max Disp	2.14	0.571	0.154	0.0495	0.0148	0.00367	0.0753
Constant $\sigma_{cm}$	$A_2$	$B_2$	$C_2$	$D_2$	$E_2$	$F_2$	$G$
Plastic $R_p$	7.5	6.3	5.0	3.3	2.2	1.6	1

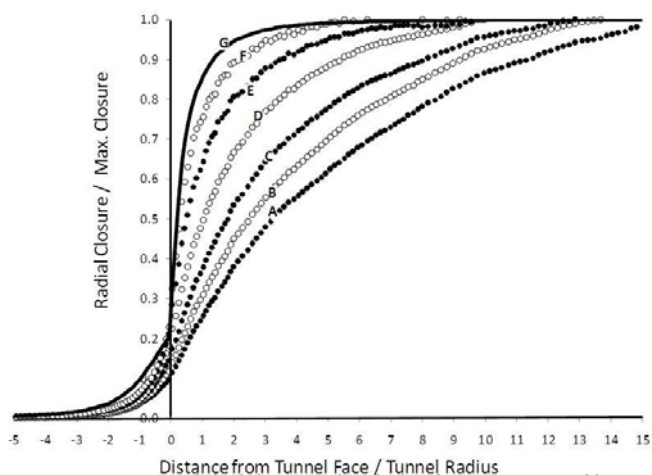
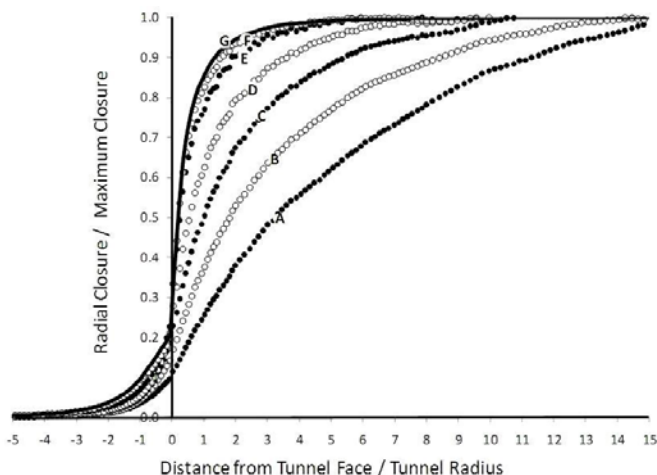


Figure A1.4: Modeled longitudinal displacement profile results for axisymmetric models: (top) constant  $P_0$  model results; (bottom) constant  $V_{crm}$  model. Labeled results (A-G) correspond to models in Table A1.3.

By inspection of Figure A1.4 it is evident that the longitudinal displacement profile does not correlate with the stress/strength index  $P_0/V_{crm}$  as the set of curves in both plots represent the same selected values for this ratio and yet have different longitudinal displacement profiles. Analysis of the data, however, shows a direct correlation with the maximum normalized plastic zone,  $R_p/R_t$ , as expected. The correlation between  $u_0/u_{max}$  at  $X/R_t = 0$  (at the face) and the maximum plastic radius,  $R_p/R_t$ , is shown in Figure A1.5. Ignoring the influence of Poisson's ratio (negligible compared to plastic yielding) the best fit relationship (independent of material parameters and stress levels) is:

$$\frac{u_0}{u_{max}} = \frac{1}{3} e^{-0.15P_r} \quad (A1.5)$$

where  $P_r = R_p / R_t$

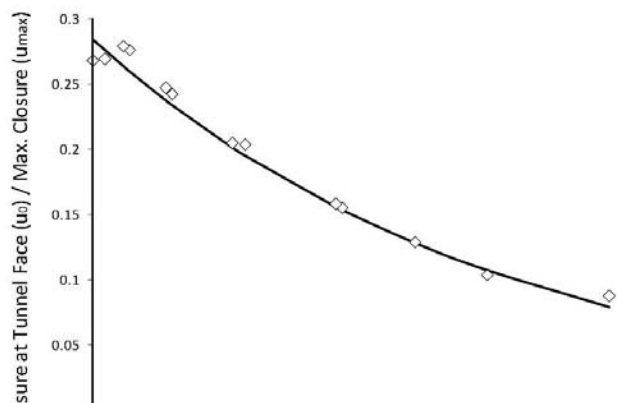


Figure A1.5: Correlation between  $u_0/u_{max}$  at  $X/R_t = 0$  (at the face) and the maximum plastic radius,  $R_p/R_t$ , for analyses in table A1.4.

The relationships proposed by Unlu and Gercek (2003) correctly illustrate that the behaviour ahead of the face ( $X < 0$  into the rockmass) does not follow the same continuous function as the behavior (progressive displacement) behind the face ( $X > 0$  in the tunnel). Their functions summarized in Equation A1.2, do not, however, capture the influence of a large developing plastic zone.

Based on the analysis in the preceding discussion, a new set of relationships are presented here that capture the influence of large plastic zone development on the longitudinal displacement profile. Equation A1.5 gives the relationship between normalized plastic radius and normalized closure at the face ( $X=0$ ). Equations A1.6 and A1.7 give the best fit longitudinal displacement profile for  $X < 0$  and  $X > 0$  as a function of normalized maximum plastic zone radius.

$$\frac{u}{u_{max}} = \frac{u_0}{u_{max}} \cdot e^{d_t} \quad \text{for } X < 0 \text{ (in the rock mass)} \quad (A1.6a)$$

$$d_t = \ln\left(\frac{u}{u_0}\right) \quad \text{for } u < u_0 \quad (A1.6b)$$

where  $u_0/u_{max}$  is given by Equation A1.5.

$$\frac{u}{u_{max}} = 1 - \left(1 - \frac{u_0}{u_{max}}\right) \cdot e^{-\frac{3d_t}{2P_r}} \quad \text{for } X > 0 \text{ (in the tunnel)} \quad (A1.7a)$$

$$d_t = -\frac{2}{3} P_r \ln\left(\frac{u_{max} - u}{u_{max} - u_0}\right) \quad \text{for } u > u_0 \quad (A1.7b)$$

The correlation with model data is shown in Figure A1.6

There is an important caveat to consider when using numerical analysis to compute longitudinal displacement profiles. When using axisymmetric or full three-dimensional models to determine the longitudinal displacement profile relationship, it is important to consider the excavation rate. A stress front builds ahead of the bullet shaped plastic zone and influences the rate of plastic zone development. Such models will yield a different apparent longitudinal displacement profile depending on the size of the excavation step. This is clearly shown in Figure A1.7, where there is a significant difference between the instantaneous excavation and the 1m (0.2D) step simulation (other excavation step sizes shown for comparison). For support sequencing it is important to simulate the actual excavation step size or, if the tunneling is continuous (TBM), to use a small step size.

be able to adjust the number and dimensions of each to accommodate the loads imposed on the lining. In current tunnel design, these loads are obtained from numerical analyses in which “beam elements” are attached to the tunnel boundary and the axial thrust, bending moments and shear forces induced in these elements are computed directly.

Note that these beam elements constitute “tunnel support” and they interact with the surrounding rock mass to limit the convergence of the tunnel. On the other hand, rockbolts act as “tunnel reinforcement” in that they change the mechanical properties of the rock mass surrounding the tunnel. Hence, it is possible to carry out a numerical analysis of a tunnel reinforced by means of rockbolts and supported by means of a composite lining. The loads imposed on the lining will be reduced by the reinforcement and the composite lining will respond to these reduced loads. The analysis that follows is valid whether rockbolts are present or not, provided that the numerical analysis correctly models the load transfer from the rock mass onto the lining.

Figure A2.1 represents the problem to be analyzed involving a section of composite liner of width  $b$  comprising  $n$  steel sets and  $n$  units of shotcrete — note that if  $n$  units of each material exist along the width  $b$ , this is equivalent to saying that the units are spaced at  $s = b/n$ . The composite section in Figure 1 can be regarded as an equivalent section of width  $b$  and thickness  $t_{eq}$ .

The steel sets are assumed to be symmetrically placed in the shotcrete lining so that the neutral axes of both the steel sets and the shotcrete lining are coincident. For the purposes of this analysis it is assumed that the complete shell behaves elastically. This is a reasonable assumption since the tunnel designer generally attempts to design the lining so that it will not fail.

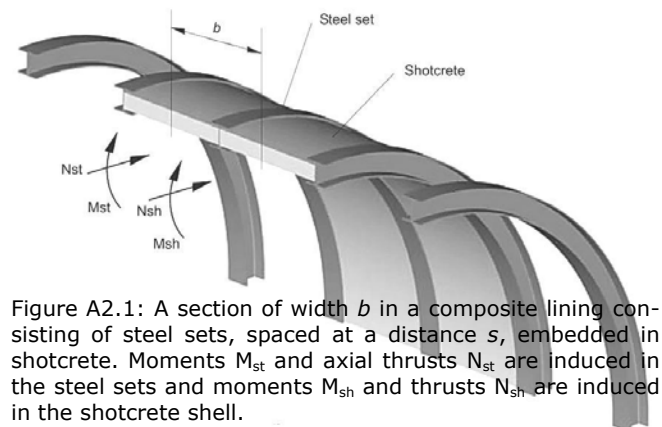


Figure A2.1: A section of width  $b$  in a composite lining consisting of steel sets, spaced at a distance  $s$ , embedded in shotcrete. Moments  $M_{st}$  and axial thrusts  $N_{st}$  are induced in the steel sets and moments  $M_{sh}$  and thrusts  $N_{sh}$  are induced in the shotcrete shell.

In order to calculate the moments and axial thrusts induced in the steel sets and the shotcrete shell and to compare these with the capacity of the steel sets and shotcrete, the following steps are required:

1. An “equivalent” rectangular section with a width of  $b$ , a thickness  $t_{eq}$  and a modulus of  $E_{eq}$ , is determined.
2. The capacity of the steel sets and the shotcrete lining are determined.
3. A numerical model of the tunnel is constructed and beam elements representing the equivalent rectangular section are applied to the tunnel perimeter.

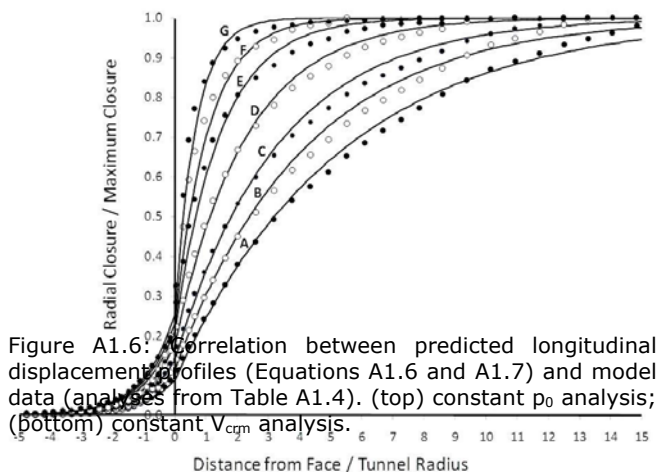
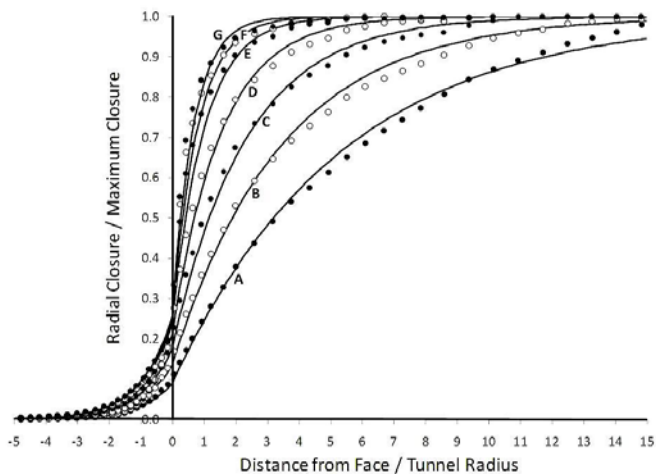


Figure A1.6: Correlation between predicted longitudinal displacement profiles (Equations A1.6 and A1.7) and model data (analyses from Table A1.4). (top) constant  $p_0$  analysis; (bottom) constant  $V_{cqm}$  analysis.

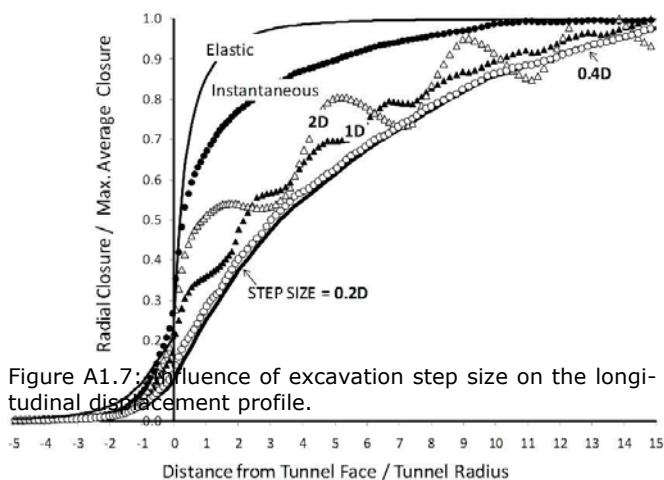


Figure A1.7: Influence of excavation step size on the longitudinal displacement profile.

## 9 APPENDIX 2 - MOMENTS AND FORCES IN LINING ELEMENTS

In a typical tunnel design in which support consists of steel sets embedded in shotcrete, the designer needs to know the contribution of each of these support elements and to

4. The bending moments and axial thrusts are redistributed back onto the steel sets and shotcrete lining.

### 9.1 Calculation of equivalent section

The properties of the equivalent rectangular section are calculated as follows. For plane strain conditions the compressibility coefficient  $D_{st}$  and flexibility coefficient  $K_{st}$  for the steel sets are:

$$D_{st} = \frac{E_{st} A_{st}}{1 - \nu_{st}^2} \quad (A2.1)$$

$$K_{st} = \frac{E_{st} I_{st}}{1 - \nu_{st}^2} \quad (A2.2)$$

where  $E_{st}$  is the Young's modulus of the steel  
 $A_{st}$  is the cross-sectional area of each steel set  
 $I_{st}$  is the moment of inertia of each steel set and  
 $\nu_{st}$  is the Poisson's ratio of the steel

For the shotcrete shell, the compressibility and flexibility coefficients are:

$$D_{sh} = \frac{E_{sh} A_{sh}}{1 - \nu_{sh}^2} \quad (A2.3)$$

$$K_{sh} = \frac{E_{sh} I_{sh}}{1 - \nu_{sh}^2} \quad (A2.4)$$

where  $E_{sh}$  is the Young's modulus of the shotcrete  
 $A_{sh}$  is the cross-sectional area of each unit of shotcrete =  $s \cdot t_{sh}$   
 $I_{sh}$  is the moment of inertia of each unit of shotcrete =  $(s \cdot t_{sh}^3) / 12$   
 $\nu_{sh}$  is the Poisson's ratio of the shotcrete

The equivalent compressibility and flexibility coefficients for the composite lining are:

$$D_{eq} = n(D_{st} + D_{sh}) \quad (A2.5)$$

$$K_{eq} = n(K_{st} + K_{sh}) \quad (A2.6)$$

The equivalent section has a width of  $b$ , an equivalent section thickness  $t_{eq}$  and the equivalent modulus  $E_{eq}$ . The equivalent compressibility and flexibility coefficients can be written as:

$$D_{eq} = b \cdot t_{eq} E_{eq} \quad (A2.7)$$

$$K_{eq} = E_{eq} \frac{b \cdot t_{eq}^3}{12} \quad (A2.8)$$

Solving for the variables  $t_{eq}$  and  $E_{eq}$ :

$$t_{eq} = \sqrt{\frac{12 K_{eq}}{D_{eq}}} \quad (A2.9)$$

$$E_{eq} = \frac{D_{eq}}{b t_{eq}} \quad (A2.10)$$

### 9.2 Calculation of support capacity

In order to check whether the induced stresses in the steel sets and shotcrete lining are within permissible limits, it is useful to plot the moments, shear forces and thrusts on support capacity diagrams. The support capacity curves are

calculated as follows:

#### 9.2.1 Moment-thrust capacity

The maximum permissible compressive and tensile stresses induced in the lining are given by:

$$\frac{\sigma_{max}}{FS} = \frac{N}{A} + \frac{Mt}{2I} \quad (A2.11)$$

$$\frac{\sigma_{min}}{FS} = \frac{N}{A} - \frac{Mt}{2I} \quad (A2.12)$$

where FS is the factor of safety.

The maximum and minimum permissible thrust capacity is obtained by substituting  $M = 0$  in equations A2.11 and A2.12, giving:

$$N_{max} = \frac{A \sigma_{max}}{FS} \quad (A2.13)$$

$$N_{min} = \frac{A \sigma_{min}}{FS} \quad (A2.14)$$

The maximum bending moment is obtained when tensile and compressive failures occur simultaneously which, by eliminating N from equations A2.11 and A2.12, gives:

$$M_{max} = \pm \left( \frac{\sigma_{max} - \sigma_{min}}{FS} \right) \frac{I}{t} \quad (A2.15)$$

The corresponding normal force  $N_{cr}$  at which these maximum moments occur is given by:

$$N_{cr} = \frac{A(\sigma_{max} + \sigma_{min})}{2FS} \quad (A2.16)$$

#### 9.2.2 Shear force-thrust capacity

In terms of shear force and axial thrust relationships:

$$\sigma_{max} = \frac{N}{A} \quad (A2.17)$$

$$\tau_{max} = \frac{3Q}{2A} \quad (A2.18)$$

$$\sigma_{1,3} = \frac{\sigma_{max}}{2} \pm \sqrt{\left( \frac{\sigma_{max}}{2} \right)^2 + \tau_{max}^2} \quad (A2.19)$$

$$FS = \frac{\sigma_c}{\sigma_1} = \frac{\sigma_t}{\sigma_3} \quad (A2.20)$$

For failure in compression:

$$N = \frac{\sigma_c A}{FS} - \frac{9Q^2 FS}{4\sigma_c A} \quad (A2.21)$$

For failure in tension:

$$N = \frac{\sigma_t A}{FS} - \frac{9Q^2 FS}{4\sigma_t A} \quad (A2.22)$$

The critical value of the shear force  $Q_{cr}$  associated with a particular factor of safety FS for both failure in compression and tension at the same time is:

$$Q_{cr} = \pm \frac{A}{FS} \sqrt{-\frac{4\sigma_c \sigma_t}{9}} \quad (A2.23)$$

Note that  $\sigma_t$  is negative.

### 9.3 Redistribution of thrust and moment onto steel sets and shotcrete

The bending moments, shear forces and axial thrusts are calculated by means of a numerical analysis and for the equivalent composite lining of width  $b$  and thickness  $t_{eq}$ . In order to consider the behavior of the steel sets and the shotcrete separately, it is necessary to redistribute these thrusts and moments back onto the individual support elements.

Since many of the linings are attached to curved surfaces and, in some cases, these linings are relatively thick compared to their radius  $R$ , it is necessary to consider the redistribution in terms of a thick curved beam solution. This solution is the most general since it automatically degenerates to a thin beam solution as the radius of curvature increases to infinity.

The equations for the redistribution of the moment  $M$ , axial thrust  $N$  and shear forces  $Q$  induced in any one of the beam elements representing the equivalent shell are:

Steel set moments:

$$M_{st} = \frac{MK_{st}}{n(K_{st} + K_{sh})} \quad (A2.24)$$

Shotcrete moments:

$$M_{sh} = \frac{MK_{sh}}{n(K_{st} + K_{sh})} \quad (A2.25)$$

Steel set thrusts:

$$N_{st} = \frac{N \cdot D_{st}}{n(D_{st} + D_{sh})} + \frac{M(D_{sh}K_{st} - D_{st}K_{sh})}{nR(D_{st} + D_{sh})(K_{st} + K_{sh})} \quad (A2.26)$$

Shotcrete thrust:

$$N_{sh} = \frac{N \cdot D_{sh}}{n(D_{st} + D_{sh})} - \frac{M(D_{sh}K_{st} - D_{st}K_{sh})}{nR(D_{st} + D_{sh})(K_{st} + K_{sh})} \quad (A2.27)$$

Steel set shear forces:

$$Q_{st} = \frac{QK_{st}}{n(K_{st} + K_{sh})} \quad (A2.28)$$

Shotcrete shear forces:

$$: Q_{sh} = \frac{QK_{sh}}{n(K_{st} + K_{sh})} \quad (A2.29)$$

### 9.4 Support capacity plots

The capacity plots described above can be calculated by means of a simple spreadsheet. The following input parameters have been assumed for this analysis

#### Steel sets

Tunnel radius	$R = 2 \text{ m}$
Steel set spacing	$s = 0.6 \text{ m}$
Steel set height	$t_{st} = 0.162 \text{ m}$
Area of steel set	$A_{st} = 4.75 \times 10^{-3} \text{ m}^2$
Moment of Inertia	$I_{st} = 2.23 \times 10^{-5} \text{ m}^4$
Modulus of steel	$E_{st} = 200,000 \text{ MPa}$
Poisson's ratio	$Q = 0.25$
Compressive strength	$V_{cst} = 500 \text{ MPa}$
Tensile strength	$V_{tst} = -500 \text{ MPa}$

#### Shotcrete lining

Shotcrete thickness	$t_{sh} = 0.2 \text{ m}$
Modulus of shotcrete	$E_{sh} = 30,000 \text{ MPa}$
Poisson's ratio	$Q = 0.15$
Compressive strength	$V_{csh} = 40 \text{ MPa}$
Tensile strength	$V_{tsh} = -2.5 \text{ MPa}$
Area of shotcrete	$A_{sh} = s \cdot t_{sh} = 0.12 \text{ m}^2$
Moment of Inertia	$I_{sh} = s \cdot t_{sh}^3 / 12 = 0.0004 \text{ m}^4$

Calculation of Support capacity diagrams for a Factor of Safety = 1.0

Steel sets	M	N
Maximum Thrust	0.00	2.38
Maximum moment	0.14	0.00
Minimum thrust	0.00	-2.38
Minimum moment	-0.14	0.00
Complete fig	0.00	2.38

Shotcrete lining	M	N
Maximum Thrust	0.00	4.80
Maximum moment	0.09	2.10
Minimum thrust	0.00	-0.60
Minimum moment	-0.09	2.10
Complete fig	0.00	4.80

Shear force - axial thrust plot

Steel sets	Q	N	N
Maximum shear force	1.58		
Minimum shear force	-1.58		
	1.58	0.00	0.00
	1.19	1.04	-1.04
	0.79	1.78	-1.78
	0.40	2.23	-2.23
	0.00	2.38	-2.38
	-0.40	2.23	-2.23
	-0.79	1.78	-1.78
	-1.19	1.04	-1.04
	-1.58	0.00	0.00
Shotcrete lining	Q	N	N
Maximum shear force	1.13		
Minimum shear force	-1.13		
	1.13	4.20	4.20
	0.85	4.46	2.10
	0.57	4.65	0.60
	0.28	4.76	-0.30
	0.00	4.80	-0.60
	-0.28	4.76	-0.30
	-0.57	4.65	0.60
	-0.85	4.46	2.10
	-1.13	4.20	4.20

The following forces induced in the lining described above are redistributed into the steel and shotcrete components as defined by Equations A2.24 to A2.29. The lining was installed in a circular tunnel with a radius of 5 m in a rock mass with properties defined by:

Modulus $E = 4000 \text{ MPa}$
Peak cohesion = 2 MPa, Residual cohesion = 1 MPa
Peak friction angle = 40q, Residual friction angle = 35q

The rock mass is subjected to a horizontal stress normal to the tunnel axis of 4 MPa and a vertical stress of 2 MPa. The horizontal stress parallel to the tunnel axis is 2 MPa.

The results of these calculations are plotted in Figure A2.2.

Redistribution of forces into steel and shotcrete lining components (Equations A2.24 to A2.29)

Total M	Total Q	Steel N	Steel M	Steel Q	Shot N	Shot M	Shot Q
0.00692	0.00242	0.40880	0.00121	0.00042	1.39360	0.00294	0.00103
0.00591	0.00049	0.43527	0.00103	0.00009	1.48383	0.00251	0.00021
0.00451	0.00371	0.49292	0.00079	0.00065	1.68034	0.00192	0.00158
0.00266	0.00206	0.57431	0.00047	0.00036	1.95781	0.00113	0.00088
-0.00057	-0.00719	0.67026	-0.00010	-0.00126	2.28492	-0.00024	-0.00305
-0.00283	-0.00224	0.77803	-0.00050	-0.00039	2.65229	-0.00120	-0.00095
-0.00518	0.00738	0.86640	-0.00091	0.00129	2.95356	-0.00220	0.00313
-0.00632	-0.00213	0.91111	-0.00111	-0.00037	3.10595	-0.00269	-0.00091
-0.00680	0.00133	0.91191	-0.00119	0.00023	3.10869	-0.00289	0.00057
-0.00519	-0.00831	0.86533	-0.00091	-0.00146	2.94989	-0.00221	-0.00353
-0.00315	-0.00787	0.79319	-0.00055	-0.00138	2.70397	-0.00134	-0.00334
-0.00121	-0.00529	0.70242	-0.00021	-0.00093	2.39454	-0.00051	-0.00225
0.00239	-0.00134	0.59056	0.00042	-0.00023	2.01320	0.00101	-0.00057
0.00456	-0.00336	0.49313	0.00080	-0.00059	1.68109	0.00194	-0.00143
0.00617	0.00073	0.43500	0.00108	0.00013	1.48290	0.00262	0.00031
0.00626	-0.00133	0.40879	0.00110	-0.00023	1.39355	0.00266	-0.00057
0.00631	-0.00002	0.42241	0.00111	0.00000	1.43999	0.00268	-0.00001
0.00500	0.00211	0.48075	0.00088	0.00037	1.63887	0.00213	0.00090
0.00241	0.00237	0.57426	0.00042	0.00042	1.95762	0.00102	0.00101
-0.00028	0.00829	0.68655	-0.00005	0.00145	2.34045	-0.00012	0.00352
-0.00324	0.00972	0.79386	-0.00057	0.00170	2.70624	-0.00138	0.00413
-0.00627	0.00100	0.87449	-0.00110	0.00017	2.98111	-0.00266	0.00042
-0.00740	-0.00508	0.91454	-0.00130	-0.00089	3.11764	-0.00314	-0.00216
-0.00738	0.00174	0.90659	-0.00129	0.00030	3.09055	-0.00313	0.00074
-0.00461	0.00103	0.85673	-0.00081	0.00018	2.92057	-0.00196	0.00044
-0.00295	-0.00449	0.76633	-0.00052	-0.00079	2.61239	-0.00126	-0.00191
0.00012	-0.01188	0.65380	0.00002	-0.00208	2.22878	0.00005	-0.00505
0.00357	-0.00367	0.54585	0.00063	-0.00064	1.86081	0.00152	-0.00156
0.00526	-0.00100	0.46110	0.00092	-0.00018	1.57188	0.00224	-0.00043
0.00680	-0.00190	0.41097	0.00119	-0.00033	1.40097	0.00289	-0.00081

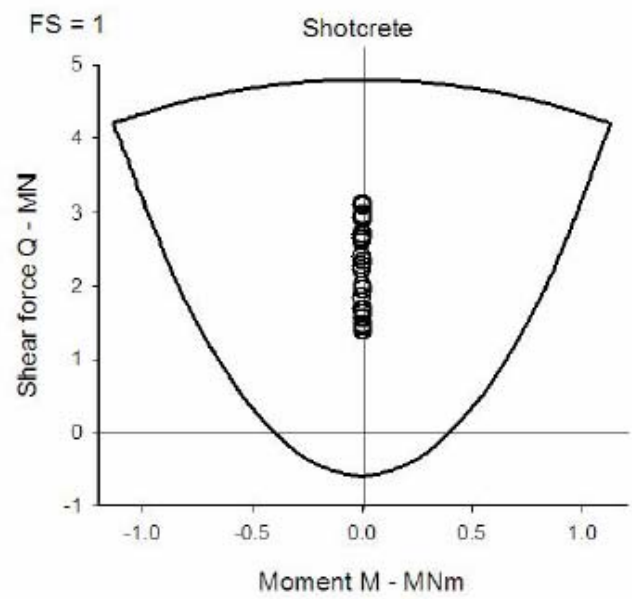
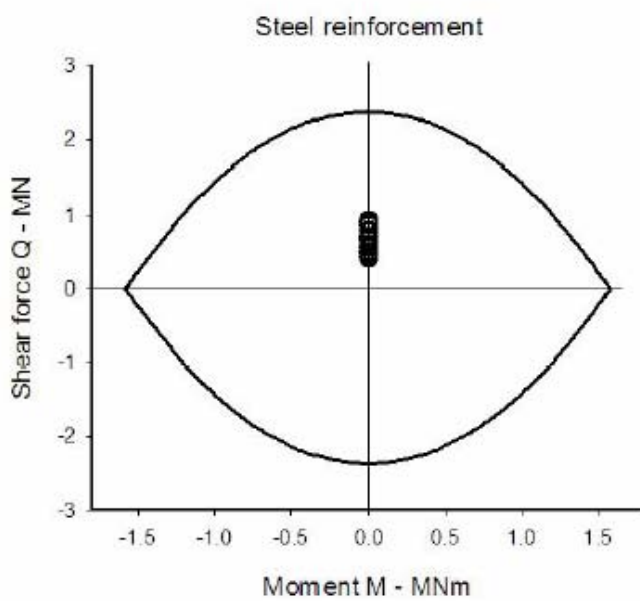
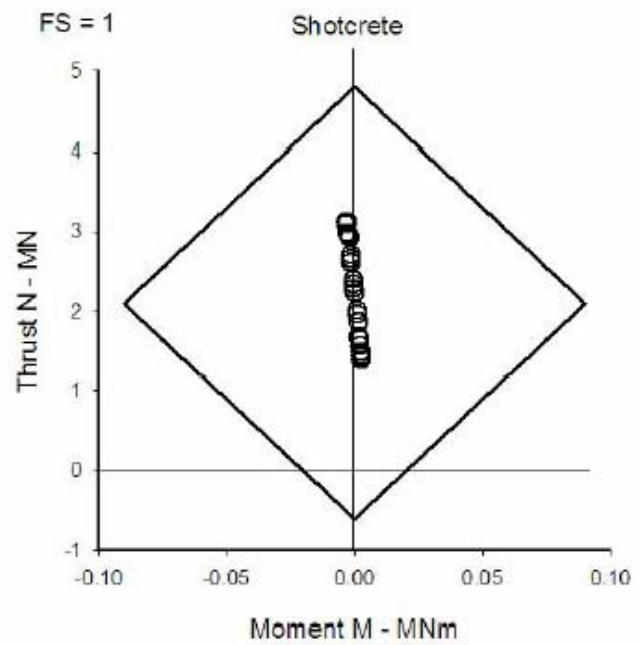
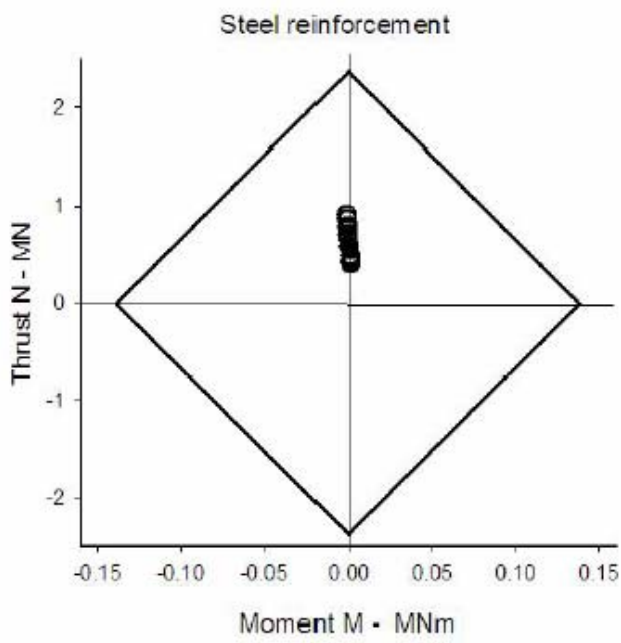


Figure A2.2. Support capacity diagrams and induced lining forces for the example described above.

## **ΕΕΕΕΓΜ**

Τομέας Γεωτεχνικής  
ΣΧΟΛΗ ΠΟΛΙΤΙΚΩΝ ΜΗΧΑΝΙΚΩΝ  
ΕΘΝΙΚΟΥ ΜΕΤΣΟΒΙΟΥ ΠΟΛΥΤΕΧΝΕΙΟΥ  
Πολυτεχνειούπολη Ζωγράφου  
15780 ΖΩΓΡΑΦΟΥ

Τηλ. 210.7723434

Τοτ. 210.7723428

Ηλ-Δι. [geotech@central.ntua.gr](mailto:geotech@central.ntua.gr)

Ιστοσελίδα [www.ntua.gr/civil](http://www.ntua.gr/civil) (υπό κατασκευή)

«ΤΑ ΝΕΑ ΤΗΣ ΕΕΕΕΓΜ» Εκδότης: Χρήστος Τσατσανίφος, τηλ. 210.6929484, τοτ. 210.6928137, ηλ-δι. [pangaea@otenet.gr](mailto:pangaea@otenet.gr)

«ΤΑ ΝΕΑ ΤΗΣ ΕΕΕΕΓΜ» «αναρτώνται» και στην ιστοσελίδα [www.pangaea.gr](http://www.pangaea.gr)